GAS SENSOR DEVELOPMENT FOR PORTABLE MONITORING

Lucy Tina Dimitrakopoulos
Bachelor of Applied Science (Phillip Institute of Technology, Melbourne, Australia) and
Master of Applied Science (Royal Melbourne Institute of Technology, Melbourne, Australia)

A thesis in fulfilment of the requirements for the Degree of

Doctor of Philosophy in Science

at the

School of Applied Sciences

Faculty of Science and Technology

University of Tasmania

Launceston, Australia

August 1998

"It is the moment that you think you can't, you discover that you can."

Celion Dion

In Memory of

Mr Rocco Di Benedetto

and dedicated to

my husband Dr. Telis Dimitrakopoulos

DECLARATION

I hereby declare that this submission is my own work and that, to the best of my knowledge and belief, it contains no material previously published or written by another person nor material which to a substantial extent has been accepted for the award of any other degree or diploma of a university or other institute of higher learning, except where due acknowledgment is made in the text.

Lucy Dimitrakopoulos
School of Applied Science,
University of Tasmania.

10th August, 1998.

ACKNOWLEDGMENTS

I wish to thank my supervisors Professor Peter W. Alexander (University of Tasmania) and Professor D. Brynn Hibbert (University of New South Wales) for their constant encouragement, support and knowledge.

I thank the School of Science and Technology for their financial support during my candidature. I also like to thank Associate Professor Don McWilliam for his support and encouragement throughout my study.

I wish to thank my dear colleague Mrs Fiona G. Beach for her advice, encouragement and friendship and I would like to thank Mr Matthew and Mrs Gabrielle Streat for their love and support.

I would like to thank with all my heart my mum and sisters for their encouragement, love and support throughout my study.

Finally, I wish to extend a special thankyou to my husband, Dr. Telis Dimitrakopoulos for his loving support and encouragement and for always being there when things were difficult.

SUMMARY

The use of multi-sensing portable analysers is of increasing importance for many applications. This thesis reports on the development of new portable battery-powered gas analysers suitable for remote site monitoring that can utilise a range of Taguchi tin-oxide sensors as detectors. Two main designs were developed and evaluated for a variety of applications employing head-space analysis.

A portable analyser employing the TGS812 and TGS824 Taguchi gas sensors was built in flow-through arrangements. The performance of the gas analyser was evaluated in terms of reproducibility, stability and sensitivity and was used to determine the ethanol content in various commercial beer and wine samples. The adsorption response mechanism of the tin-oxide gas sensors was also investigated using the Langmuir adsorption isotherm model and this model was validated by determining the ethanol content of beer and wine samples.

A portable, battery-powered, multi-sensor gas analyser, containing six different Taguchi tin-oxide semiconductors was developed and evaluated. The performance of the portable, battery-powered, multi-sensor gas analyser was evaluated in terms of stability, sensitivity, selectivity and reproducibility. The portable multi-sensor gas analyser was used to determine the ethanol content in various beer samples employing the Langmuir isotherm mentioned above.

The portable battery-powered multi-sensor gas analyser mentioned above was used together with back-propagation artificial neural networks and applied to discriminate between beer brands, grades of olive oils, as well as the estimation of the age of olive oil samples.

LIST OF PUBLICATIONS

Refereed Journal Publications:

(1) L. T. Di Benedetto, P. W. Alexander and D. B. Hibbert, "Portable Battery-Powered Flow Injection Analyser for Volatile Alcohols using Semiconductor Gas Sensors", Analytica Chimica Acta, **321**, 61-67, (1996).

(2) P. W. Alexander, L. T. Di Benedetto, T. Dimitrakopoulos, D. B. Hibbert, J. C. Nglia, M. Sequeira and D. Sheils, 'Field-Portable Analysers for Monitoring of Air and Water Pollution', Talanta, **43**, 915-925, (1996).

(3) L. T. Di Benedetto, P. W. Alexander and D. B. Hibbert, "Adsorption Response of Semiconductor Gas Sensors using a Portable Flow-Through Monitor", Field Analytical Chemistry and Technology, **1** (6), 357-366, (1997).

(4) P. W. Alexander, L. T. Di Benedetto and D. B. Hibbert, "A Field-Portable Gas Analyser with an Array of Six Semiconductor Sensors - Part 1 - Quantitative Determination of Ethanol", Field Analytical Chemistry and Technology, **2** (3), 135-143, (1998).

(5) P. W. Alexander, L. T. Di Benedetto and D. B. Hibbert, "A Field-Portable Gas Analyser with an Array of Six Semiconductor Sensors - Part 2 - Identification of Beer Samples using Artificial Neural Networks", Field Analytical Chemistry and Technology, **2** (3), 145-153, (1998).

Conference Publications:

Poster Papers:

(1) P. W. Alexander, L. T. Di Benedetto and D. B. Hibbert, "Flow Injection Determination of Volatile Alcohols with Semiconductor Gas Sensors", 13th Australian Analytical / 4th Environmental Conference, Darwin, July, 1995.

Oral Papers:

(1) P. W. Alexander, L. T. Di Benedetto, T. Dimitrakopoulos, D. B. Hibbert, J. C. Nglia, M. Sequeira and D. Sheils, "Field-Portable Analysers for Monitoring of Air and Water Pollution", 7th International Flow Injection Analysis Conference (ICFIA '95), Seattle, WA, USA, August 1995.

(2) P. W. Alexander, L. T. Di Benedetto, and D. B. Hibbert, "A Portable Gas Monitor for Flow Analysis in the Gas Phase using an Array of Six Semiconducting Sensors", 14th Australian Symposium on Analytical Chemistry, Adelaide, July, 1997.

TABLE OF CONTENTS

Chapter One: General Introduction

Chapter Three: The Evaluation of a Portable, Battery-Powered Gas Analyser with an Array of Six Tin-Oxide Semiconductor Sensors

Chapter Four: The Discrimination of Beer Brands using the Portable Battery-Powered Multi-Sensor Gas Analyser and Artificial Neural Network

Chapter One: General Introduction

1.1 Sensors

The aim of the work presented in this thesis was to develop and evaluate a portable, battery-powered gas analyser suitable for remote site monitoring. The portable analyser developed in this study employs multiple Taguchi tin-oxide semiconductor gas sensors in an array type arrangement, in order to determine the feasibility of the system.

A sensor converts a physical parameter that is to be measured into an electrical signal that is processed or transmitted electronically. Classification of physical parameters that are measured by sensors are presented in Figure 1.1.

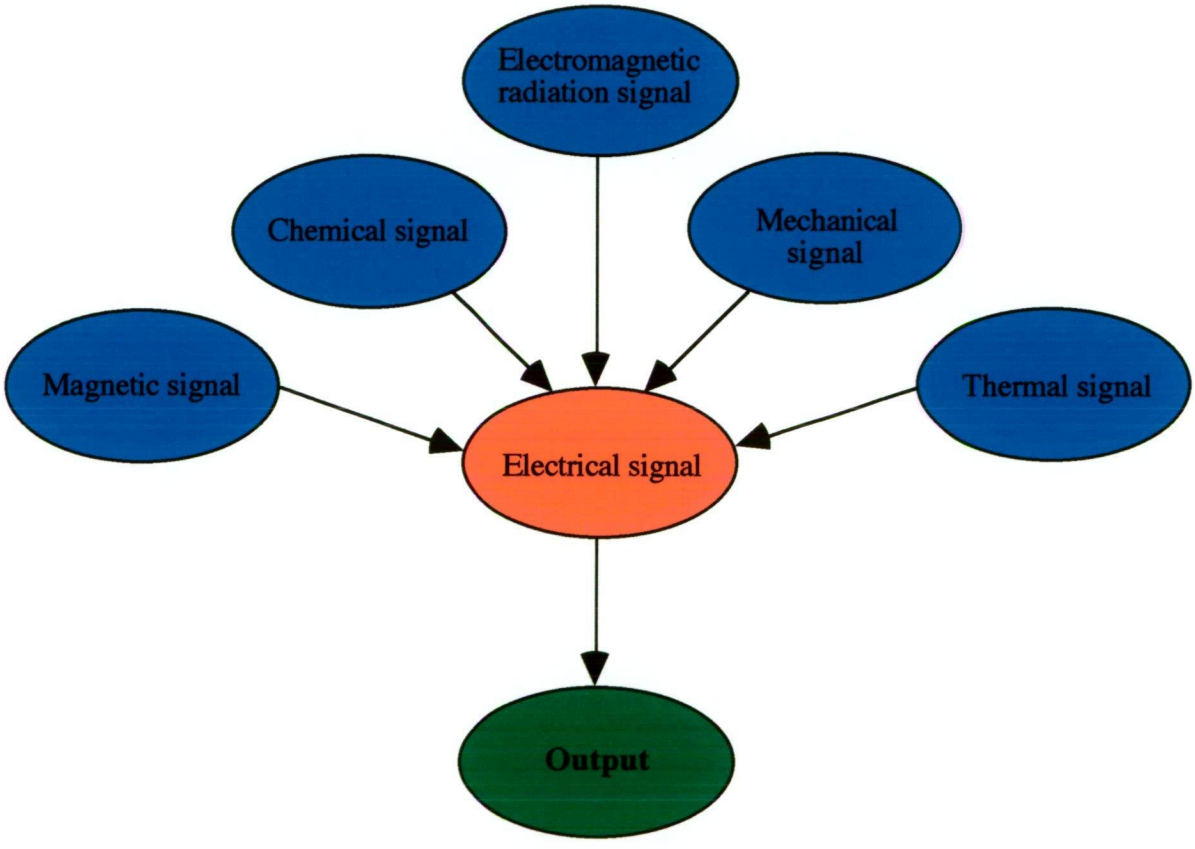

Figure 1.1. Physical parameters that are converted into an electrical signal by sensors.

Examples of physical parameters that sensors have been employed to monitor include:

(1) Magnetic signals used in measuring the earth's gravitational field [1],

(2) Chemical signals used to measure the concentration of chemical species such as pH, Na^+, Cl^-, and CO_2 [1],

(3) Electromagnetic radiation emitted from telecommunication devices [1],

(4) Mechanical signals used to determine pressure, viscosity and velocity of flow for gases and liquids [1] and,

(5) Thermal signals used to measure temperature and heat flow [1].

An ideal sensor should be highly sensitive, reproducible, reversible, selective, reliable, durable, small in size, low in background noise, simple to calibrate, of low cost, rapid in response and capable of producing a digital output. However, in practice, it is not possible to satisfy all these characteristics, so a compromise between cost and performance must always be reached. The characteristics of a sensor must be chosen in relation to particular requirements needed [1].

The aim of the work presented in this thesis was to develop and evaluate a portable battery-powered gas analyser employing various types of tin-oxide semiconductor gas sensors.

1.2 Gas Sensors

There are many gas sensors available commercially and many more are currently being researched, due to the recent interest in occupational health and the need for environmental pollution monitoring. Various types of gas sensors have been applied to detect gases of interest including; catalytic gas sensors, mass sensors such as piezoelectric sensors and surface acoustic wave sensors, optical gas sensors and electrochemical sensors such as potentiometric, amperometric and conductimetric gas sensors and each of these sensors will be discussed in turn.

1.2.1 Catalytic Gas Sensors

Catalytic gas sensors are widely used throughout industry for estimating the concentration of flammable gases in air [2]. Generally, the concentration of the gas of interest is measured as the heat is liberated in a controlled chemical reaction [2].

A typical catalytic gas sensor consists of a catalyst surface, a temperature sensor and a

heater to maintain the catalyst at the operating temperature. An example of a catalytic gas sensor is the pellistor-type sensor [2] as shown in Figure 1.2. This sensor uses palladium supported on thoria as the catalyst. This is deposited on the surface of a refractory bead of approximately 0.5 - 1.0 mm in diameter encapsulating the platinum coil which acts as a heater and temperature sensor. Encapsulation of the coil within a spherical bead in this way produces a device which is insensitive to orientation and also resistant to shock. It is possible to use any type of temperature sensor without changing the basic concept of this sensor [2].

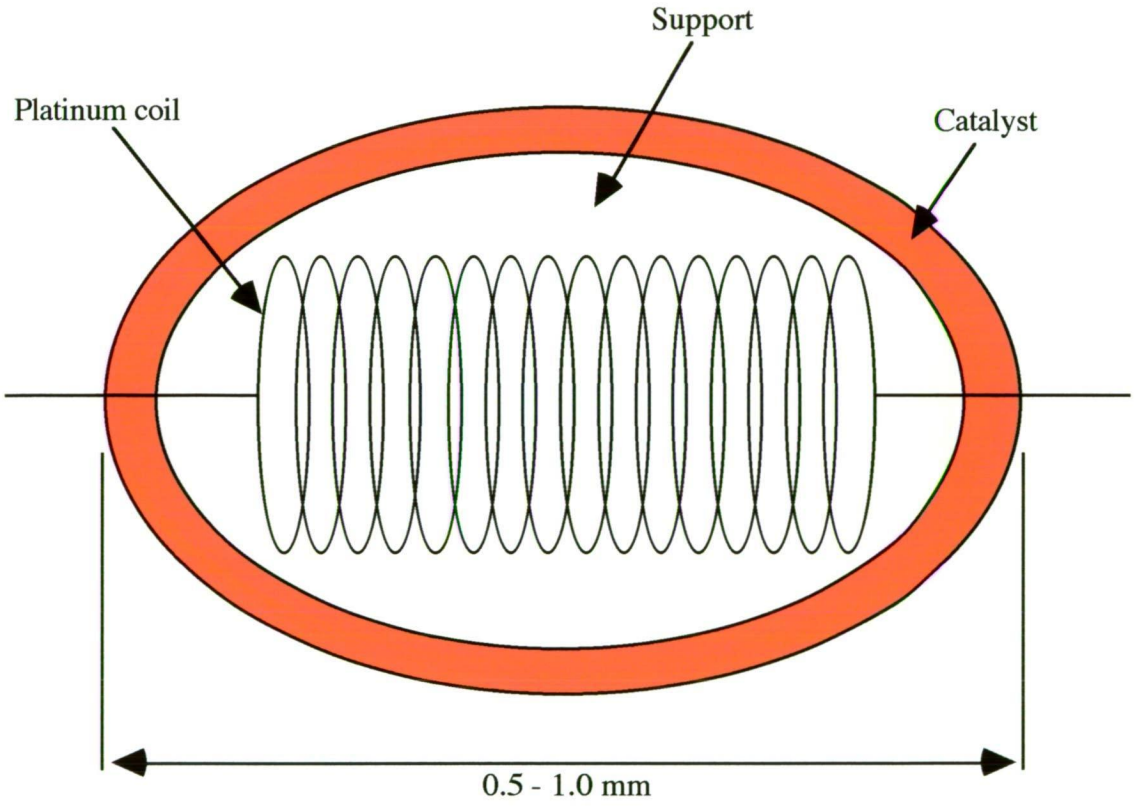

Figure 1.2. A typical catalytic gas sensing element: the pellistor.

When the combustible gas reacts at the catalytic surface, heat evolved from this reaction increases the temperature. The pellistor is usually connected to one arm of the Wheatstone bridge circuit, which provides the output signal. For small temperature changes, the out-of-balance signal (V) across the bridge is proportional to the rate of reaction and the heat of combustion [2]:

$$V = K\, r\, \Delta H \qquad (1.1)$$

where K is the constant defined by the components of the system, r is the reaction rate and ΔH is the heat of combustion. As a result, the out-of-balance voltage of the bridge is proportional to the concentration of the flammable gas [2].

Catalytic gas sensors have been used to distinguish between different flammable gases by monitoring the sensor over a range of temperatures [3-4]. These gas sensors are known to be very reliable for the quantitative analysis of flammable gases in air, giving a measure of explosiveness irrespective of the composition of the gas mixture. However, the major limitation of catalytic gas sensors is that various gases such as organosulfur compounds will poison the catalyst [2-4].

1.2.2 Mass Sensors

1.2.2.1 Piezoelectric Sensors (Quartz Resonance Sensors)

Piezoelectric sensors are based on thin crystals which oscillate in an applied electric field at a fixed frequency usually in the range of 5-15 MHz [1]. A schematic diagram of a piezoelectric sensor is illustrated in Figure 1.3.

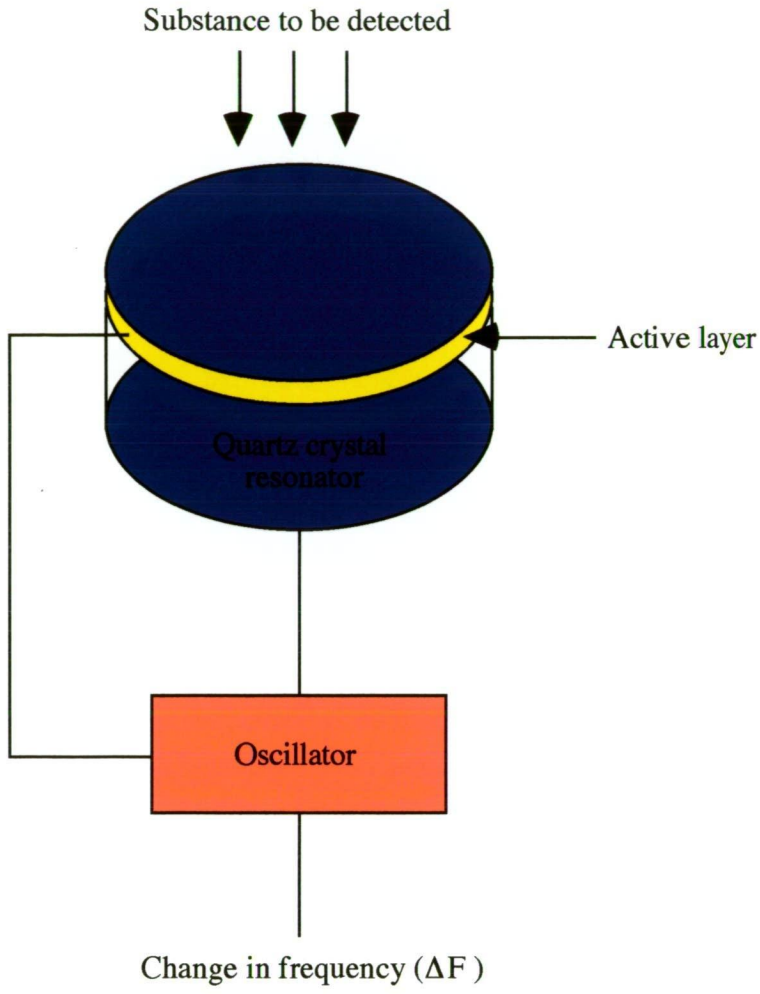

Figure 1.3. Piezoelectric sensor.

There are several types of materials that can exhibit the piezoelectric effect. α-Quartz is the most common material used because it is inexpensive, has a relatively high piezoelectric coefficient and possesses a hexagonal crystallographic structure with no centre of symmetry. The magnitude of the piezoelectric coefficient and its temperature dependence depends on the orientation of the cut of the crystal with respect to the main axes. The optimum orientation is chosen so that the crystal exhibits minimum temperature dependence within the operating range of temperatures. Therefore, for sensor applications under ambient conditions, the AT cut (35 ° 15' inclination in the y-z plane) is commonly used [1].

Quartz crystals have been used as microbalances in the determination of thin layer thickness and in gas-sorption studies [5]. The principle was based on the mass change (ΔM, g) on the surface of the crystal which was directly proportional to the frequency change (ΔF, Hz)

according to the Sauerbrey equation [1,5]:

$$\Delta F = 2.3 \times 10^6 F^2 \Delta M / A \qquad (1.2)$$

where F is the frequency of the quartz crystal (MHz), ΔM is the mass change on the surface of the quartz crystal (g) and A is the surface area of the crystal (cm^2).

Piezoelectric gas sensors have been used for the determination of ammonia [6], carbon monoxide [7], hydrogen chloride [8], nitrogen dioxide [6], sulfur dioxide [9], organophosphorus compounds [10] and mononitrotoluene [11]. The advantages of piezoelectric sensors include their small size, light weight, high sensitivity and reliability, simple construction and operation and low power requirement [12]. The main disadvantage of piezoelectric sensors is that the quartz crystal requires frequent cleaning and the accuracy and precision may be affected by temperature and humidity changes [12].

1.2.2.2 Surface Acoustic Wave Sensors

Surface acoustic wave (SAW) sensors employ a piezoelectric crystal to electronically induce a periodic wave on the surface of the crystal [1]. The most common SAWs are the Rayleigh waves [1]. These waves are generated by affixing two pairs of comb-shaped, interlocking metal electrodes at the two ends of a piezoelectric substrate using lithographic methods as shown in Figure 1.4 [1]. It is usual to have the electrode configuration repeated at the two ends of the substrate. In this way, one side can be the reference and the other can be the sensing element [1].

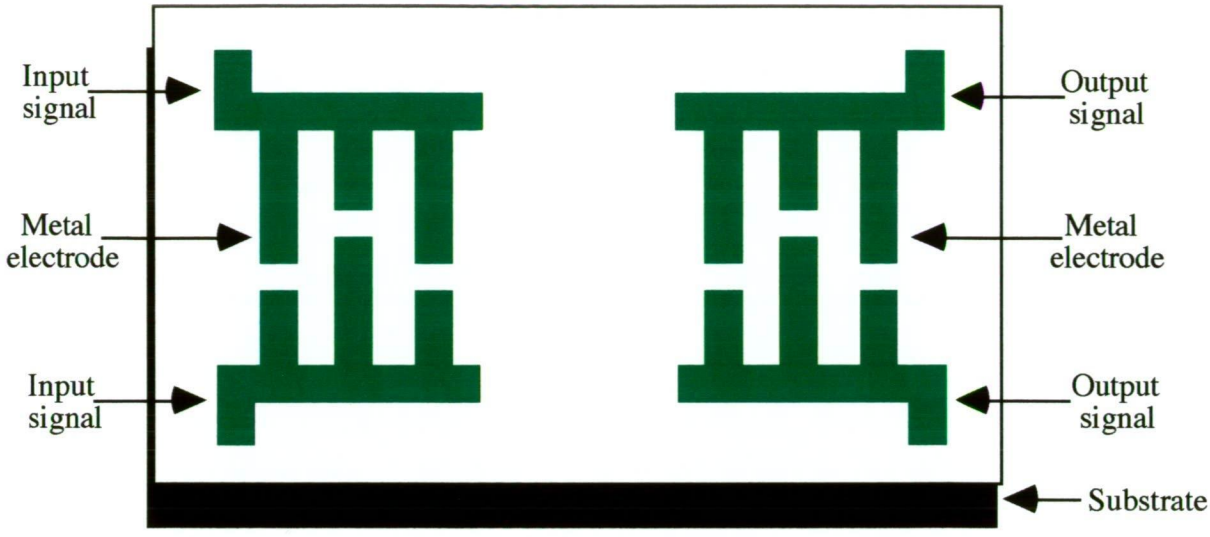

Figure 1.4. SAW element.

The frequency of the SAW varies between 10 MHz and 1 GHz [1]. Quartz, lithium niobate, piezoceramics or thin piezoelectric layers such as ZnO can be used as the piezoelectric substrate material [13]. These thin layers are located on a non-piezoelectric base such as glass, silicon or a ceramic.

The transmission of the SAW is dependent on the mass of material adsorbed onto the crystal and therefore the gas or vapour adsorbed between the sets of electrodes causes a change in frequency, which is proportional to the weight of adsorbed species according to the equation [1]:

$$\Delta F = k f_o^2 h \rho \qquad (1.3)$$

where k is the material constant of the SAW substrate, f_o is the resonant frequency, h is the coating thickness and ρ is the coating density. SAW sensors have been used for the detection of various gases including styrene [14], carbon dioxide [15] and nitrogen dioxide [16].

SAW sensors are attractive for chemical microsensor applications because of their small size, low cost, high sensitivity and reliability [15,16]. The main disadvantage with SAW sensors is their lack of selectivity and reproducibility of surface coating layer thickness [12].

1.2.3 Optical Gas Sensors

Optical gas sensors are based on optical fibres that employ a single indicator dye, which is located at the tip of the fibre and immobilised in an inert polymer [17]. Absorbance and fluorescence are the two main parameters that are used to monitor the optical signal [17,18]. An example of an indicator dye used for an oxygen sensing optode is the tris(4,7-diphenyl-1,10-phenanthroline)ruthenium (II) perchlorate, which is a luminescent transition metal complex that was immobilised in a plasticised poly (vinyl chloride) membrane [17]. A cross-section of a typical optode that employs a polymer membrane is illustrated in Figure 1.5.

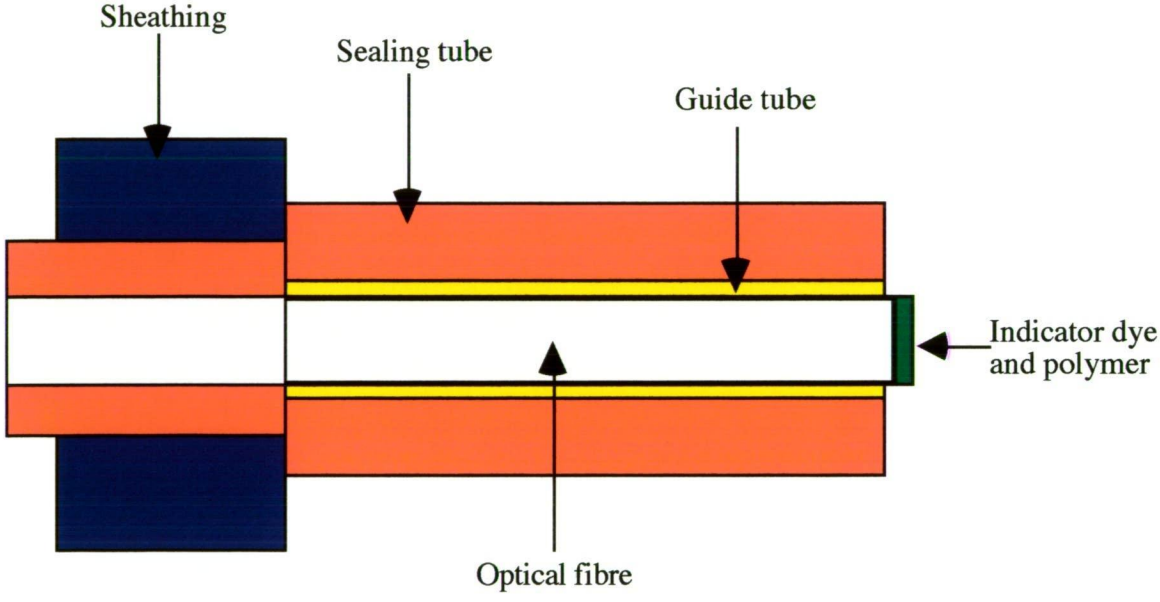

Figure 1.5. Schematic diagram of a typical optical gas sensor.

Optodes have been developed to respond to ammonia [18], carbon dioxide [19] and oxygen [20]. The main advantage of optodes is that no reference is required compared to electrochemical methods, they are easily miniaturised, the signal can be transferred to optical fibres over large distances without amplification compared to electrical signals, they are relatively inexpensive, simple in design and can easily be replaced [21].

The disadvantages of optodes include the interferences of ambient and stray light if the sensor is not optically isolated, the membrane exhibits limited stability due to leaching of the immobilised indicator dye and most optodes do not exhibit a linear relationship between the analyte concentration and the optical signal [21].

1.2.4 Electrochemical Sensors

1.2.4.1 Potentiometric Gas Sensors

The Severinghaus-type electrode is an example of a potentiometric gas sensor and it was originally developed to measure the partial pressure of carbon dioxide in blood [22]. A diagram is illustrated in Figure 1.6. The Severinghaus-type potentiometric gas sensors commonly employ a pH glass electrode surrounded by an intermediate electrolyte solution (eg., sodium bicarbonate-sodium chloride) and enclosed by a gas-permeable membrane, usually silicone. An internal reference electrode is used so that the sensor is a complete electrochemical cell. The Severinghaus-type electrode can be used for measurements in either gaseous or liquid samples. When carbon dioxide from the outer sample diffuses through the semipermeable membrane, it lowers the pH of the inner solution [23]:

$$CO_2 + H_2O \Leftrightarrow HCO_3^- + H^+$$

Such changes in the pH are measured by the inner glass electrode and the overall cell potential is therefore determined by the carbon dioxide concentration in the sample.

The permeable membrane is responsible for the electrode's gas selectivity. Two types of polymeric material, microporous and homogeneous, are used to form gas-permeable membranes. These membranes are usually 0.01- 0.1 mm in thickness and are impermeable to water and ions [23]. By employing different membranes and internal electrolyte solutions, it is possible to obtain potentiometric gas sensors for gases such as ammonia [24] and hydrogen cyanide [25]. These sensors employ similar acid-base or other equilibrium processes.

Potentiometric gas sensors exhibit excellent selectivity compared with many ion selective electrodes, however the response characteristics are often affected by the composition of the internal solution and the variables of geometry [26].

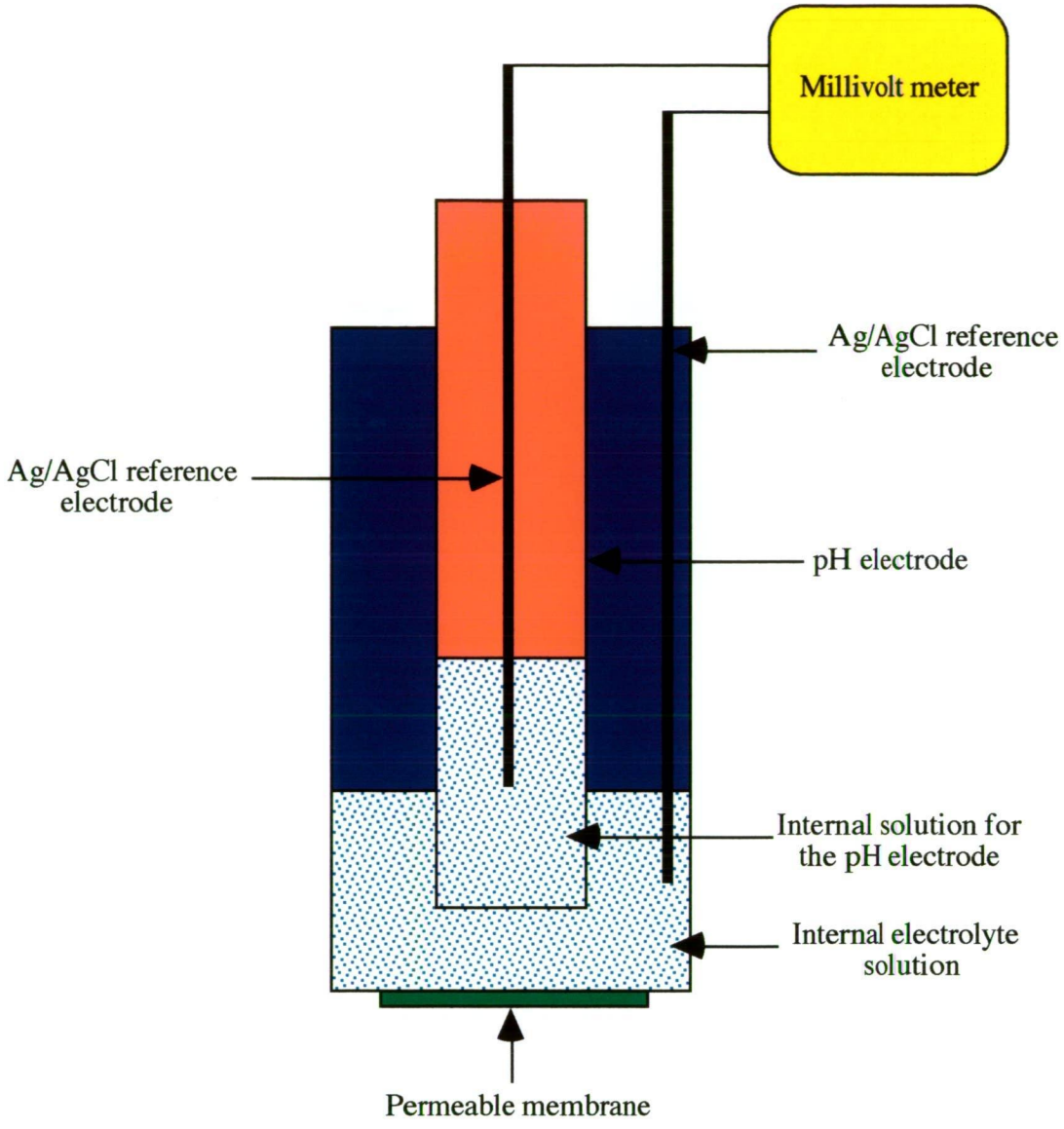

Figure 1.6. Schematic diagram of the Severinghaus-type potentiometric gas sensor.

1.2.4.2 Amperometric Gas Sensors

The Clark electrode is an example of an amperometric gas sensor which was originally developed to analyse blood oxygen [27] and a schematic diagram is illustrated in Figure 1.7. The Clark amperometric gas sensors is based on a pair of electrodes immersed in an electrolyte solution and separated from the test solution by a gas-permeable hydrophobic membrane [23]. The membrane is usually made of teflon, silicon rubber, or polyethylene and the electrolyte is a solution of potassium chloride and buffer [23]. Oxygen diffuses through the membrane and is reduced at the surface of the sensing electrode as follows [23]:

$$O_2 + 2H_2O + 2e^- \longrightarrow [H_2O_2] + 2OH^-$$

$$[H_2O_2] + 2e^- \longrightarrow 2OH^-$$

The resulting electrolytic current is proportional to the rate of diffusion of oxygen to the cathode, and therefore to the partial pressure of the gas in the sample [23]. The actual potential applied at the cathode (with respect to the anode / reference electrode) depends on the particular design. The cathode is commonly made of platinum, gold or silver. The applied potential usually maintains the cathode on the diffusion-limited plateau region for the oxygen reduction process [23].

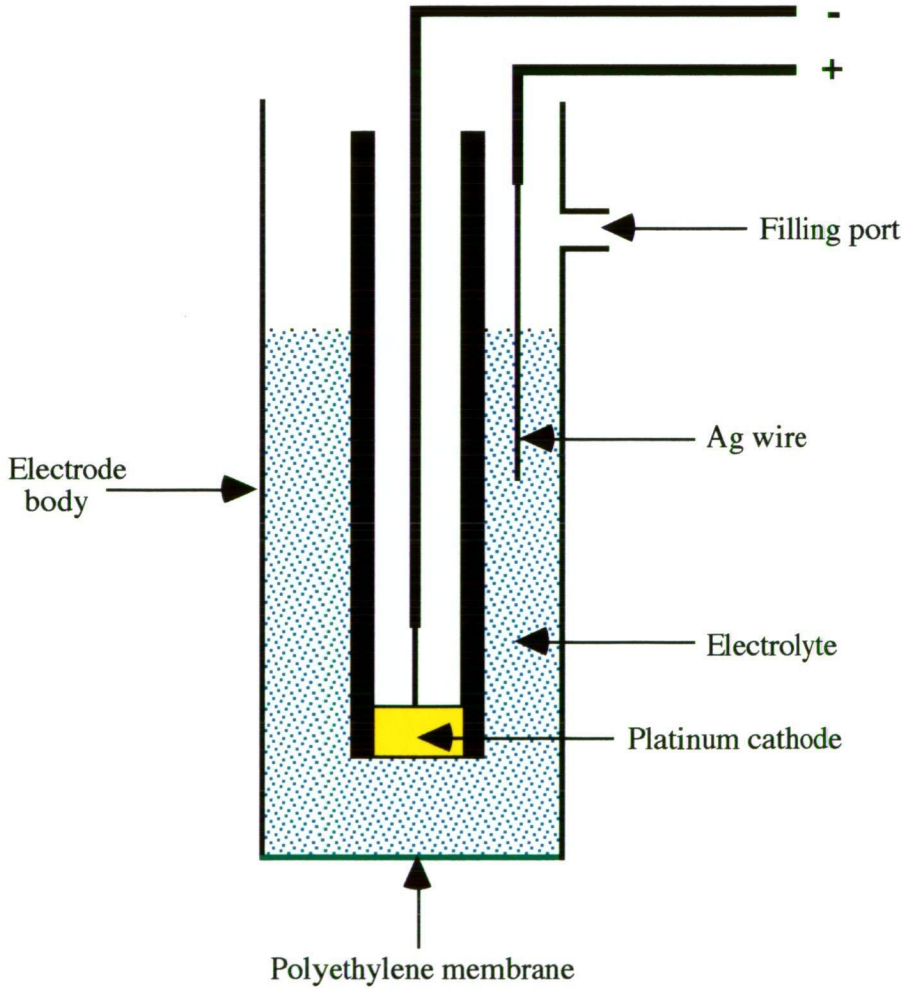

Figure 1.7. A schematic diagram of a Clark oxygen electrode.

The operation and the sensor design of the amperometric gas sensor can be applied to

any gas which can be reduced or oxidised such as nitrogen monoxide [28], nitrogen dioxide [28] and carbon dioxide [29].

1.2.4.3 Fuel Cell Gas Sensors

An alternative amperometric gas sensor is the fuel cell sensor. The fuel cell sensor is constructed and contains a solvent / supporting electrolyte combination, and a voltage can be applied to the working electrode so that the gas species can be oxidised or reduced with some degree of selectivity [30]. The relationship between the cell current is proportional to the concentration of gas species of interest. An example of a fuel cell type amperometric sensor is shown in Figure 1.8. The sample enters the cell through porous electrodes. Porous platinum / teflon electrodes separate the electrolytic cell from the gaseous reference chamber on one side, and the sample chamber on the working electrode side [30]. The applied voltage between the working and the platinum / air electrodes are maintained constant and the potential of the platinum / air reference electrode is measured against the potential of a regular Ag / AgCl electrode. This is an unusual arrangement from the electrochemical point of view, because the potential of the working electrode is affected both the cathodic processes taking place at the platinum / air reference electrode and by the IR drop across the cell [30]. The sample enters into the electrolytic cell through the porous electrodes, the pore size of which needs to be also closely controlled in order to prevent their flooding with the solvent.

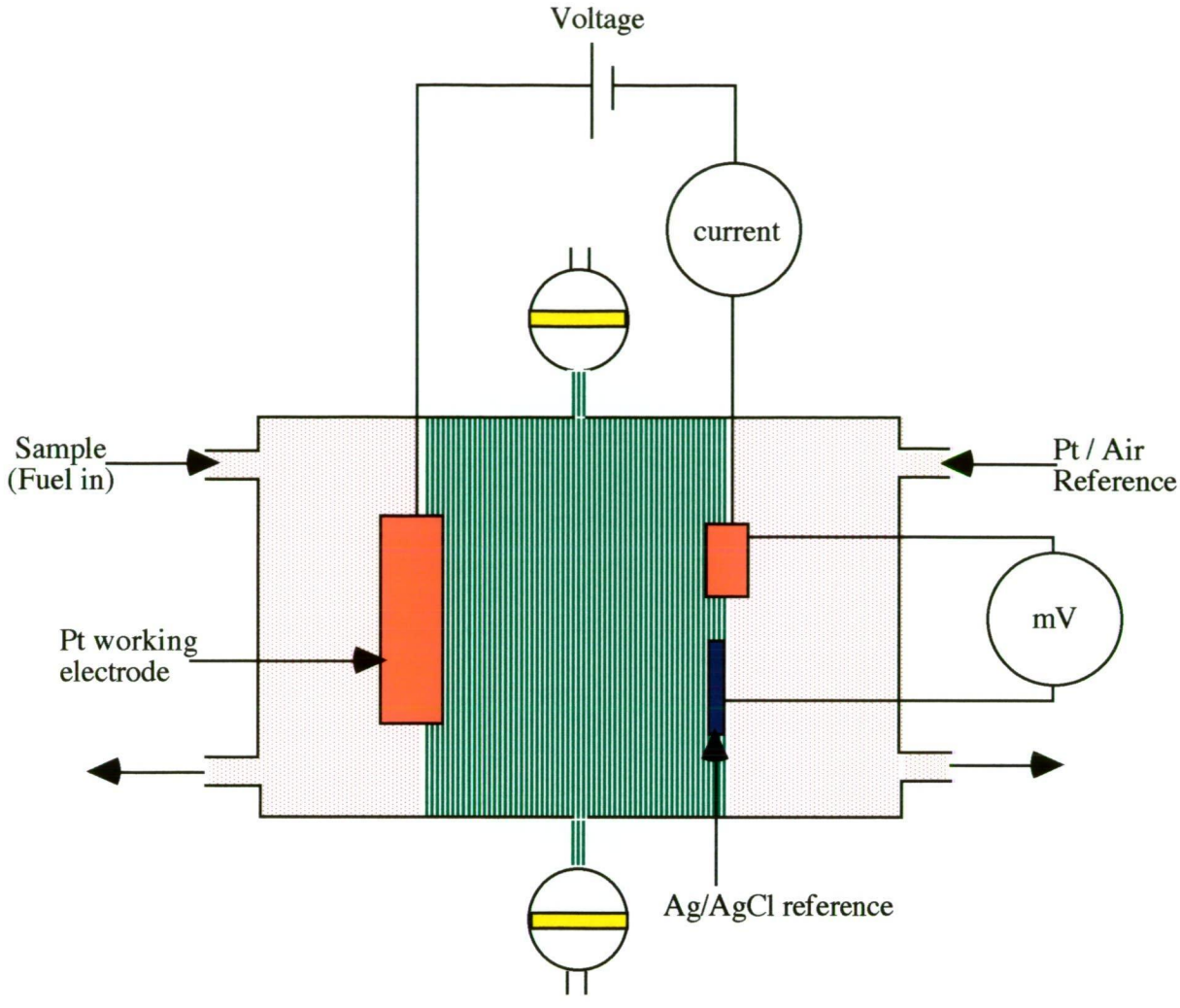

Figure 1.8. A schematic diagram of the fuel cell gas sensor.

Fuel cell sensors are primarily used in the areas of evidential breath testing and environmental monitoring [31]. The ability to detect component gases in a mixture is significantly improved when an array of fuel cell sensors are employed [31]. The advantages of the fuel cell sensors are their simple construction [30]. However, because the processes which affect the response are not fully known, it is difficult to correct problems when they arise or to make suitable design changes [30].

1.2.5 Conductimetric Gas Sensors

The most common conductimetric gas sensors are the semiconducting metal oxide sensors, because of their chemical and thermal stability. The primary mechanism responsible for gas reactions with metal oxide semiconductors in air at high temperatures (200 - 600 ^{o}C)

relates to the change in the concentration of the adsorbed oxygen at the semiconductor surface [32]. Oxygen ions are formed at the metal oxide surface by removing electrons from the semiconductor solid. As the charge carrier density is reduced, a potential barrier develops that slows the oxygen adsorption rate and corresponding electron movement through the grain junctions [32]. Conductivity of the semiconductor material is therefore limited by the oxygen adsorption rate and the potential barrier effects at grain junctions. At the surface of an n-type semiconductor, reducing gases combines with the adsorbed oxygen reducing the height of potential barrier and the semiconductor resistance, and vice versa for oxidising gases and this phenomenon is illustrated in Figure 1.9. For p-type metal oxide semiconductor gas sensors, reducing gases will increase the semiconductor resistance, while oxidising gases will decrease it [32]. Semiconductor sensor materials are therefore classified as n or p type based on the resistance changes to decreasing partial pressures of oxygen or to reducing gases in fixed partial pressures of oxygen. Solid state doping can set a metal oxide to n or p type, as desired, although many materials switch behaviour from n type to p type with increasing partial pressures of oxygen [32].

Other mechanisms affecting resistance changes in the semicondutor are adsorption of ions other than oxygen at the surface, changes in ambient humidity, or water formed by combining with adsorbed oxygen. The reactions for an n-type semiconductor as shown in Figure 1.9 are below [32]:

$$\text{Adsorption of oxygen: } (SnO_2 + e^-) + 1/2\,O_2 \longleftrightarrow SnO_2\,(O^-)_{ad}$$

$$\text{Reducing gas: } SnO_2\,(O^-)_{ad} + CO \longrightarrow (SnO_2 + e^-) + CO_2$$

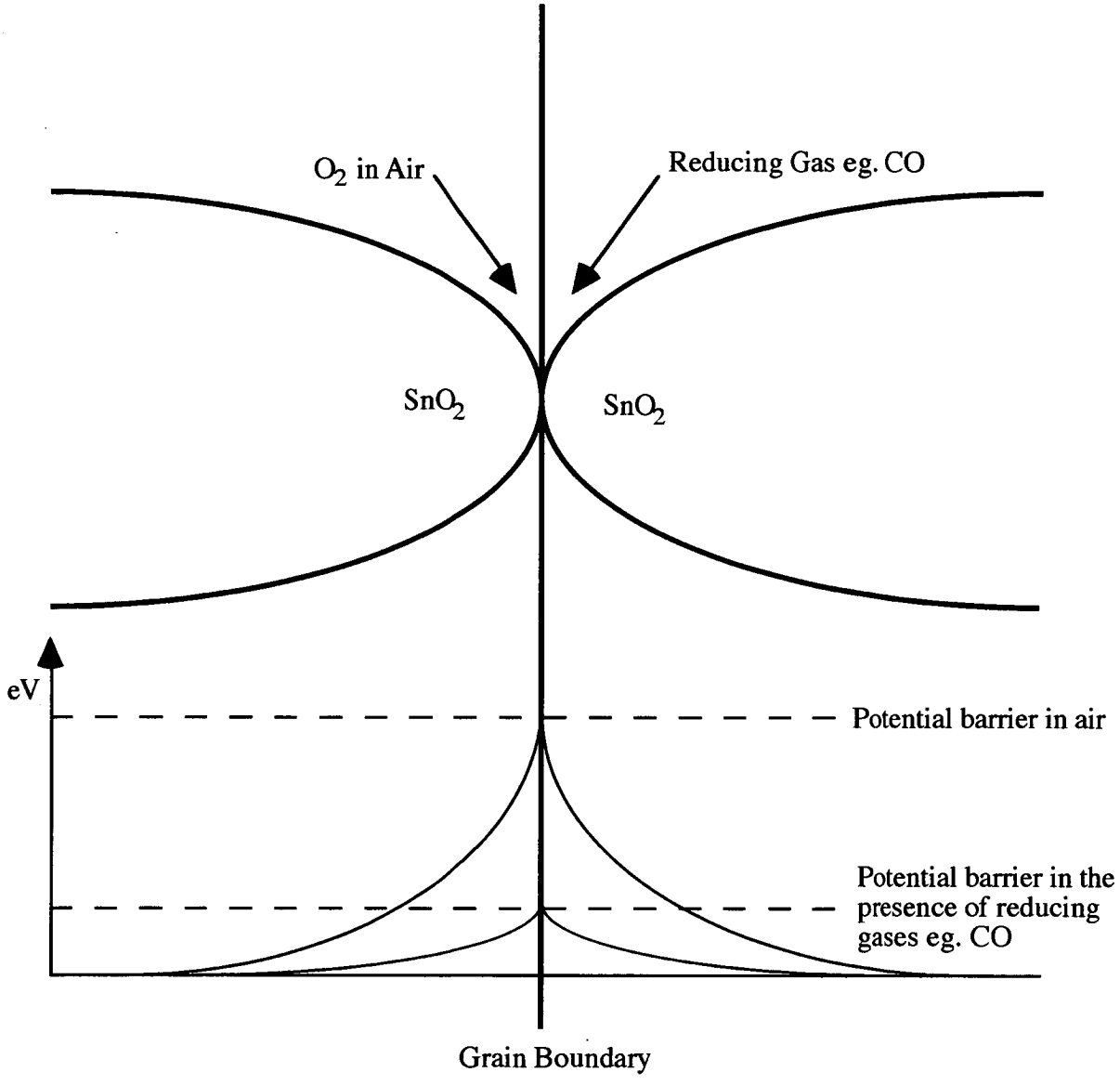

Figure 1.9. Model of the potential barrier at the grain boundary for metal oxide semiconductor gas sensors.

Examples of n-type semiconductor gas sensors include SnO_2, ZnO and Fe_2O_3, and p-type semiconductor gas sensors include CuO, NiO and CoO. Figure 1.10 illustrates a schematic diagram of two possible configurations of metal oxide semiconductor gas sensors.

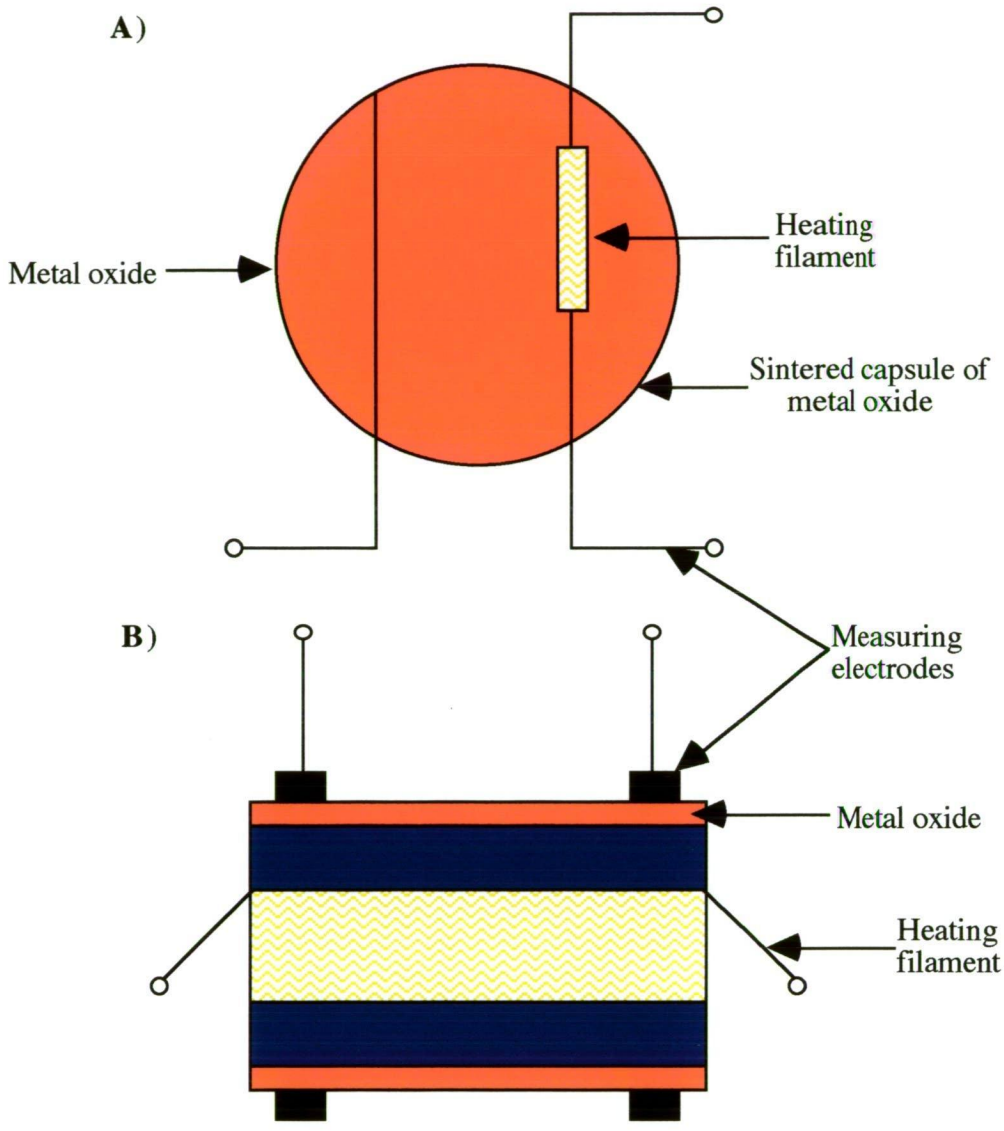

Figure 1.10. Schematic diagram of A) polycrystalline sensor with sintered platinum heating filament and B) polycrystalline sensor with a separate heating element.

Metal oxide semiconductor gas sensors are frequently modified and optimised through doping of other metal atoms, commonly Pd, Pt, Cu, Au and Ag [33,34] and this gives a certain degree of selectivity. The most commonly used metal oxide gas sensors are based on SnO_2, ZnO and Fe_2O_3. Table 1.1, summarises gases detected by various metal oxide gas sensors.

Table 1.1. Selectivity of some metal oxide semiconductor gas sensors [1].

Metal oxide Semiconductor Gas Sensors	Detected Gases
TiO_2, Fe_2O_3, CoO, ZnO, ZrO_2, SnO_2, La_2O_3	O_2
Cr_2O_3, NiO, ZnO, ZrO_2, SnO_2, In_2O_3	CO
Fe_2O_3, Fe_3O_4, Co_3O_4, ZnO	CH_4
SnO_2, VO	NO_X
ZnO, Al_2O_3, SnO_2	Halogens

1.2.5.1 Tin-oxide Gas Sensors

The tin-oxide (SnO_2) semiconductor gas sensor was originally developed in 1968 for the detection of domestic gas leaks [35]. However, it was soon discovered that this sensor could be applied for breath alcohol analysers, automatic cooking controls in microwave ovens, air quality monitors and fire alarm systems [32,35]. SnO_2 is the most common type of metal oxide material used in gas sensors because this material exhibits higher sensitivity than other metal oxides at relatively low temperatures and it remains stable without a thermal phase change in the crystal structure. A schematic diagram of a commercial SnO_2 sensor element and configuration developed by Figaro Engineering Inc. is shown in Figure 1.11. This sensor consists of a small ceramic tube coated with tin (IV) oxide and a suitable catalyst. A heater coil maintains the tin-oxide temperature between 200 and 500 ^{o}C. The signal is measured by the resistance between the two printed gold electrodes at opposite ends of the ceramic tube. These sensor elements are protected by a plastic housing, with an open area to allow gases to enter, which is covered by two flame arresters of stainless steel double-gauze. A photograph of the commercial Figaro Taguchi gas sensors (TGS) are shown in Figure 1.12.

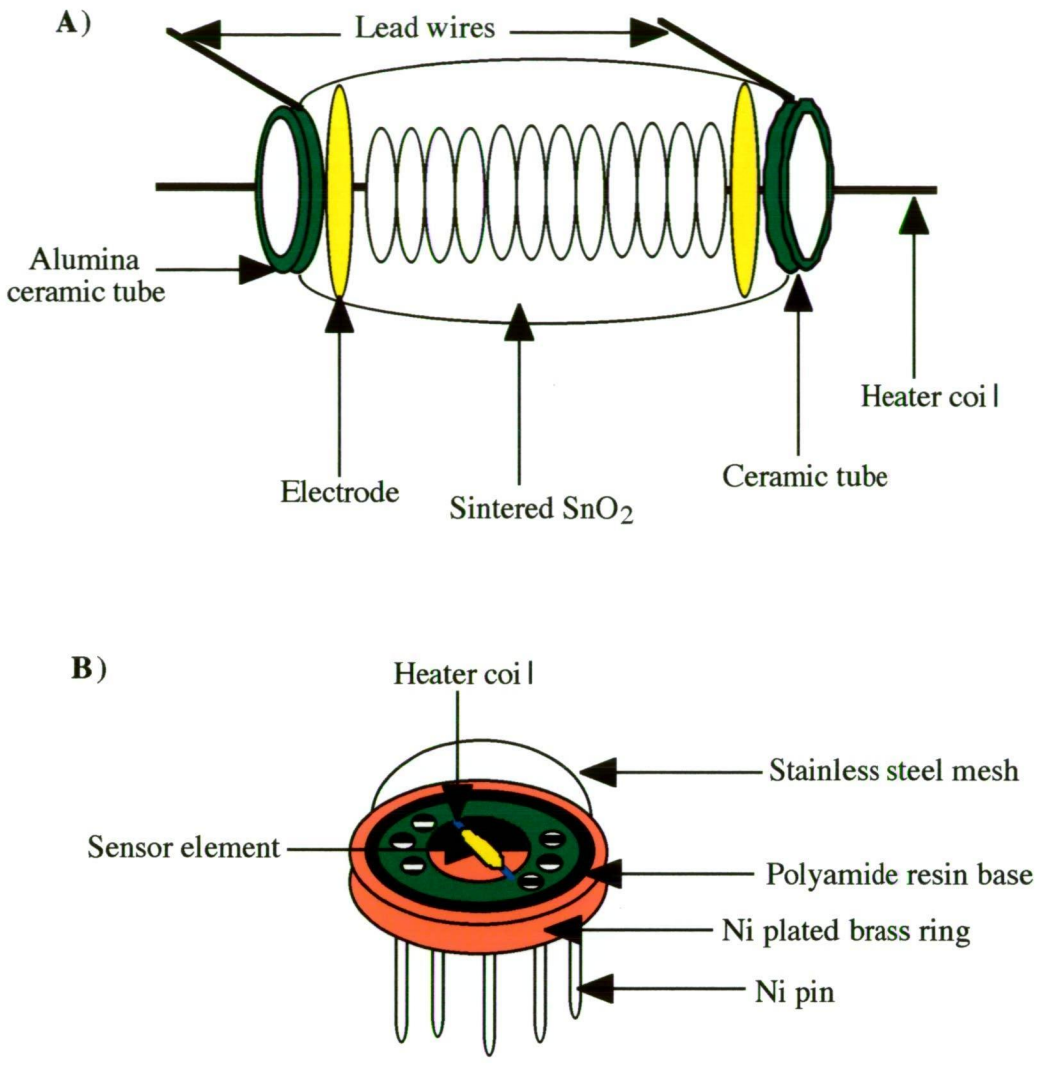

Figure 1.11. Schematic diagram (A) sensor element (B) configuration of Taguchi gas sensor.

Figure 1.12. Photograph of the commercial TGS813, TGS822 and TGS824 Taguchi gas sensors.

The advantages of the TGSs include, a long lifetime (3 to 5 years) and good reliability, high sensitivity and a rapid response, good reproducibility, highly resistant to poisoning, small size (19.5 mm internal diameter), excellent durability and shock proof, low power consumption (0.6 to 1.2 W) and are inexpensive [36].

1.2.5.2 Preparation of Tin Dioxide Sensors

There are various alternative laboratory methods for the preparation of tin dioxide sensors and the sequence for a typical preparation method is described below.

High-purity tin is dissolved in acid and an alkali is added to precipitate out the tin hydroxide. The tin hydroxide is then calcined, usually at about 450 ^{o}C, in order to obtain very pure SnO_2 powder and the temperature and time of calcination defines the sensor properties [37]. An equal weight of high-purity alumina is added to the SnO_2 powder to enhance the strength of the ceramic and to modify the conductivity. Distilled water is then added to form a paste which is allowed to air-dry. This is usually carried out after portions of the paste have been mounted on to whatever structure is used to support the final sensor material [37].

The final process involves sintering of the paste typically over 700 ^{o}C. In principle, sintering fuses individual particles together and therefore increases strength radically, but unfortunately this process is not efficient in some materials, including tin dioxide, and therefore a binder must be added. Tetraethyl orthosilicate is one example of a binder [38] and it decomposes to leave silica in the resultant tin dioxide ceramic. Above 3% silica content, the strength of the final ceramic is considerably increased, due to the formation of a network of bridges around the grains of SnO_2 and alumina. The presence of silica in the ceramic has the added advantage of lowering the absolute resistance of the material by a factor of 10, consequently simplifying the circuitry for the developed sensor.

1.2.5.3 Tin-Oxide Sensor Arrays

The use of sensor arrays are extremely attractive for multi-analyte determinations, since analysis time and expense can be significantly reduced. A recent publication has reviewed the progress in sensor array research, reporting on a range of multi-gas monitors, many of which

are portable and applicable for field operation [39]. These mainly utilise electrochemical sensors developed to detect gases such as carbon monoxide, hydrogen sulfide, nitric oxide, sulfur dioxide and nitrogen dioxide. In addition there has been considerable research devoted to the development of multi-gas analysers based on tin-oxide sensors, including two chemically modified tin-oxide sensors used for the identification of carbon monoxide and methane [40], three tin-oxide sensors for the discrimination between alcohols and tobaccos [41], a sensor array of four tin-oxide semiconductor thin-film devices used to characterise smoke [42], an array of six tin-oxide gas sensors used for the detection of single and mixtures of gases [43] and twelve tin-oxide semiconductor sensing elements employed for the discrimination of coffees [44].

1.3 Portable Gas Analysers for Remote-site Monitoring

Two recent publications have highlighted the need for portable instrumentation based on flow injection analysis [45] and gas analysers [46] for the purpose of remote site monitoring. The use of portable gas analysers for chemical analysis is of increasing interest and has been reviewed recently [46]. Portability ideally allows operators to perform chemical analysis outside the conventional laboratory limits.

In gas analysis, advances have occurred in many instrumental areas including the development of a miniaturised gas chromatograph employing a micromachined thermal conductivity detector used to separate mixtures of hydrocarbons [47], laser radar spectroscopy using a CO_2 wavelength for air pollution monitoring [48], the combination of gas chromatography with mass spectrometry for the detection of organic contaminants at chemical accident locations [49], and ion mobility spectrometry for the detection of chemical warfare agents [50]. In addition X-ray fluorescence spectrometry has been developed in a portable analyser which has the capability of simultaneous multi-elemental non-destructive analysis of transition elements [51]. This portable X-ray fluorescence spectrometer was employed by NASA in one of the lunar missions to analyse in-situ the composition of the lunar crust [51]. However, there is still little research devoted to the development of portable gas analysers based on metal oxide semiconductor gas sensors that are battery-powered and for use in field

monitoring at remote locations.

1.4 Pattern Recognition in Gas Sensing

Pattern recognition is the term used to describe the methodology of solving classification type problems encountered in the physical and engineering sciences [52]. Establishing a classification is desirable for various applications such as the analysis of chemical composition, detection of food contamination, food quality testing and exploratory data analysis. Recent developments in gas sensors have led towards the application for the identification or classification of gases, gas mixtures or odours employing gas sensor arrays and this has been made possible through the use of pattern recognition [52]. Most gas sensor materials exhibit poor selectivity, therefore the application of gas sensor arrays provides researchers with a response pattern as a means for identification.

Pattern recognition may be regarded as a branch of artificial intelligence that involves the mimicking or modelling of human intelligence [52]. There are two main types of pattern recognition: parametric and non-parametric, as illustrated in Figure 1.13.

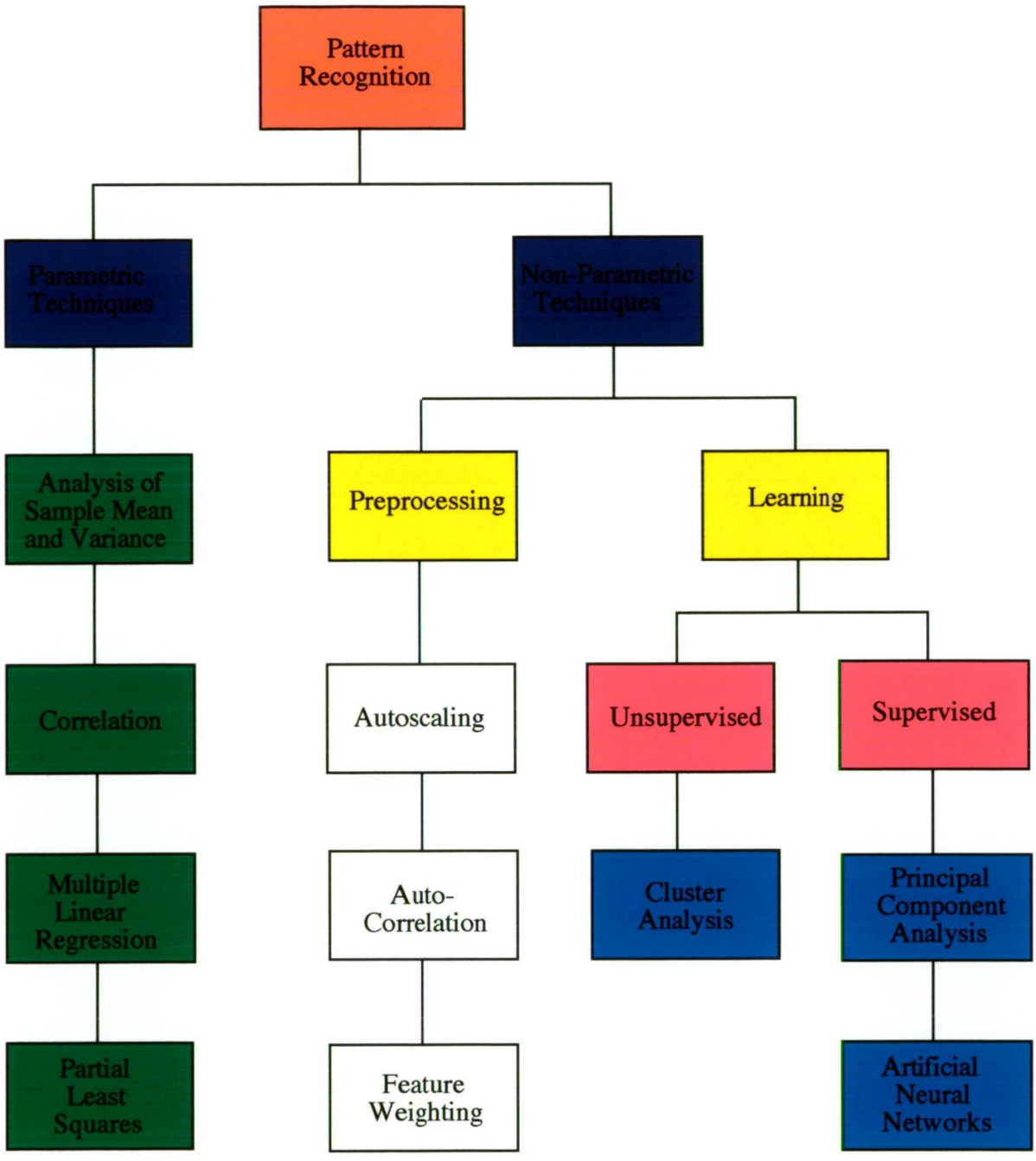

Figure 1.13. Classification of pattern recognition techniques applied in gas sensing.

Parametric techniques rely upon obtaining or estimating the probability density function of the parameters used to characterise the response of a system [52]. In univariate analysis, examples include tests on the sample mean or variance, such as a Student's t test or Snecodor F test and in bivariate analysis, examples are least-squares fit and linear regression methods [52]. In multivariate systems, examples include multiple linear regression (MLR) and partial least-squares (PLS). In general these methods require considerable effort in establishing a large

database, although some techniques are used to model smaller data sets, with a reduced confidence level. Conversely, non-parametric techniques require no assumption about the statistical distributions of the data. Examples of pre-processing techniques are: autoscaling, correlating and feature weighting [52]. These techniques all involve the transformation of the data to promote and display underlying patterns within the data. There are also two types of non-parametric learning techniques: unsupervised and supervised [52]. Unsupervised techniques make no prior assumptions about the sample classes but try to separate them in groups or clusters such as in cluster analysis (CA). In contrast, supervised techniques involve learning based on previous knowledge of the classification and examples include principal component analysis (PCA) and artificial neural network (ANN) techniques [52]. These techniques use optimal rules, algorithms or paradigms in order to classify and identify unknown samples.

1.4.1 Multiple Linear Regression (MLR)

The linear model employed for multiple linear regression (MLR) assumes that the dependent variable, Y, is a function of the k^{th} independent variable, X, in a given population and is represented by the following equation [53]:

$$Y_j = \alpha + \beta_1 X_1 + \beta_2 X_2 + \ldots\ldots\ldots \beta_k X_k + E \qquad (1.4)$$

where Y_j is the dependent variable for the j^{th} observation, α, β_1, β_2 and β_k are coefficients that represent the population parameters, X_1, X_2 and X_k are the independent variables, and E is the error term which represents deviations for Y_j from the mean distribution of the j^{th} observation. It is assumed that the relationship between the expected Y_j variable is linear for X_k and the effect of the k independent variables in equation 1.4 is an additive one [53].

MLR has been applied for the identification of gas mixtures consisting of carbon tetrachloride and ethyl methyl ketone from the response of a gas sensor array based on ZnO, SnO_2, MoO and CdS semiconductor sensors [54]. In this study, the independent variables were the composition of the gas mixtures and the dependent variables were the response of each

gas sensor in the array.

1.4.2 Partial Least Squares (PLS)

The partial least squares (PLS) method is a development of the PCA. PLS is a multivariate regression technique that models multiple independent variables (sensor responses) to one or more dependent variables (concentration), and this method calibrates one dependent variable at a time [55].

Calibration with the use of PLS is performed by decomposition of both the concentration, C, consisting of n mixtures (columns) and m components (rows) and sensor response, R, containing n columns and p sensors (rows) matrices into latent variables [55]:

$$C = F_C L_C + E_C \quad (1.5)$$

$$R = F_R L_R + E_R \quad (1.6)$$

where F_C is the latent concentration matrix with n rows (mixtures) and d columns (number of dimensions), L_C represents the concentration loading matrix with d rows and m columns (number of components), F_R is the n X d latent response matrix, L_R is the d X p response loading matrix (with p the number of sensors) and E_C and E_R are error matrices that have the same dimensions as the original concentration matrix (n X m) and response matrix (n X p), respectively. Relating the latent variable matrix from equation 1.5 to that in equation 1.6, a diagonal regression matrix V is given as [55]:

$$F_C = F_R V + E_d \quad (1.7)$$

where E_d is an error matrix. The matrix V is used in the prediction step for the estimation of the unknown concentrations (c_o) from the response of the sensors (rs_o) of a given sample as follows [55]:

$$c_o = r s_o (F_C R) V L_C \quad (1.8)$$

where the matrices F_C, L_C and R are determined from the calibration series.

In gas sensing, PLS has been used for the identification of ethyl acetate, acetone, ethanol and pentane solvents using an array of three tin-oxide gas sensors [56]. In a separate study PLS was used to analyse two and three component mixture sets of toluene, benzene, acetone and trichlorethylene using an array of eight Taguchi gas sensors [57].

1.4.3 Cluster Analysis (CA)

Many unsupervised pattern recognition techniques rely upon the principle of identifying groups or clusters of points within the data [52]. In cluster analysis (CA), points are grouped together according to their proximity in n-dimensional space. The general distance metric is given by [52]:

$$d_{ij} = \left(\sum_{K=1}^{N} \left(g_{ik} - g_{jk} \right)^{N} \right)^{1/N} \qquad (1.9)$$

where d_{ij} is the n-space Euclidean distance when N = 2. The proximity of the two points is defined in terms of a similarity value S_{ij} [52]:

$$S_{ij} = 1 - d_{ij} \Big/ \max\left(d_{ij}\right) \qquad (1.10)$$

where d_{ij} is the distance metric of data points i, j in n-dimensional vector space and max (d_{ij}) is its maximum value. The similarity value, or index, calculated in this manner is 0 for the two most distant points and 1.0 for two identical points [52]. There are many clustering techniques developed including hierarchical techniques, the K-means algorithm and fuzzy clustering. In hierarchical cluster analysis, every point is initially assumed to be a lone cluster. Therefore, for n points there are initially n clusters. Clusters which are 'close' together are then merged to reduce the total number of clusters. This can be achieved in a number of ways depending upon the method chosen to determine the 'closeness' of two clusters. Some commonly applied methods include single linkage (nearest neighbour), complete linkage (furthest neighbour),

centroid, median and group average [52]. In single linkage the closeness of two clusters is determined by the distance between the nearest pair of points, one from each cluster. In complete linkage the distance between the furthest pair of points is used. These two methods are the simplest since they only use one point from each cluster [52]. The more sophisticated centroid, median or group average methods use all the points within each cluster. In each of these cases the appropriate parameter is first calculated for each cluster and the distance between pairs of resulting values is then used to calculate the similarity or nearest index [52].

CA can be applied to the response matrix of a gas sensor array in order to compute the similarity indices for either the sensors or the measurands. In gas sensing CA has been applied to the response of a coated piezoelectric quartz sensor array [58] and SAW devices [59,60].

1.4.4 Principal Component Analysis (PCA)

Principal component analysis (PCA) is a powerful linear supervised learning pattern recognition technique that is usually applied in conjunction with cluster analysis [52]. The objective of PCA is to take the n variables g_r which define the rows of the response matrix, G, (these might be the responses of a given sensor to different gas component or the response of different sensors to a given gas component) and to find combinations of these which produce n indices X_r (the principal components) which are uncorrelated. Therefore, the response vectors are expressed in terms of linear combinations of orthogonal vectors. The indices X_r are ordered so that X_1 displays the greatest amount of variation, X_2 the next greatest and so on. If the original data set were uncorrelated to begin with, then this type of analysis is meaningless [52].

The first principal component X_1 is calculated as a linear combination of the response vectors g_i for n variables and p individuals [52]:

$$X_1 = a_{11} g_1 + a_{21} g_2 + \ldots + a_{n1} g_n \qquad (1.11)$$

such that the variance of X_1 is as large as possible under the constraint that [52]:

$$\sum_{i=1}^{n} a_{ir} = 1 \qquad (1.12)$$

The second principal component X_2 is then calculated in a similar manner but subject to the additional constraint that it is uncorrelated with X_1. The analysis proceeds in this way for each additional component, subject to the constraint that each new component is uncorrelated with any of the previous components. The coefficients a_{ir} are the elements of the orthogonal vectors, or eigenvectors, determined so that the maximum information in the form of variance or eigenvalue is preserved with the minimum number of eigenvectors. PCA essentially removes any redundancy or correlation that exists within the response data [52].

In gas sensing, PCA has been employed to analyse the response of seven coated piezoelectric element arrays using seven components [61]. The work was later extended to analyse the response of 27 piezoelectric sensing elements using 14 components [58]. Similar work has been carried out to characterise the response of gas sensitive SAW device arrays [59,60].

1.4.5 Artificial Neural Networks (ANN's)

Artificial Neural Networks (ANN's) is a pattern recognition technique employed for complex non-linear data and are formed from numerous simulated neurons that are connected in much the same way as the human brain's neurons and are thus capable of learning in a similar manner as humans [62]. ANN's use a highly interconnected group of neurons that process information in parallel. The human brain is a complex biological network of billions of highly interconnected cells called neurons. These cells receive information from as many as 10,000 other cells and send signals to other cells based upon the incoming signal pattern. The exact mechanism by which thought arises from these neuron signals is still unknown [62]. However, enough is known about the human brain to be able to mimic some of its abilities, such as learning, pattern recognition and generalisation [62]. Figure 1.14 illustrates the similarities of a biological and an artificial neuron.

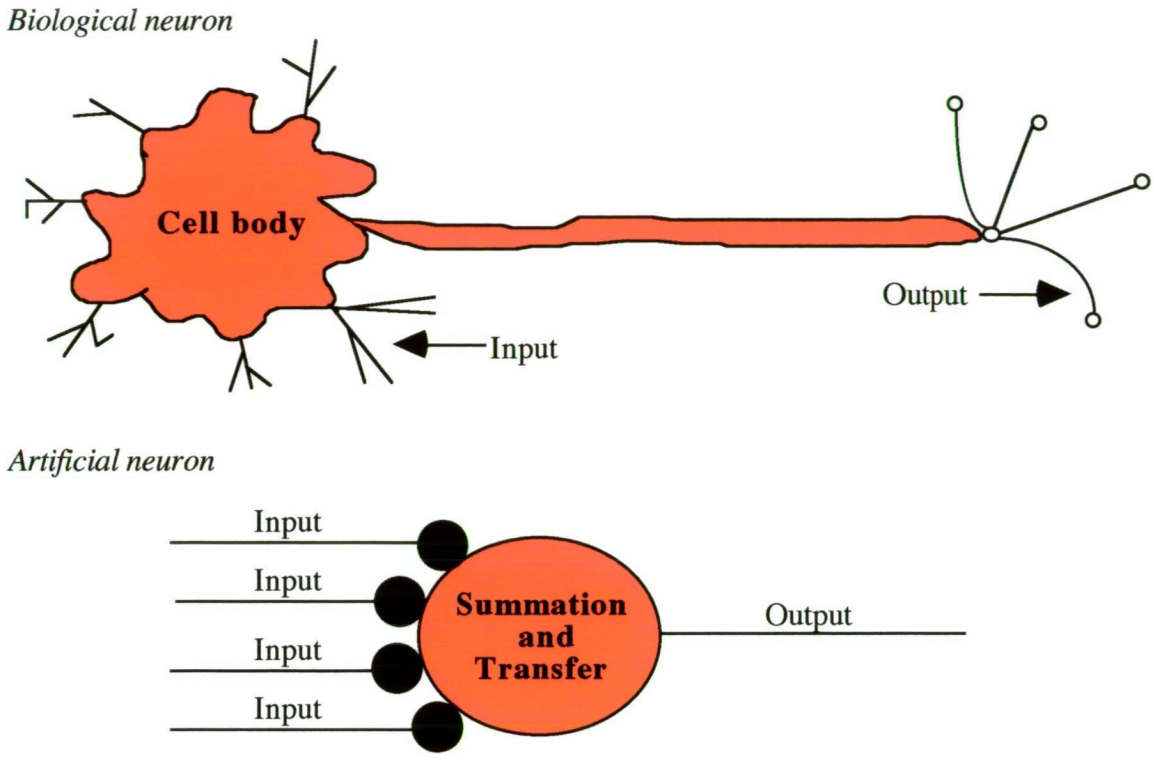

Figure 1.14. Illustrates the similarities between a biological and an artificial neuron.

A neuron in the brain has four basic parts: the body, the incoming channels, the outgoing channel and the connecting points between the neurons, which are called synapses. A neuron receives many signals from other neurons at the synapses. In the synapses, some processing occurs before the signals are sent down the incoming channels to the neuron body.

The synapses attach "weights" to incoming signals so that each of the signals will have a different effect on the neuron. A synapse can "turn up" or "turn down" the volume of a signal so that it has a stronger or weaker effect on the receiving neuron than other signals do [62]. The synapses change over time as signals are received and this constitutes learning and knowledge is "captured" in bits and pieces by the weights synapses attached to incoming signals.

1.4.5.1 Neurons

Both biological and artificial neural networks contain neurons, real or simulated. These neurons have many connections to each other which transfer information. The knowledge of a network is distributed across the interconnections between the neurons, not as bits of

intelligence stored within the neurons [62].

Artificial neurons are also called processing elements, nodes, units or cells. Each neuron receives the output signals from many other neurons. A neuron calculates its own output by finding the weighted sum of its inputs, generating an activation level and passing that through an output or transfer function. The point where two neurons communicate is called a connection (analogous to a synapse). The strength of the connection between two neurons is called a weight. The collection of weights arranged in rows and columns is called the weight matrix [62].

1.4.5.2 Layers

An ANN consists of three layers of neurons which are connected to each other: the input layer, the output layer and the hidden layer. The input neurons receive data from the outside world, such as from a digitising pad, a data file or another program. The input layer neurons send information to the hidden layer neurons. The hidden neurons are all the neurons in between the input and output layers. Their inputs and outputs can not be seen as they connect only to other neurons. The output neurons provide us with the neural network's response to the input data [62]. A typical structure of a simple neural network is shown in Figure 1.15.

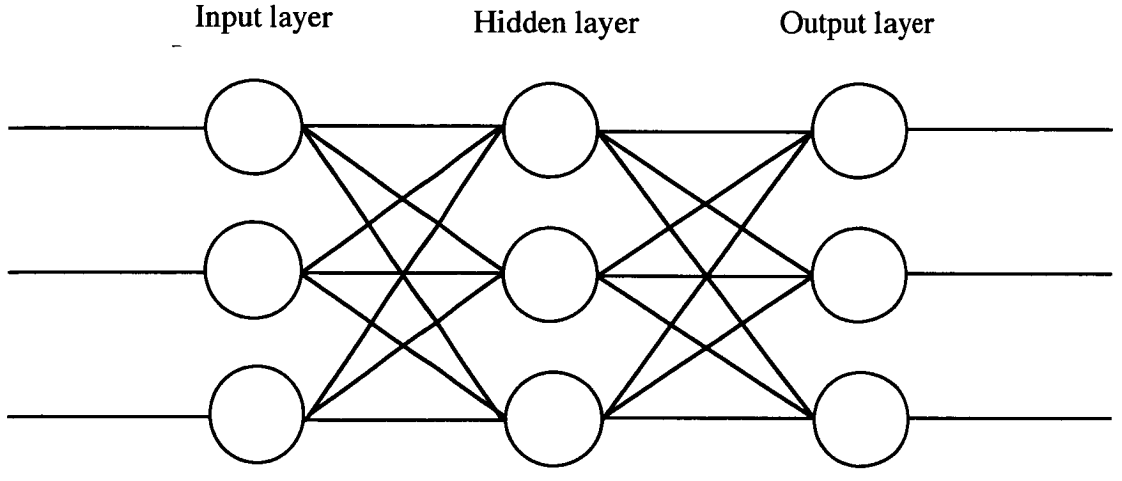

Figure 1.15. Typical structure of a simple neural network.

1.4.5.3 Connections

A connection is a unique line of communication that goes from one sending neuron to

one receiving neuron. There are two types of connections going to a neuron: excitatory and inhibitory. Inhibitory connections tend to prevent the activity, whereas excitatory connections tend to cause the activity of the neuron [62].

The network structure may involve inhibitory connections from one neuron to the rest of the neurons in the same layer. This is called lateral inhibition. Sometimes a network has such strong lateral inhibition that only one neuron in a layer, usually the output layer, can be activated at a time. This effect of minimising the number of active neurons is one type of competition.

The way in which the neurons are connected to each other has an enormous effect on the operation of the network. Specifying the connections determines the type of processing that will occur. Connections may go from the output of one layer to the input of a previous layer, or to the same layer. This is known as feedback [62]. The most common type of feedback model connects every neuron to every other neuron.

An ANN built with today's technology has very few connections compared to the number of connections in the brain. The human brain has about one hundred billion neurons and ten million billion connections. Most problems can be solved by an ANN with less than 500 neurons and 30,000 connections. It is likely that the brain also has many smaller neural networks in this size range that solve pieces of problems, with higher level networks that bring the pieces together [62].

1.4.5.4 Learning Methods

An ANN learns by changing its response as the inputs change. ANN's developed to date are associators. That is, they learn that pairs of things go together. For example, 'green' goes with 'go' and 'red' goes with 'stop'. The learning rule is the very heart of a neural network; it determines how the weights are adjusted as the neural network gains experience (trains) [62].

There are many different learning rules namely Hebb's Rule, the Delta Rule and the Back Propagation Rule. Back propagation is a supervised learning scheme by which a layered feed forward network is trained to become a pattern matching engine [62].

1.4.5.5 Transfer Functions

Neurons process input and produce output. Each neuron in the hidden layer will sum up all the inputs and then transform the sum by a sigmoidal non linear transfer function, similar to that illustrated in Figure 1.16.

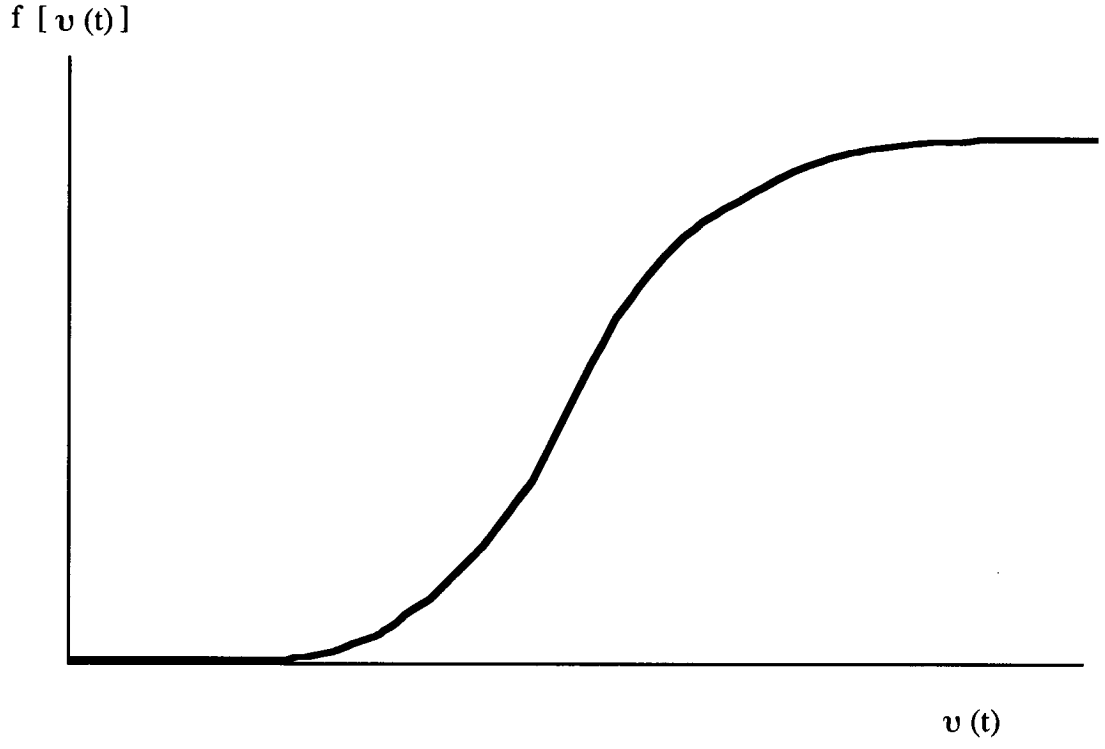

Figure 1.16. A sigmoidal transfer function.

The output of the i^{th} hidden neuron in the l^{th} layer, $x^{l}_{i}(t)$ can be expressed as follows [62]:

$$x^{l}_{i}(t) = f(\upsilon^{l}_{i}(t)), \quad l = 1,2,\ldots., m, \quad i = 1,2,\ldots.n_{l} \qquad (1.13)$$

where n_l is the size of layer l and $f(\upsilon(t))$ is the non-linear sigmoidal function,

$$f(\upsilon(t)) = 1 / (1 + e^{-\upsilon(t)}) \qquad (1.14)$$

and

$$\upsilon^{l}_{i}(t) = \sum_{j=1}^{n_l - 1} w^{l}_{ij}\, x^{l-1}_{j}(t) + b^{l}_{i} \qquad (1.15)$$

where b is the network threshold, w^{l}_{ij} is the weight connection between the j^{th} neuron of the (l - 1)th layer and the i^{th} neuron of the l^{th} layer and $n_l - 1$ is the number of neurons in the (l - 1)th layer. When combining equations 1.13 and 1.15, the output of each neuron can be expressed as:

$$x^{l}_{i}(t) = f\left(\sum_{j=1}^{n_l - 1} w^{l}_{ij}\, x^{l-1}_{j}(t) + b^{l}_{i}\right) \qquad (1.16)$$

In ANN, the neuron in the output layer is normally considered to be the same as for the neurons in the hidden layer, however this will limit the dynamic range of the output neurons to be ≤ 1.0.

The aim of training a ANN is to determine the predicted output to as close to the desired output as possible.

1.5 Objectives of this Research

The objectives of the research undertaken were as follows:

1) to develop and evaluate the viability of a portable battery-powered gas analyser employing two different Taguchi tin-oxide sensors, in terms of stability, sensitivity, selectivity and reproducibility,

2) to determine the ethanol content in various commercial liquor samples employing the above mentioned gas analyser,

3) to evaluate the viability of a portable battery-powered six-sensor gas analyser in terms of stability, sensitivity, selectivity and reproducibility and,

4) to apply the ethanol response pattern to discriminate between various beer brands and to determine the ethanol content of commercial beer samples.

5) to establish whether the above mentioned multi-sensor gas analyser together with a three-layer artificial neural network technique using the back propagation model could be trained successfully to recognise various beer and olive oil samples.

In Chapter two, the application is described of two commercial Taguchi sensors

employed in a portable battery-powered gas analyser. The performance of the sensors was evaluated in terms of stability, sensitivity, selectivity and reproducibility. The ethanol content of commercial liquor samples was determined.

In Chapter three, six Taguchi semiconductor sensors arranged in an array and employed in a portable battery-powered gas analyser is described. The performance of the six sensor array was studied and validation of this analyser was performed with various ethanol standard solutions. The response pattern of ethanol is used to discriminate between various beer samples.

In Chapter four, a method employing the above mentioned multi-sensor gas analyser together with an artificial neural network to discriminate between six different beer brands is described. The artificial neural network employed was based a back propagation model, employing a three layer network.

Chapter five describes the strategies to discriminate between different varieties of olive oils and determine the age of the individual olive oils. Similar to Chapter four, an artificial neural network based on the back propagation model will be employed.

1.6 References

1. P. Hauptmann, 'Sensors: Principles and Applications', Carl Hanser Verlag, (1991).

2. S. J. Gentry, 'Catalytic Devices' in T. E. Edmonds, Chemical Sensors, Chapman and Hall, New York, (1988).

3. S. J. Gentry and P. T. Walsh, 'Poison-Resistant Catalytic Flammable-Gas Sensing Elements', Sensors and Actuators, **5**, 239-251, (1984).

4. S. J. Gentry and A. Jones, 'Poisoning and Inhibition of Catalytic Oxidations 1. The Effect of Silicone Vapour on the Gas-Phase Oxidations of Methane, Propene, Carbon Monoxide and Hydrogen over Platinum and Palladium Catalysts', Journal of Applied Chemical Biotechnology, **28**, 727-732, (1978).

5. W. H. King, Jr., 'Piezoelectric Sorption Detector', Analytical Chemistry, **36**, 1735-1739, (1964).

6. K. H. Karmarkar and G. G. Guilbault, 'The Detection of Ammonia and Nitrogen Dioxide at the Parts Per Billion Level with Coated Piezoelectric Crystal Detectors', Analytica Chimica Acta, **75**, 111-117, (1975).

7. M. H. Ho, G. G. Guilbault and E. P. Scheide, 'Detection of Carbon Monoxide in Ambient Air with a Piezoelectric Crystal', Analytical Chemistry, **54**, 1998-2002, (1982).

8. J. Hlavay and G. G. Guilbault, 'Detection of Hydrogen Chloride Gas in Ambient Air with a Coated Piezoelectric Quartz Crystal', Analytical Chemistry, **50**, 965-967, (1978).

9. J. L. Cheney and J. B. Homolya, 'A Systematic Approach for the Evaluation of Triethanolamine as a Possible Sulfur Dioxide Sorption Detector Coating', Analytical Letters, **8**, 175-193, (1975).

10. J. Kristoff and G. G. Guilbault, 'Application of Uncoated Piezoelectric Crystals for the Detection of an Organic Phosphonate', Analytica Chimica Acta, **149**, 337-341, (1983).

11. Y. Tomita, M. H. Ho and G. G. Guilbault, 'Detection of Explosives with a Coated Piezoelectric Quartz Crystal', Analytical Chemistry, **51**, 1475-1478, (1979).

12. M. H. Ho, 'Applications of Quartz Crystal Microbalances in Aerosol Mass Measurement' in C. Lu and A. W. Czanderna, Applications of Piezoelectric Quartz Crystal Microbalances, Volume 7, Elsevier, Amsterdam, (1984).

13. A. D' Amico and E. Verona, 'SAW Sensors', Sensors and Actuators, **17**, 55-66, (1989).

14. E. T. Zellers, N. Hassold, R. M. White and S. M. Rappaport, 'Selective Real-Time Measurement of Styrene Vapor using a Surface-Acoustic-Wave Sensor with a Regenerable Organoplatinum Coating', Analytical Chemistry, **62**, 1227-1232, (1990).

15. M. S. Nieuwenhuizen and A. J. Nederlof, 'A SAW Gas Sensor for Carbon Dioxide and Water. Preliminary Experiments', Sensors and Actuators B, **2**, 97-101, (1990).

16. M. S. Nieuwenhuizen and A. J. Nederlof, 'Surface Acoustic Wave Gas Sensor for Nitrogen Dioxide using Phthalocyanines as Chemical Interfaces. Effect of Nitric Oxide, Halogen Gases, and Prolonged Heat Treatment', Analytical Chemistry, **60**, 236-240, (1988).

17. C. Preininger, I. Klimant and O. S. Wolfbeis, 'Optical Fiber Sensor for Biological Oxygen Demand', Analytical Chemistry, **66**, 1841-1846, (1994).

18. M. A. Arnold and T. J. Ostler, 'Fiber Optic Ammonia Gas Sensing Probe', Analytical Chemistry, **58**, 1137-1140, (1986).

19. Z. Zhujun and W. R. Seitz, 'A Carbon Dioxide Sensor Based on Fluorescence', Analytica Chimica Acta, **160**, 305-309, (1984).

20. Z. Zhujun and W. R. Seitz, 'Optical Sensor for Oxygen Based on Immobilized Hemoglobin', Analytical Chemistry, **58**, 220-222, (1986).

21. B. H. Weigl, PhD Thesis, 'Design and Characterization of Opto-Chemical Sensor Modules for Measurement of Carbon Dioxide', Karl-Franzens-UniversitSt Graz, (1993).

22. J. W. Severinghaus and A. F. Bradley, 'Electrodes for Blood pO_2 and pCO_2 Determination', Journal of Applied Physiology, **13**, 515-520, (1957).

23. J. Wang, 'Analytical Electrochemistry', VCH Publishers, New York, (1994).

24. M. E. Meyerhoff, 'Polymer Membrane Electrode Based Potentiometric Ammonia Gas Sensor', Analytical Chemistry, **52**, 1532-1534, (1980).

25. J. Langmaier and J. Janata, 'Sensitive Layer for Electrochemical Detection of Hydrogen Cyanide', Analytical Chemistry, **64**, 523-527, (1992).

26. J. W. Ross, J. H. Riseman and J. A. Krueger, 'Potentiometric Gas Sensing Electrodes',

Pure Applied Chemistry, **36**, 473-487, (1973).

27. L. C. Clark, Jr., R. Wolf, D. Granger and Z. Taylor, 'Continuous Recording of Blood Oxygen Tensions by Polarography', Journal of Applied Physiology, **6**, 189-193, (1953).

28. G. Alberti, F. Cherubini and R. Palombari, 'Amperometric Solid-State Sensor for NO and NO_2 Based on Protonic Conduction', Sensors and Actuators B, **37**, 131-134, (1996).

29. T. Ishiji, K. Takahashi and A. Kira, 'Amperometric Carbon Dioxide Gas Sensor Based on Electrode Reduction of Platinum Oxide', Analytical Chemistry, **65**, 2736-2739, (1993).

30. J. Janata, 'Principles of Chemical Sensors', Plenum Press, New York, (1989).

31. D. R. Bull, G. J. Harris and A. B. Ben Rashed, 'A Connectionist Approach to Fuel Cell Sensor Array Processing for Gas Discrimination', Sensors and Actuators B, **15-16**, 151-161, (1993).

32. R. F. Taylor and J. S. Schultz, 'Handbook of Chemical and Biological Sensors' in B. Hoffheins, Solid State, Resistive Gas Sensors, Institute of Physics Publishing, Bristol, (1996).

33. W. Gopel, 'Chemisorption and Charge Transfer at Ionic Semiconductor Surfaces: Implications in Designing Gas sensors', Progress in Surface Science, **20**, 9-103, (1985).

34. G. Heiland and P. Kohl, 'Problems and Possibilities of Oxidic and Organic Semiconductor Gas Sensors', Sensors and Actuators, **8**, 227-233, (1985).

35. A. Chiba, 'Development of the TGS Gas Sensor', Chemical Sensors and Technology, **4**, 1-18, (1992).

36. Figaro Engineering Inc., 'Figaro Gas Sensors', Product Document, Osaka, August, (1990).

37. K. Ihokura, 'The Effects of Crystallite Size of Sintered Tin-Dioxide on Changes of Electric Conductivity in Deoxidizable Gases', Journal of Electrochemical Society of Japan, **50**, 99-104, (1982).

38. K. D. Biddle, A. K. Das, K. Jones and H. G. Emblem, 'The Chemistry of Ethyl Silicate Binders in Refractory Technology', Journal of Applied Chemical Biotechnology, **27**, 565-573, (1977).

39. D. Diamond, 'Progress in Sensor Array Research', Electroanalysis, **5**, 795-802, (1993).

40. K. D. Schierbaum, U. Weimar and W. Gopel, 'Multicomponent Gas Analysis: An Analytical Chemistry Approach Applied to Modified SnO_2 Sensors', Sensors and Actuators B, **2**, 71-78, (1990).

41. H. V. Shurmer, J. W. Gardner and H. T. Chan, 'The Application of Discrimination Techniques to Alcohols and Tobaccos using Tin-Oxide Sensors', Sensors and Actuators, **18**, 361-371, (1989).

42. J. Mizsei, 'Response Pattern of SnO2 Sensor System for Smoke of Different Origins', Sensors and Actuators B, **18-19**, 264-267, (1994).

43. C. Di Natale, F. A. M. Davide, A. D' Amico, W. Gopel and U. Weimar, 'Sensor Arrays Calibration with Enhanced Neural Networks', Sensors and Actuators B, **18-19**, 654-657, (1994).

44. J. W. Gardner, H. V. Shurmer and T. T. Tan, 'Application of an Electronic Nose to the Discrimination of Coffees', Sensors and Actuators B, **6**, 71-75, (1992).

45. K. N. Andrew, N. J. Blundell, D. Price and P. J. Worsfold, 'Flow Injection Techniques for Water Monitoring', Analytical Chemistry, **13**, 252-299, (1994).

46. H. L. C. Meuzelaar, Ed., 'Special Issue on: Field Portable Analytical Instrumentation', Trends in Analytical Chemistry, **13**, 252-299, (1994).

47. E. B. Overton and K. R. Carney, 'New Horizons in Gas Chromatography: Field Applications of Microminiaturized Gas Chromatographic Techniques', Trends in Analytical Chemistry, **13**, 252-257, (1994).

48. P. I. Richter, 'Air Pollution Monitoring with LIDAR', Trends in Analytical Chemistry, **13**, 263-266, (1994).

49. G. Baykut and J. Franzen, 'Mobile Mass Spectrometry; A Decade of Field Applications', Trends in Analytical Chemistry, **13**, 267-275, (1994).

50. R. B. Turner and J. L. Brokenshire, 'Hand-Held Ion Mobility Spectrometers', Trends in Analytical Chemistry, **13**, 275-280, (1994).

51. S. Piorek, 'Principles and Applications of Man-Portable X-Ray Fluorescence Spectrometry', Trends in Analytical Chemistry, **13**, 281-286, (1994).

52. J. W. Gardner and P. N. Bartlett, 'Pattern Recognition in Gas Sensing', in P. T. Moseley, J. O. W. Norris and D. E. Williams, Techniques and Mechanisms in Gas Sensing, Adam Hilger, Bristol, (1991).

53. W. D. Berry and S. Feldman, 'Multiple Regression in Practice', Sage Publications, Newbury Park, (1985).

54. M. S. Nayak, R. Dwivedi and S. K. Srivastava, 'Application of Iteration Technique in Association with Multiple Regression Method for Identification of Mixtures of Gases using an Integrated Gas-Sensor Array', Sensors and Actuators B, **21**, 11-16, (1994).

55. P. Geladi and B. R. Kowalski, 'Partial Least-Squares Regression: A Tutorial', Analytica Chimica Acta, **185**, 1-17, (1986).

56. A. D. Walmsley, S. J. Haswell and E. Metcalfe, 'Evaluation of Chemometric Techniques for the Identification and Quantification of Solvent Mixtures using a Thin-Film Metal Oxide Sensor Array', Analytica Chimica Acta, **250**, 257-264, (1991).

57. W. P. Carey and S. S. Yee, 'Calibration of Nonlinear Solid-State Sensor Arrays using Multivariate Regression Techniques', Sensors and Actuators B, **9**, 113-122, (1992).

58. W. P. Carey, K. R. Beebe, B. R. Kowalski, D. L. Illman and T. Hirschfeld, 'Selection of Adsorbates for Chemical Sensor Arrays by Pattern Recognition', Analytical Chemistry, **58**, 149-153, (1986).

59. D. S. Ballantine, Jr., S. L. Rose, J. W. Grate and H. Wohltjen, 'Correlation of Surface Acoustic Wave Device Coating Responses with Solubility Properties and Chemical Structure using Pattern Recognition', Analytical Chemistry, **58**, 3058-3066, (1986).

60. S. L. Rose-Pehrsson, J. W. Grate, D. S. Ballantine, Jr., and P. C. Jurs, 'Detection of Hazardous Vapors Including Mixtures using Pattern Recognition Analysis of Responses from Surface Acoustic Wave Devices', Analytical Chemistry, **60**, 2801-2811, (1988).

61. W. P. Carey and B. R. Kowalski, 'Chemical Piezoelectric Sensor and Sensor Array

Characterization', Analytical Chemistry, **58**, 3077-3084, (1986).

62. J. Lawrence, 'Introduction to Neural Networks', California Scientific Software Press, Nevada City, (1994).

Chapter Two: Development and Evaluation of a Portable Battery-Powered Flow-Through Analyser Employing Two Tin-Oxide Gas Sensors for Alcohols

2.1 Introduction

This chapter is concerned with the development and evaluation of a portable battery-powered gas analyser suitable for remote site monitoring. This portable gas analyser was evaluated with two Taguchi tin-oxide gas sensors in an array.

The use of portable instrumentation for chemical analysis is of increasing interest, and has been reviewed recently for monitoring of both liquid [1] and gas analysers [2]. Portable analysers allows chemical analysis to be performed outside conventional laboratory limits. In gas analysis, advances have occurred in many instrumental areas including gas chromatography [3], gas chromatography with mass spectroscopy [4], infrared spectroscopy [5], laser induced radar spectroscopy [6], ion mobility spectroscopy [7] and X-ray fluorescence spectroscopy [8]. However, there is still a need for portable analysers which are battery-powered and of light weight for use in field monitoring at remote locations.

There are many gas sensors available commercially including catalytic gas sensors, piezoelectric and surface acoustic wave sensors, optical gas sensors, electrochemical sensors and conductimetric gas sensors such as semiconductor metal oxide sensors. Taguchi gas sensors (TGS) produced by the Japanese company, Figaro Engineering Inc [9,10] have been available for many years. They are based on sintered powdered tin dioxide and are known to respond to various gases and vapours including hydrogen, carbon monoxide, methane, ethane, propane, alcohols and hydrocarbons [9,10]. A model electronic nose was first described by Persaud and Dodd [11], who showed that a system incorporating three broadly-tuned tin-oxide gas sensors could provide discrimination between chemically similar odours.

The design of a 12-element conducting polymer chemoresistor based electronic nose was employed for monitoring the flavour of lager beers [12]. This instrument relies upon the manual injection of an odorant into the chamber containing the sensor array. In a separate

study, the development of a multi-sensor array of 18 conducting polymers in an automated flow injection system with self-diagnostics was used for monitoring beer flavours [13]. The conducting polymers used in the above studies were based on polypyrrole membranes.

An array of three Taguchi tin-oxide gas sensors were used for the discrimination between methanol, ethanol and propan-2-ol as well as different blends of cigarette smoke [14]. A sensor array of four metal oxide based gas sensors was employed for the recognition of various wines, having the same denomination but coming from different vineyards [15]. In another study, tin-oxide gas sensors were used to determine the ethanol content of various wines [16].

This chapter describes the design and operation of a portable battery-powered gas analyser employing two different types of Taguchi tin-oxide sensors. The response of ethanol was used to evaluate the gas analyser in terms of reproducibility, stability and sensitivity. The portable gas analyser was used also to determine the ethanol content in various commercial liquor samples. The adsorption response mechanism of the tin-oxide gas sensors was investigated using the Langmuir adsorption isotherm model and will be discussed.

2.1.1 Langmuir Adsorption Isotherm Model for the Tin-Oxide Semiconductor Gas Sensors

There has been considerable interest shown concerning the mechanism of the non-linear response of these gas sensors to changes in gas or vapour concentrations [17-19]. The response to gases has been attributed to adsorption mechanisms in a number of publications mostly based on various adsorption isotherms [20-22].

The simplest description of the adsorption mechanism may be represented by a Langmuir isotherm [23,24], which will be considered in this study. The Langmuir isotherm is based on the assumption that every adsorption site is equivalent and that the ability of a molecule to bind on the surface of the sensor is independent of whether or not nearby sites are occupied [23,24]. When the gas is at a certain partial pressure above an aqueous solution containing the dissolved gas at a certain concentration (C), the fraction of the surface of the sensor that is covered by the gaseous molecules is defined as the extent of surface coverage (θ)

[23,24].

The response of these semiconductor sensors is dependent on the adsorbed oxygen on the tin-oxide surface reacting with ethanol, which is oxidised to acetaldehyde, as given below:

$$1/2\,O_2 + (SnO_2 + e^-) \longrightarrow SnO_2\,(O^-)_{ad}$$

$$CH_3CH_2OH + SnO_2\,(O^-)_{ad} \longrightarrow CH_3CHO + H_2O + (SnO_2 + e^-)$$

with rate constants k_a for adsorption and k_d for desorption. Therefore, the adsorption rate (R_a) is proportional to the concentration of the ethanol vapour and the number of unoccupied sites on the tin-oxide sensor surface, $N(1-\theta)$, as described by equation 2.1 [23,24]:

$$R_a = k_a C N (1 - \theta) \qquad (2.1)$$

and the desorption rate (R_d) of O_2 depends not only on the number of adsorbed O^- species, $N\theta$, but also on the concentration of the ethanol, which can be written as [23]:

$$R_d = k_d N \theta \qquad (2.2)$$

At equilibrium $R_a = R_d$, and the Langmuir equation is expressed as shown below [23,24]:

$$\theta = C / (a + C) \qquad (2.3)$$

where $a = k_a / k_d$ and θ can be expressed in terms of the amount of gas adsorbed (y) at a particular concentration and the amount of gas needed to form a monolayer coverage (y_m) on the surface of the sensor as [23,24]:

$$y / y_m = \theta \qquad (2.4)$$

The Langmuir equation can then be rearranged to give:

$$y = y_m C / (a + C) \qquad (2.5)$$

and this equation will be manipulated and discussed further in this chapter.

2.2 Experimental

2.2.1 Solutions and Samples

The standard ethanol solutions were made up in Ultrapure water (Barnstead Ultrapure water systems) by dilution of stock absolute ethanol (Ajax Chemicals, Analytical UNIVAR Reagent). Solutions in the concentration range 0.1 - 20% (v/v) were prepared in 100 mL volumetric flasks and used for head-space analysis at room temperature (22 ± 2 °C). The beer and wine samples used in this study were obtained commercially from local suppliers, and are listed below, with the labelled ethanol content in brackets: Light beer (2.7%), Normal beer (4.9%), White wine (10.0%) and Red wine (10.9%).

2.2.2 Design of the Portable Flow-Through Gas Analyser

The portable analyser was fitted with two Taguchi gas sensors (TGS), the TGS812 and the TGS824, obtained from Figaro Inc. (Osaka, Japan) [25] and built into a flow-through compartment. A schematic diagram of the portable gas analyser is given in Figure 2.1. The ethanol vapour of the standards and samples was pumped into the flow-through compartment using a diaphragm pump at a constant flow rate of 1 L / minute. Using a 5 seconds sampling time, a vapour volume of 83 mL was pumped from the head-space of the 100 mL flasks, which were open to the air. Therefore the dilution factor due to air intake was similar for all the standards and samples analysed. The sensors and pump were controlled by an electrical circuit that was powered with a rechargeable Ni-Cd battery pack of 7.2 V and 1.4 A hours output. The power required to operate the two Taguchi sensors and the pump was 3.6 W and the voltage output was displayed on an LCD unit of the monitor.

The data from each sensor were acquired using an 8-channel, 12-bit analog-to-digital converter (ADC) with a RS232C output to a serial port of a Macintosh PowerBook 150 computer. The ADC was built in the chemistry workshop at the University of Tasmania and a block diagram and circuit design are both presented in Appendix 1.

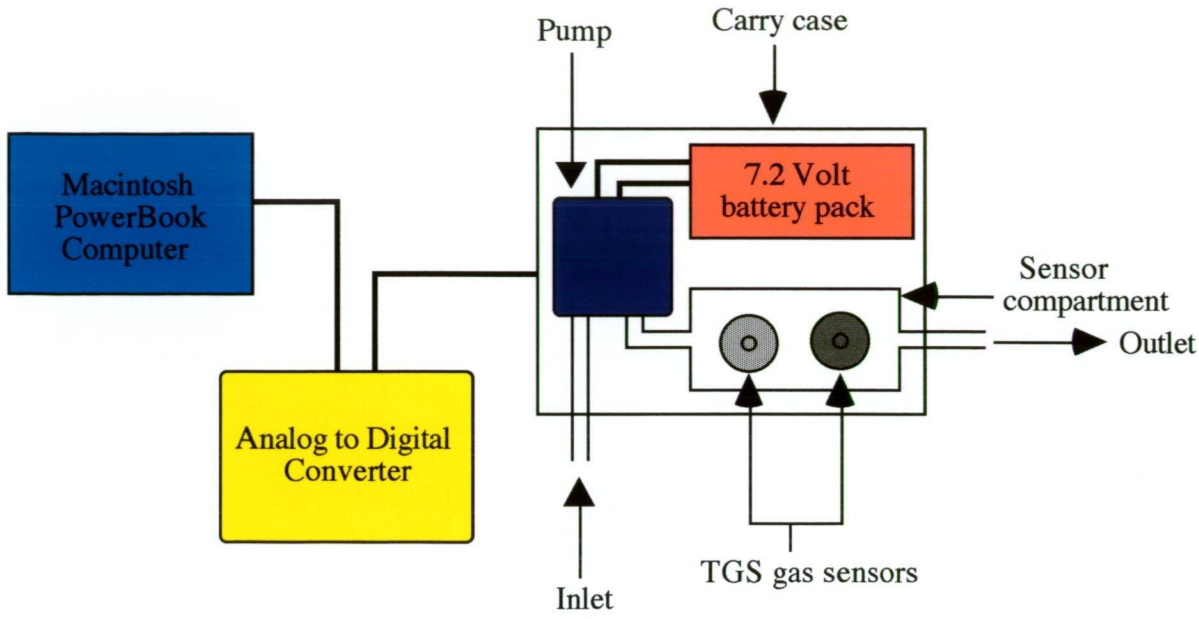

Figure 2.1. Schematic diagram of the portable battery-powered gas analyser employing the TGS812 and TGS824 gas sensors used in this study.

2.2.3 Gas Chromatography Instrumentation

A Perkin-Elmer Sigma 3 Gas Chromatograph with a Flame Ionisation Detector (FID) was used for the analysis of ethanol where nitrogen was employed as the carrier gas. A Chromosorb W column (length of 6 ft, 1/8 in. internal diameter) was used at a temperature of 70 °C. 0.5 μL sample injection volumes were used, using a SGE 1.0 μL syringe. The data collected were saved as text files and a software application called 'IGOR' (AD Instruments, Sydney, Australia) was used for data analysis.

2.2.4 Head-Space Analysis and Gas Chromatography Procedure

The tin-oxide semiconductor gas sensors were allowed to warm up by pumping air (carrier gas) through the analyser for 30 minutes prior to measurements to ensure a stable baseline was obtained. The standard ethanol solutions and samples were left standing at room temperature (22 ± 2 °C) for 2-3 hours to produce adequate head-space vapour. The ethanol solutions and samples were shaken prior to measurement in the 100 mL volumetric flasks and the sample inlet tube of the gas analyser was simply introduced into the head-space of the flasks. A vapour sample volume of 83 mL was pumped from the head-space of the 100 mL flasks into the flow-through compartment for a fixed period of 5 seconds at a constant

temperature and relative humidity. The response of each standard solution and sample for each sensor was recorded in duplicate, sampled from low to high ethanol concentration, displayed in real time millivolt readings and plotted as a function of time on the Macintosh PowerBook 150 computer screen using a data acquisition program called 'Satod' © Version 1.46. Satod was written by Dr J. Morgan (University of New South Wales, Sydney, Australia) in Think C for a Macintosh PowerBook computer and 'IGOR' was used for data analysis and graphical representation of the data.

MacCurve Fit © Version 0.7 was used to calculate the Langmuir isotherm constants and the standard deviations (95% confidence) of each gas sensor. This program was written and supplied by Dr Kevin Raner (CSIRO, Division of Chemicals and Polymers, Victoria, Australia).

For the gas chromatography analysis, the same ethanol standard solutions and samples were left standing at room temperature for 2-3 hours, in order to produce adequate head-space vapour. Sample injection volumes of 0.5 μL were used and the data collected were stored as text files.

2.3 Results and Discussion

2.3.1 Design of the Portable Gas Analyser

The TGS812 and the TGS824 Taguchi tin-oxide semiconductor gas sensors were arranged in a flow-through compartment as described previously in this chapter, Section 2.2.2, whereby the gas or vapour sample was pumped over the surface of the sensors. The major advantage of this arrangement is that it allows for a minimal exposure of the sensors to the gas sample and thus minimises the chance of poisoning the sensor's surface.

The TGS series are sintered n-type semiconductor bulk devices mainly composed of tin dioxide. These Taguchi sensors have a heater in an alumina ceramic tube and the semiconductor material is mounted on the tube with two printed gold electrodes. The TGS812 sensor type has a polyamide resin base whereas the TGS824 type has a heat resistant ceramic base and are reported to be more sensitive to combustible gases and ammonia, respectively [25]. These TGS gas sensors were used because they are reported to be the most suitable

commercial sensors available at present [26]. The sensor elements were protected by a plastic housing with two flame arresters of stainless steel double-gauze on the top and bottom. The advantages of these Taguchi sensors include, a long life-time and good reliability, high sensitivity, highly resistant to poisoning, compact in size (up to 19.5 mm internal diameter), easy to install, excellent durability and shock proof and inexpensive [25].

The portable gas analyser is small in size (20 x 11 x 6 cm), light weight (1.1 kg), requires low power consumption (3.6 W) and is connected to a Macintosh PowerBook computer for real-time display of data and data acquisition. The gas analyser was in continuous operation for 4 hours before recharging was necessary. Photographs of the entire portable gas analyser and the internal electronic circuitry are presented in Figure 2.2 and Figure 2.3.

(A)

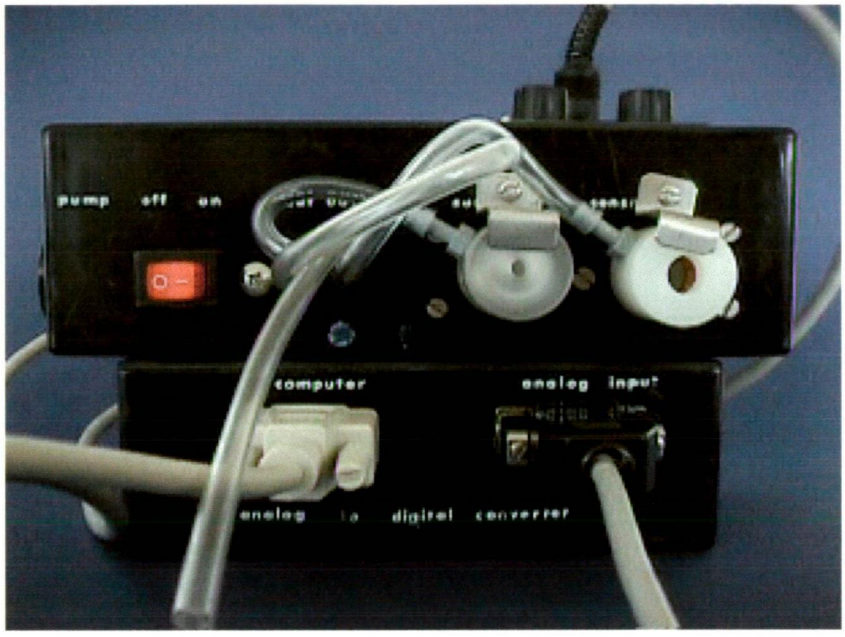

(B)

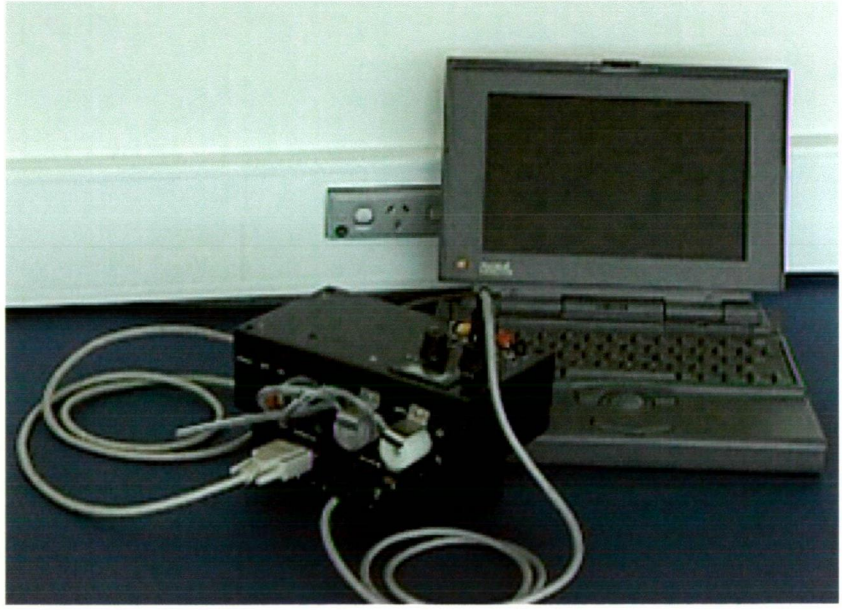

Figure 2.2. Photographs of (A) the portable gas analyser and the analog-to-digital converter and (B) the portable gas analyser and analog-to-digital converter connected to a Macintosh PowerBook computer.

(A)

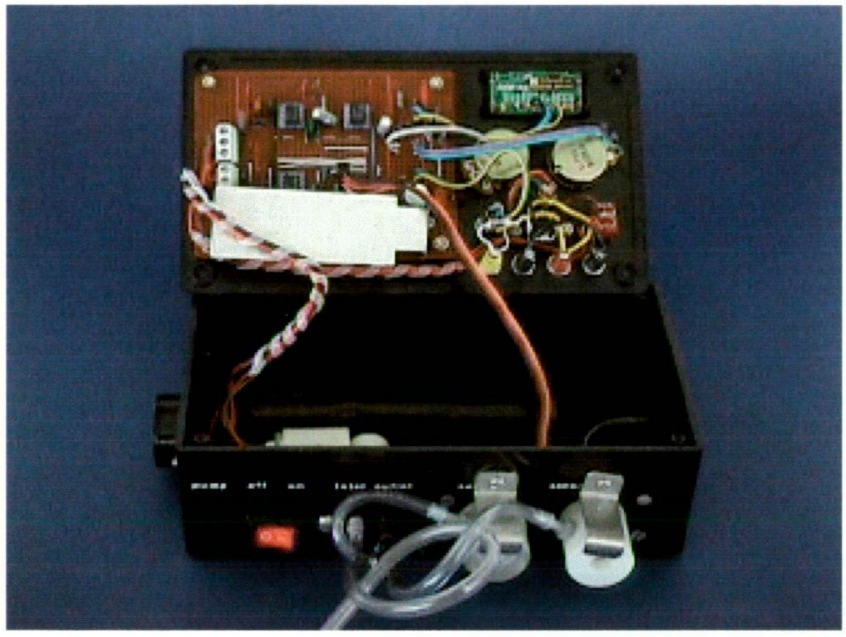

(B)

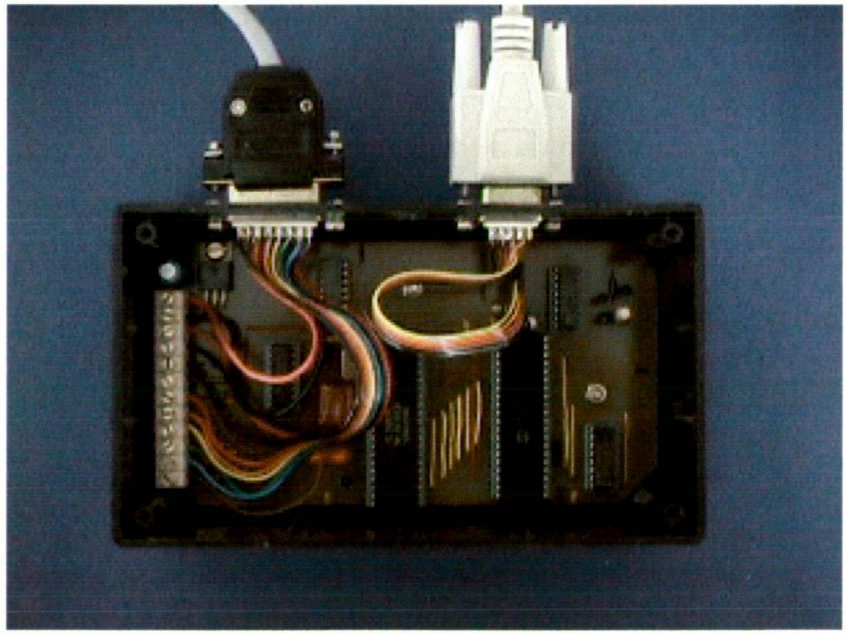

Figure 2.3. Photographs of the circuitry of (A) the portable flow-through gas analyser and (B) the analog-to-digital converter.

2.3.2 Response to Ethanol

The voltage response of each sensor in the presence of ethanol is dependent on the change in electrical resistance when ethanol is adsorbed on the sensor surface. An example of typical ethanol peak responses in duplicate observed by the TGS812 and TGS824 gas sensors are given in Figure 2.4. Figure 2.4, shows that the peak height response range was between 0 and 3.8 V and 0 and 3.2 V for the TGS812 and the TGS824 sensors, respectively. Therefore, the TGS812 sensor was observed to be more sensitive towards changes in ethanol concentrations than the TGS824 type sensor. However, both sensors showed a rapid response with peak widths of approximately 30 seconds for a 5 seconds sampling time at 1 L / minute flow rate.

Calibration plots for the TGS812 and TGS824 sensors for ethanol are presented in Figure 2.5. These sensors exhibited a non-linear response to ethanol, however both sensors showed no loss of activity and no baseline drift during the course of the study.

The precision of replicate peak heights recorded simultaneously for the TGS812 and the TGS824 sensors after sampling the same ethanol solution is presented in Figure 2.6. A relative standard deviation (RSD) of < 3% was observed for a 1% ethanol standard solution for both gas sensors. For replicate measurements of the 10% ethanol solution, the RSD values for the TGS812 and TGS824 sensors were 0.5% and 1.6%, respectively. These tin-oxide sensors are known to be limited by the lack of stability, sensitivity and reproducibility [27]. However, the results presented in this chapter demonstrate that TGS812 and TGS824 tin-oxide gas sensors in a flow-through arrangement, exhibit high stability, sensitivity and reproducibility.

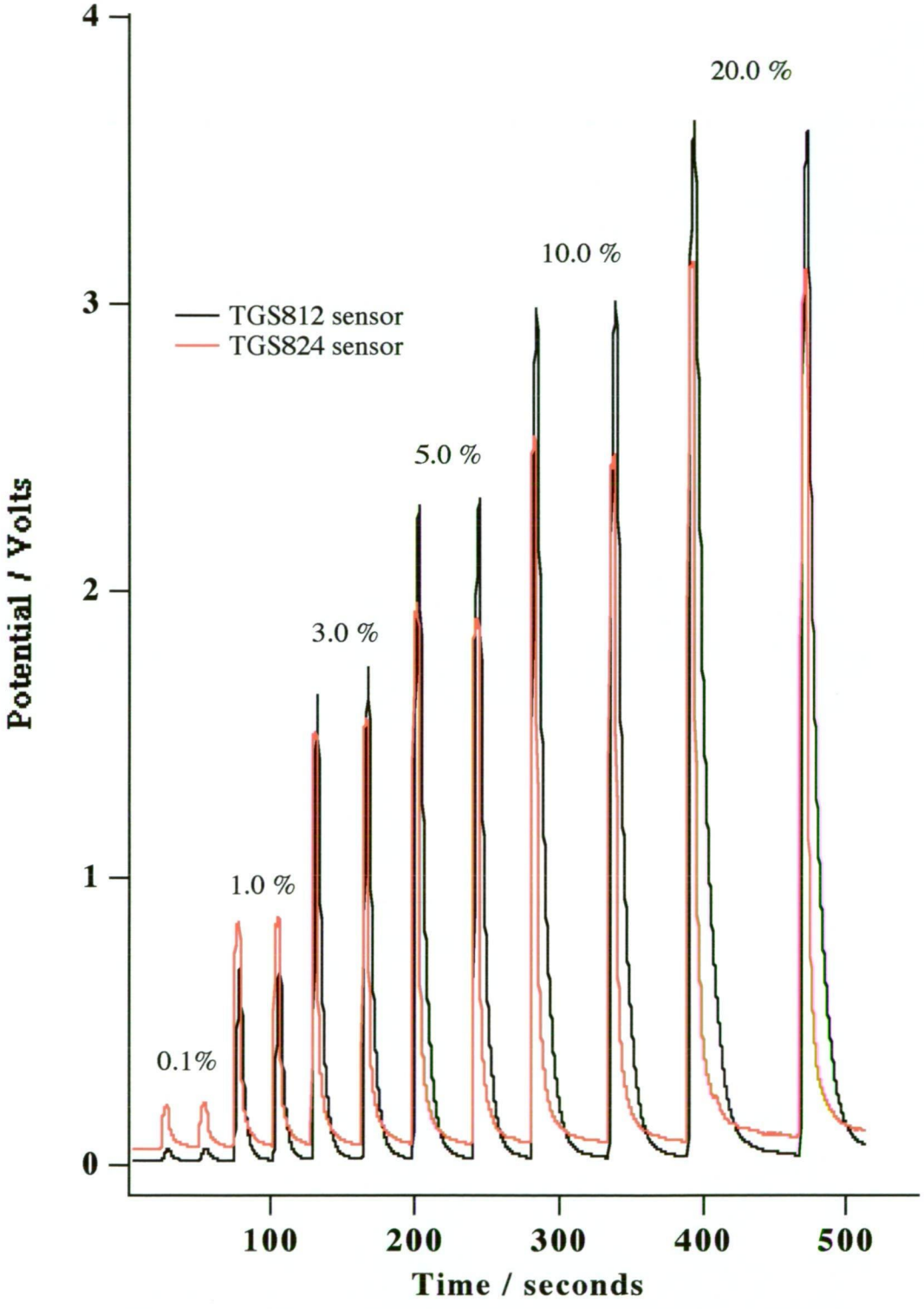

Figure 2.4. Sample peaks for increasing concentrations of ethanol.

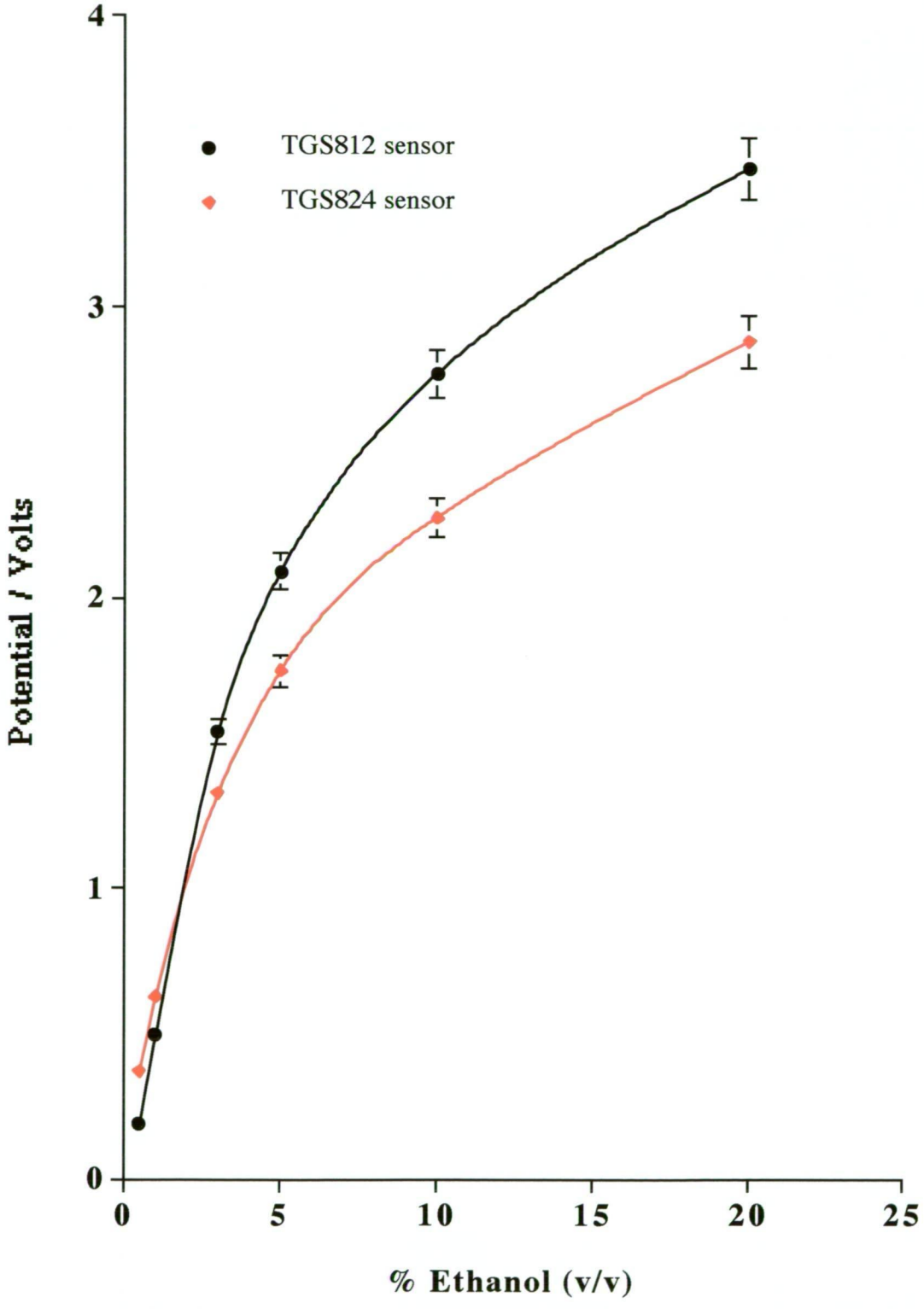

Figure 2.5. Calibration plots for the TGS812 and TGS824 gas sensor responses to ethanol.

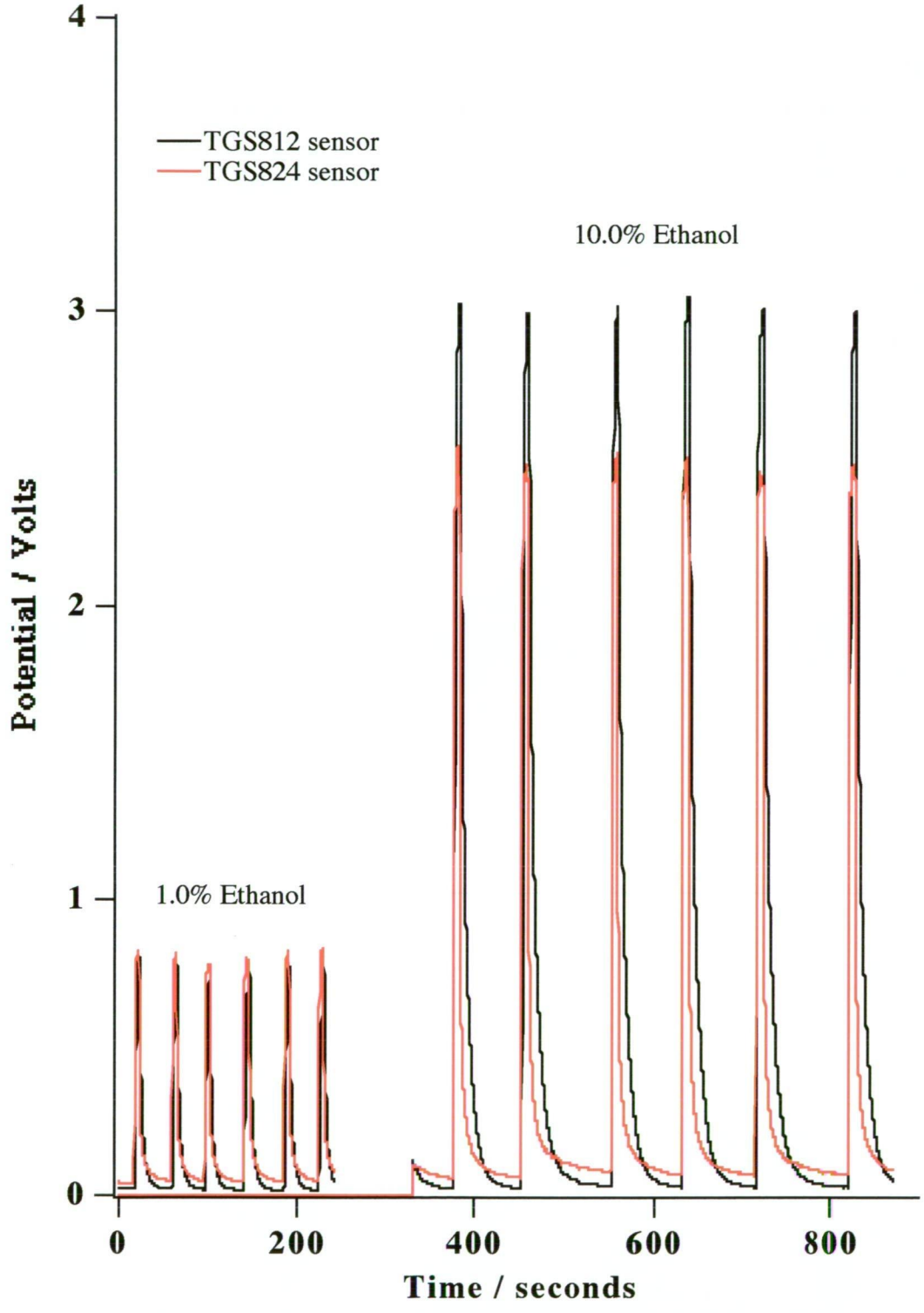

Figure 2.6. Reproducibility of the TGS812 and TGS824 gas sensors.

2.3.3 Mechanism of Response to Alcohol

The mechanism of response of these Taguchi semiconductor gas sensors has been discussed in a number of papers [17-19]. The response of the tin-oxide semiconductors was dependent on the chemisorbed oxygen on the surface reacting with reducing gases or vapours on the oxide layer of the semiconductor. For example, ethanol is oxidised to ethanal:

$$O_2 + 2e^- \longrightarrow 2O^-$$

$$2O^- + 2CH_3CH_2OH \longrightarrow 2CH_3CHO + 2H_2O + 2e^-$$

There is a resulting change in resistance of the TGS sensor which is dependent on the concentration of the ethanol introduced [20,27]. An electronic circuit can be constructed to produce a voltage output to a voltmeter which can then be plotted as a function of time after introduction of the ethanol vapour sample to the sensor. The voltage output is given by [25]:

$$V_C / V_S = (R_L + R_S) / R_L \qquad (2.6)$$

where V_C is the constant circuit voltage, V_S is the voltage difference between the carrier gas and the sample, R_L is the constant circuit load resistance and R_S is the electrical resistance due to adsorption of the sample on the surface of the sensor. Rearranging equation 2.6 gives:

$$1 / V_S = 1 / V_C + R_S / V_C R_L$$

$$= k_1 + k_2 R_S \qquad (2.7)$$

where k_1 and k_2 are constants depending on the circuit design. The relationship between V_S and concentration of the gas, C_S, is proportional as shown in Figure 2.7. Therefore, R_S is inversely related to the concentration of the sample due to the decrease in electrical resistance as the concentration adsorbed on the surface of the sensor increases and equation 2.7 can be rearranged to give:

$$1 / V_S = k_1 + k_2 / C_S \qquad (2.8)$$

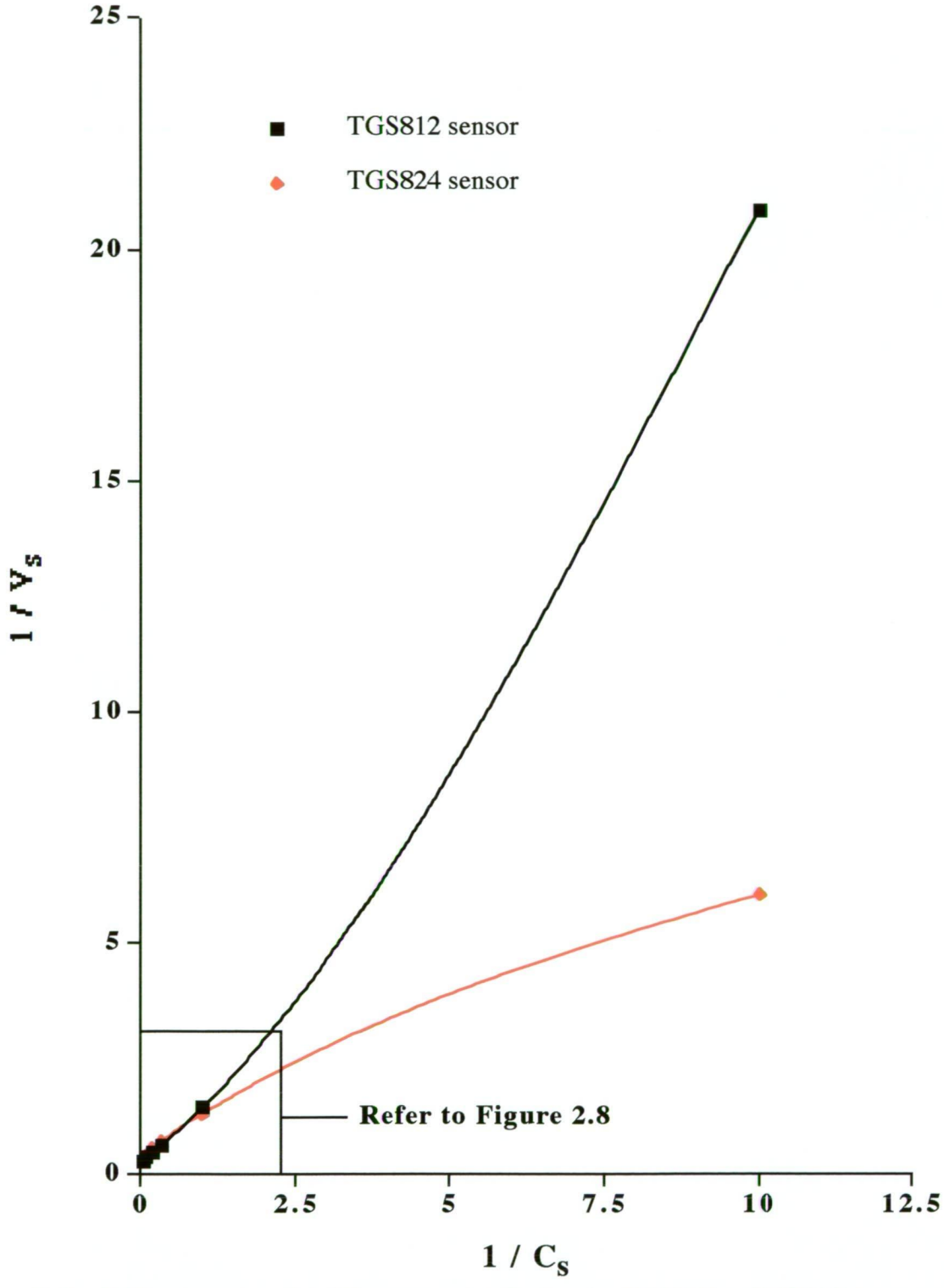

Figure 2.7. Calibration plot of 1 / V_S versus 1 / C_S for the TGS812 and TGS824 gas sensor responses to ethanol between 0.1 and 20% (v/v).

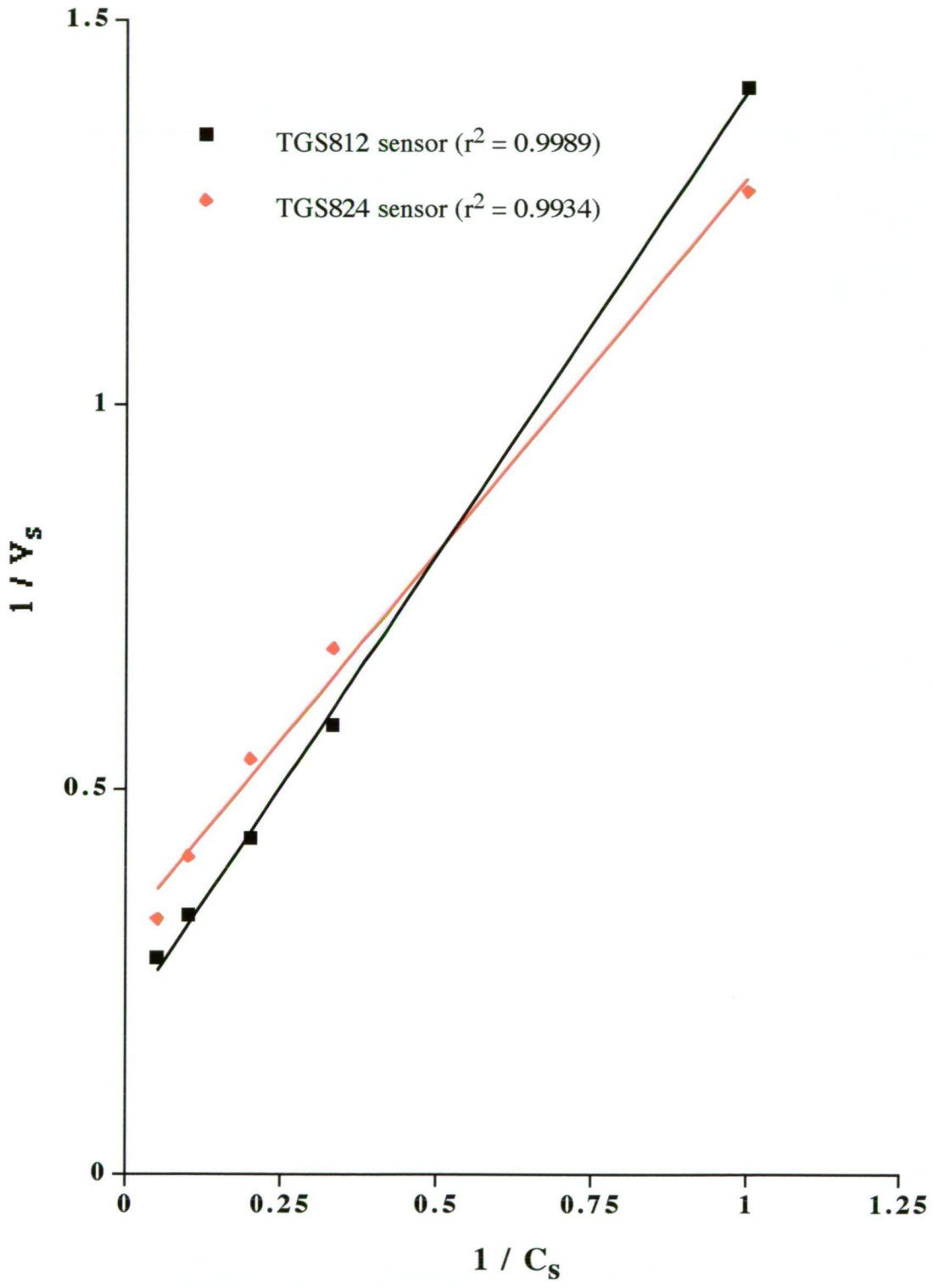

Figure 2.8. Calibration plot of $1 / V_S$ versus $1 / C_S$ for the TGS812 and TGS824 gas sensor responses to ethanol between 1.0 and 20% (v/v).

Figure 2.7, shows the inverse of the voltage response (1 / V_S) for the TGS812 and the TGS824 sensors against the inverse of the ethanol concentration (1 / C_S). These plots were used to calibrate both the Taguchi gas sensors. As shown in Figure 2.7, the last point exhibits deviation from linearity due to the detection limit of ethanol. Figure 2.8 shows the same calibration plot as in Figure 2.7, but excludes the 0.1% (v/v) ethanol and clearly a linear relationship is observed as shown by the correlation coefficients (r^2); for the TGS812 sensor r^2 = 0.9989 and for the TGS824 sensor r^2 = 0.9934.

Other linearisation techniques such as using an operational amplifier linearising circuit [14] and adsorption isotherm models [20,22] have been reported. Later in this chapter an investigation of the Langmuir adsorption model will be applied to the ethanol response of the Taguchi TGS812 and TGS824 tin-oxide gas sensors.

2.3.4 Analysis of Alcoholic Samples

Various alcoholic samples were analysed for their ethanol content using the portable analyser, and the results are presented in Table 2.1.

Table 2.1. Comparison of the label data for commercial liquors and the data determined with the TGS812 and TGS824 gas sensors and gas chromatography.

Alcohol	GC %Ethanol (v/v)	TGS812 sensor %Ethanol (v/v) (%RSD)	TGS824 sensor %Ethanol (v/v) (%RSD)	Labelled %Ethanol (v/v)
Light beer	2.0	2.0 (1.9)	2.0 (2.1)	2.7
Normal beer	4.6	4.6 (1.1)	4.2 (1.0)	4.9
White wine	11.2	11.4 (2.2)	10.5 (1.4)	10.0
Red wine	9.7	10.3 (0.4)	8.8 (3.1)	10.9

The ethanol concentrations were calculated from the calibration plots shown in Figure 2.8. It was observed that the results obtained with the TGS812 sensor were slightly higher than the TGS824 sensor for all the alcoholic samples analysed. The likely reason was that the TGS824 sensor was responding to other volatiles present in the alcoholic samples and

consequently resulting in a lower ethanol content. The RSD exhibited for the TGS812 and TGS824 sensors for the alcoholic samples analysed were typically $\leq 3.1\%$. These results were compared to gas chromatography analysis and showed agreement with a correlation coefficient of 0.9980 and 0.9985 for the TGS812 and TGS824 sensors, respectively. The gas chromatography analysis was also performed using an isopropanol internal standard and the results showed no improvement in the accuracy and precision, therefore the same ethanol solutions used to calibrate the TGS sensors were also used in the gas chromatography procedure. The labelled ethanol content was also compared to the results obtained with the TGS812 and the TGS824 sensors and showed agreement with a correlation coefficient of 0.9633 and 0.9290, respectively.

2.4 Application of the Langmuir Isotherm Model to the Ethanol Response of the Tin-Oxide Gas Sensors

The Langmuir adsorption isotherm is based on the assumption that every adsorption site is equivalent and that the ability of a molecule to bind on the surface of the sensor is independent of whether or not nearby sites are occupied as described in Section 2.1.1.

The measured voltage (E) of the ethanol vapour from the semiconductor gas sensor depends on the circuit design recommended by Figaro [25] and is expressed as:

$$E = V_S - V_O \tag{2.9}$$

where V_S is the voltage output due to the sample and V_O is the output voltage due to the carrier gas (air) in the flow-through analyser. Rearranging equation (2.6), the voltage output of the sample can be written as [25]:

$$V_S = V_C R_L / (R_S + R_L) \tag{2.10}$$

where V_C is the constant circuit voltage, R_L is the constant load resistance and R_S is the sample resistance. The load resistance and the response behaviour of the gas sensors are dependent on

the amount of gas adsorbed onto the semiconductor surface (ie. on the surface coverage).

The relationship of the voltage output of the sample is described in equation 2.10. When the sample voltage output V_S increases, the sample resistance R_S decreases due to the above mentioned reaction of adsorbed oxygen. However, the relationship between the measured voltage (E) and the ethanol concentration is not linear because of the complex nature of the adsorption mechanism as shown by the calibration plots for the TGS812 and the TGS824 type gas sensors presented in Figure 2.5. The sample output and the surface coverage of the semiconductor sensor by the adsorbed alcohol molecules can be described in terms of ag Langmuir adsorption mechanism as given in equation 2.5.

Experimental results exhibited for both the TGS812 and the TGS824 sensors can be compared with the Langmuir adsorption isotherm theory most easily if equation 2.5 is rearranged to:

$$C / y = a / y_m + C / y_m \qquad (2.11)$$

where C is the % ethanol (v/v), a and y_m are constants and y is the measured output voltage for a particular concentration of ethanol. This is based on the assumption that the surface coverage of the sensor will determine the change in resistivity of the surface, and hence gives a change in voltage output of the electrical circuit. The concentration of the ethanol vapour is therefore proportional to the concentration of ethanol in the aqueous solution.

Hence a plot of C / y [% Ethanol (v/v) / Measured output voltage (V)] versus C [% Ethanol (v/v)] should result in a linear calibration. As shown in Figure 2.9, the above plot resulted in a linear fit to the experimental data with correlation coefficients (r^2) of 0.9992 and 0.9978 for the TGS812 and TGS824 semiconductor gas sensors, respectively. Clearly, this response mechanism for the TGS812 and the TGS824 gas sensors indicates that the surface is uniform and each adsorption site is independent of nearby sites.

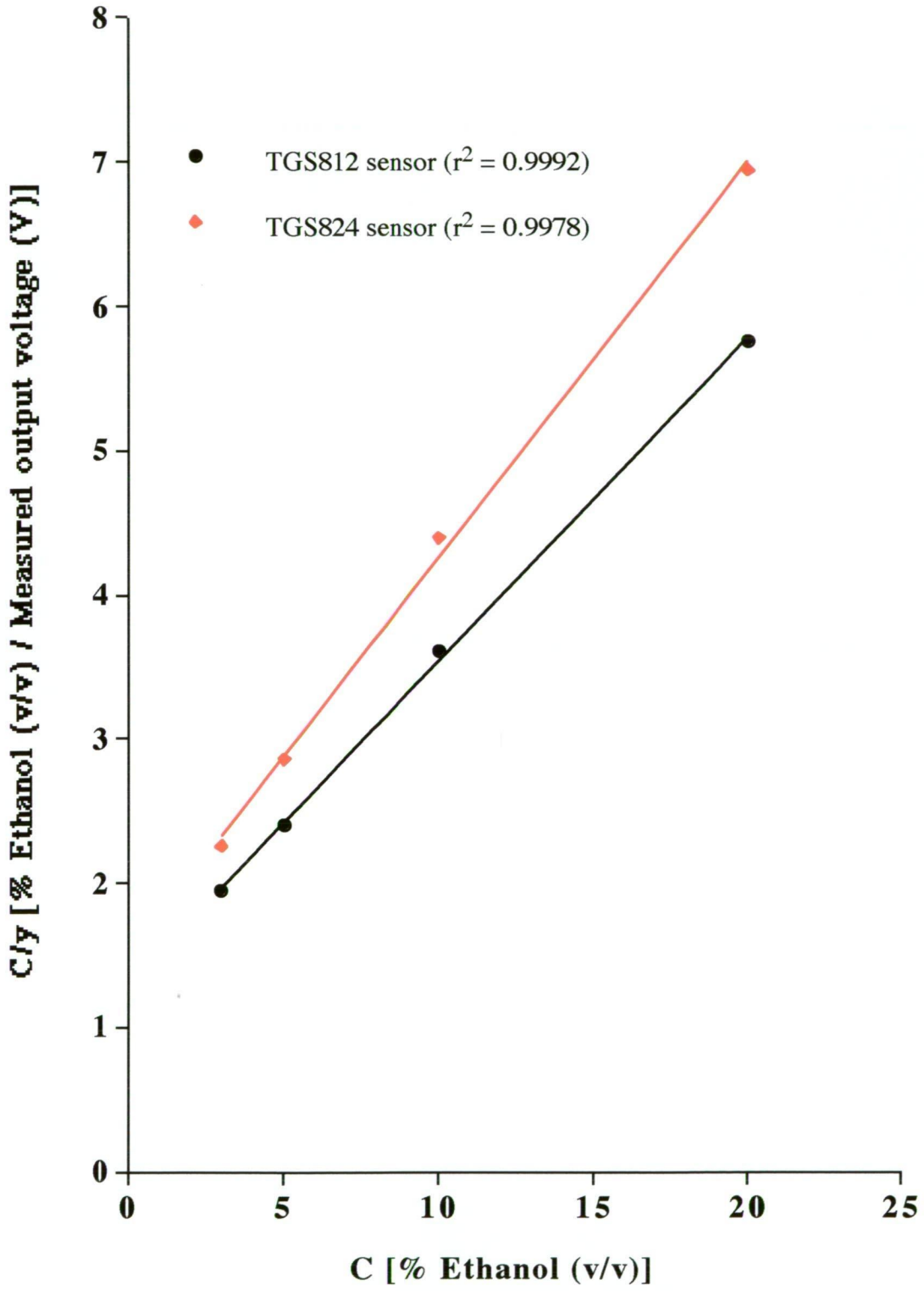

Figure 2.9. Calibration plot for the TGS812 and TGS824 gas sensor response to ethanol using the Langmuir isotherm model.

2.4.1 Validation of the Langmuir Model using Alcoholic Samples

The beer and wine samples were analysed for their ethanol content using the portable flow-through analyser, and the results are presented in Table 2.2. The ethanol content was calculated from the linear Langmuir model calibration plots as shown in Figure 2.9 for both the TGS812 and the TGS824 sensors. Similar to Section 2.3.4, the ethanol content determined with the TGS812 sensor were slightly higher than the TGS824 sensor for all the alcoholic samples analysed except for the light beer. These results were compared to the gas chromatography analysis and showed agreement with a correlation coefficient (r^2) of 0.9989 and 0.9996 for the TGS812 and the TGS824 sensors, respectively. The RSD exhibited for the TGS812 and TGS824 sensors for the alcoholic samples analysed were typically $\leq$ 2.4%. The labelled ethanol content was also compared to the results obtained with the TGS812 and the TGS824 sensors and showed agreement with a correlation coefficient of 0.9587 and 0.9363, respectively.

Table 2.2. Comparison of the label data for commercial liquors, the data determined using the linearised Langmuir model and gas chromatography.

Alcohol	GC %Ethanol (v/v)	TGS812 sensor %Ethanol (v/v) (%RSD)	TGS824 sensor %Ethanol (v/v) (%RSD)	Labelled %Ethanol (v/v)
Light beer	2.0	2.1 (1.2)	2.3 (1.4)	2.7
Normal beer	4.6	4.6 (1.9)	4.4 (1.1)	4.9
White wine	11.2	10.7 (1.7)	9.5 (2.4)	10.0
Red wine	9.7	9.6 (1.5)	8.2 (1.9)	10.9

2.5 Conclusions

The portable flow-through gas analyser developed and evaluated in this study is of a simple design, small in size, light weight, battery-powered and requires low power consumption. The gas analyser was used continuously for up to 4 hours, before recharging was necessary. The use of gas sensors in flow-through analysis allows the operator to conduct rapid measurements without significant interference from other volatile organics in the liquor

samples analysed.

The TGS812 and TGS824 gas sensors exhibited excellent peak height reproducibility of < 3% RSD, good baseline stability and sensitivity and a rapid response with peak widths of 30 seconds for ethanol in the range between 0.1 to 20% (v/v). A calibration plot of $1 / V_S$ versus $1 / C_S$ exhibited a linear plot for the TGS812 and TGS824 sensor response to ethanol and this plot was employed to determined ethanol content in beer and wine samples, and the results were in agreement compared to gas chromatography analysis and the labelled ethanol content.

The ethanol response exhibited by the TGS812 and TGS824 gas sensors were fitted to the Langmuir isotherm model and a linear calibration plot was achieved. The Langmuir isotherm model calibration plots were validated by determining the ethanol content in various beer and wine samples and these results were in agreement compared to gas chromatography analysis and the labelled ethanol content.

2.6 References

1. K. N. Andrew, N. J. Blundell, D. Price and P. J. Worsfold, 'Flow Injection Techniques for Water Monitoring', Analytical Chemistry, **66**, 917A-922A, (1994).

2. H. L. C. Meuzelaar, Ed., 'Special Issue on: Field Portable Analytical Instrumentation', Trends in Analytical Chemistry, **13**, 252-299, (1994).

3. E. B. Overton and K. R. Carney, 'New Horizons in Gas Chromatography: Field Applications of Microminiaturized Gas Chromatographic Techniques', Trends in Analytical Chemistry, **13**, 252-257, (1994).

4. G. Baykut and J. Franzen, 'Mobile Mass Spectrometry; A Decade of Field Applications', Trends in Analytical Chemistry, **13**, 267-275, (1994).

5. S. P. Levine and G. M. Russwurm, 'Fourier Transform Infrared Optical Remote Sensing for Monitoring Airborne Gas and Vapor Contaminants in the Field', Trends in Analytical Chemistry, **13**, 258-262, (1994).

6. P. I. Richter, 'Air Pollution Monitoring with LIDAR', Trends in Analytical Chemistry, **13**, 263-266, (1994).

7. R. B. Turner and J. L. Brokenshire, 'Hand-Held Ion Mobility Spectrometers', Trends in Analytical Chemistry, **13**, 275-280, (1994).

8. S. Piorek, 'Principles and Applications of Man-Portable X-Ray Fluorescence Spectrometry', Trends in Analytical Chemistry, **13**, 281-286, (1994).

9. N. Taguchi, 'Gas Detecting Device', U.S. Patent 3 631 436, December, (1971).

10. N. Taguchi, 'Gas Detecting Device', U.S. Patent 3 695 848, October, (1972).

11. K. Persaud and G. Dodd, 'Analysis of Discrimination Mechanisms in the Mammalian Olfactory System using a Model Nose', Nature, **299**, 352-355, (1982).

12. T. C. Pearce, J. W. Gardner, S. Friel, P. N. Bartlett and N. Blair, 'Electronic Nose for Monitoring the Flavour of Beers', Analyst, **118**, 371-377, (1993).

13. J. W. Gardner, T. C. Pearce, S. Friel, P. N. Bartlett and N. Blair, 'A Multisensor System for Beer Flavour Monitoring using an Array of Conducting Polymers and Predictive Classifiers', Sensors and Actuators B, **18-19**, 240-243, (1994).

14. H. V. Shurmer, J. W. Gardner and H. T. Chan, 'The Application of Discrimination Techniques to Alcohols and Tobaccos using Tin-oxide Sensors', Sensors and Actuators, **18**, 361-371, (1989).

15. C. Di Natale, F. A. M. Davide, A. D' Amico, P. Nelli, S. Groppelli and G. Sberveglieri, 'An Electronic Nose for the Recognition of the Vineyard of a Red Wine', Sensors and Actuators B, **33**, 83-88, (1996).

16. L. Promsong and M. Sriyudthsak, 'Thin Tin-Oxide Film Alcohol-Gas Sensor, Sensors and Actuators B, **24-25**, 504-506, (1995).

17. P. T. Moseley, J. O. W. Norris and D. E. Williams, *Eds.*, 'Techniques and Mechanisms in Gas Sensing', Adam Hilger, Bristol, (1991).

18. G. S. V. Coles, G. Williams and B. Smith, 'Selectivity Studies on Tin Oxide-Based Semiconductor Gas Sensors', Sensors and Actuators B, **3**, 7-14, (1991).

19. H. P. Kim, J. J. Choi, H. W. Cheong, J. M. Kim and J. M. Kim, 'Sensing Mechanism of SnO_2-based Sensors for Alcohols', Sensors and Actuators B, **13-14**, 511-512, (1993).

20. R. K. Srivastava, P. Lal, R. Dwivedi and S. K. Srivastava, 'Sensing Mechanism in Tin Oxide-based Thick-film Gas Sensors', Sensors and Actuators B, **21**, 213-218, (1994).

21. H. Geistlinger, 'Electron Theory of Thin-film Gas Sensors', Sensors and Actuators B, **17**, 47-60, (1993).

22. D. M. Oglesby, B. T. Upchurch, B. D. Leighty, J. P. Collman, X. Zhang and P. C. Herrmann, 'Surface Acoustic Wave Oxygen Sensor', Analytical Chemistry, **66**, 2745-2751, (1994).

23. G. M. Barrow, 'Physical Chemistry', 4th Edition, McGraw-Hill, Tokyo, (1979).

24. P. W. Atkins, 'Physical Chemistry', 5th Edition, Oxford University Press, Tokyo, (1994).

25. Figaro Engineering Inc., 'Figaro Gas Sensors', Product Document, Osaka, August, (1990).

26. H. V. Shurmer, 'Basic Limitations for an Electronic Nose', Sensors and Actuators B, **1**, 48-53, (1990).

27. S. R. Morrison, 'Semiconducting-Oxide Chemical Sensors', IEEE Circuits and Devices, **7**, 32-35, (1991).

Chapter Three: The Evaluation of a Portable, Battery-Powered Gas Analyser with an Array of Six Tin-Oxide Semiconductor Sensors

3.1 Introduction

In this chapter, a portable, battery-powered, multi-sensor array gas analyser, containing six different Taguchi tin-oxide semiconductors was developed and evaluated. This multi-sensor array gas analyser was based on the electronic circuitry of the portable gas analyser described in Chapter two. The advantage of a multi-sensor array response over a single sensor response is that it produces a response pattern rather than a single signal that can be used to improve the identification of a particular sample [1]. However, there is little point in having an array of sensors, all of which respond in the same manner to a sample [1].

A wide range of portable analysers have been used for many applications, such as monitoring airborne gas [2] and vapour contaminants in the field [2], air pollution monitoring [3], analyses of soil contamination [4], detection of chemical warfare agents [5] and hazardous waste screening [6]. The use of sensor arrays has advantages for multi-analyte determinations, and the progress of sensor array research, reporting on a range of multi-gas monitors, many of which are portable and applicable for field operation have been reviewed [7]. These mainly utilise electrochemical sensors developed to detect gases such as carbon monoxide, hydrogen sulfide, nitric oxide, sulfur dioxide and nitrogen dioxide.

In addition there has been considerable research devoted to the development of multi-sensor array systems based on tin-oxide sensors. Examples include: two chemically modified tin-oxide sensors used for the identification of carbon monoxide and methane in mixtures [8]; an array of three thin film metal oxide sensors were employed for the identification of ethyl acetate, acetone, ethanol and pentane and the determination of ethanol in various mixtures [1] and the discrimination between alcohols and tobaccos [9]; a sensor array of four tin-oxide semiconductor thin-film devices were used to characterise smoke from different origins [10]; an array of six modified tin-oxide gas sensors were used for the detection of single and mixtures of

gases [11]; and an array of twelve tin-oxide sensors were employed for the discrimination of coffees [12] and the discrimination between various alcoholic beverages [13,14]. Other gas sensors include catalytic [15], piezoelectric [16,17], surface acoustic wave [18,19] conducting polymers [20-22] and electrochemical gas sensors [23,24]. However, some of these gas monitors have complex designs, are fixed-site instruments which require voltage main power supply, have limited sensor life and are expensive.

In this chapter, a portable, battery-powered, multi-sensor gas analyser, containing six different Taguchi tin-oxide semiconductors is described and evaluated. This portable gas analyser employed in a flow-through mode, is of a simple design, relatively inexpensive and has low power consumption. The performance of the portable, battery-powered, multi-sensor gas analyser was evaluated in terms of stability, sensitivity, selectivity and reproducibility using the response to ethanol. The portable multi-sensor gas analyser was used to determine the ethanol content in various beer samples employing the Langmuir isotherm described in Chapter two. The response pattern of the multi-sensor array to discriminate between various beer samples was also investigated.

3.2 Experimental

3.2.1 Solutions

The following general reagents were used: acetaldehyde (Merck-Schuchardt), acetone (BDH Chemicals, AnalaR), butan-1-ol (BDH Chemicals, AnalaR), ethanol (Ajax Chemical, Analytical UNIVAR Reagent) and propan-1-ol (BDH Chemicals, AnalaR). All solutions were prepared in Ultrapure water (Barnstead Ultrapure water systems) in 100 mL volumetric flasks and used for head-space analysis at room temperature (22 ± 2 °C). A standard cigarette lighter was used as a source for pure butane. The beer samples used in this study were obtained commercially from local suppliers, and are listed below, with the labelled ethanol content in brackets: Beer A (2.7%), Beer B (2.8%) and Beer C (2.8%).

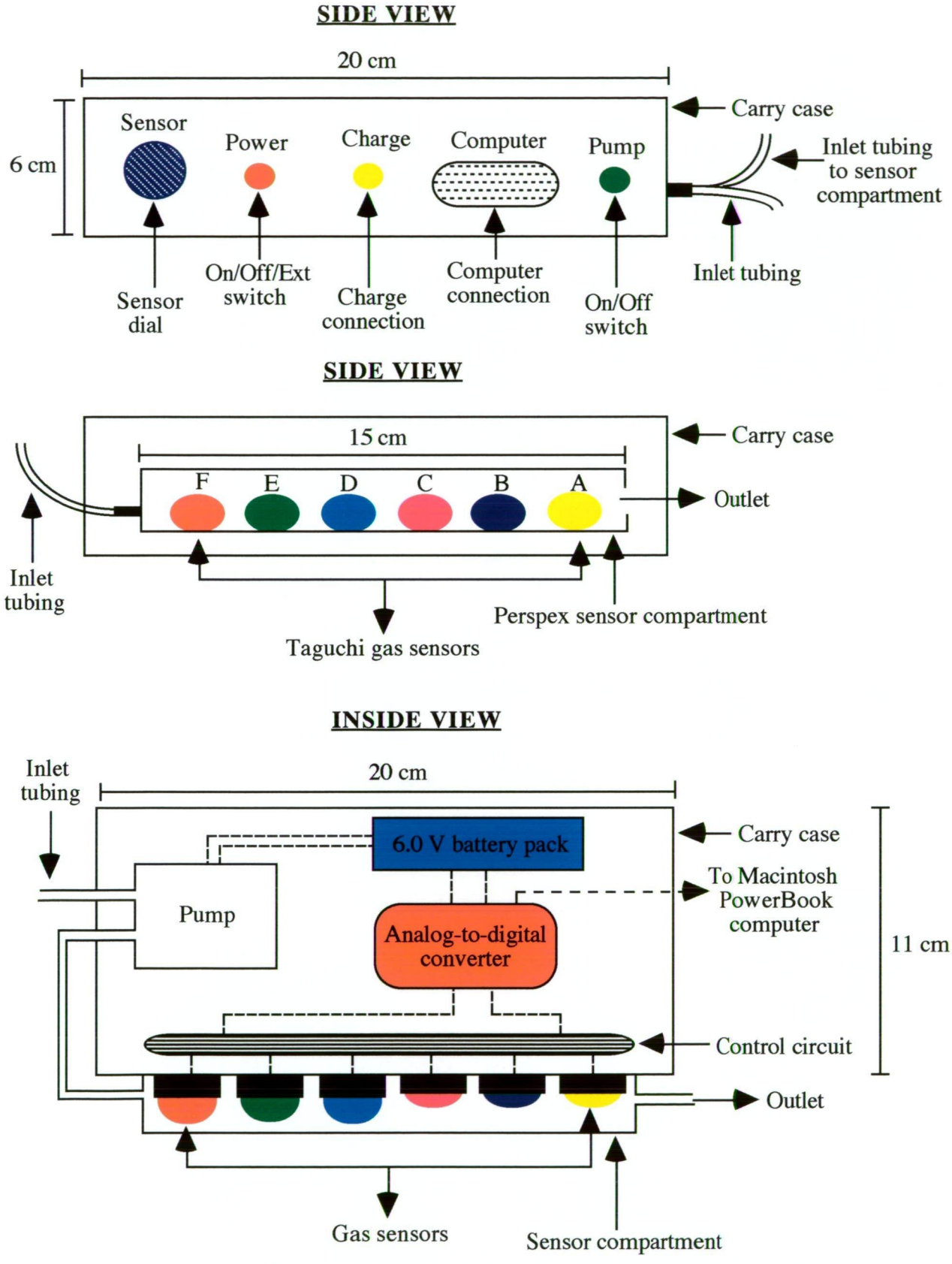

Figure 3.1. Schematic diagram of the portable multi-sensor gas analyser used in this study.

(A)

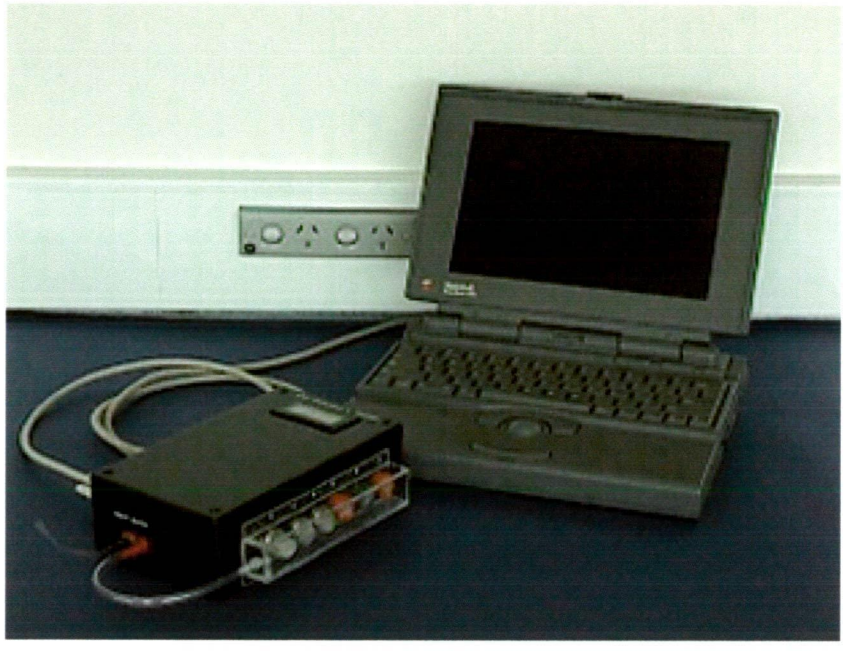

(B)

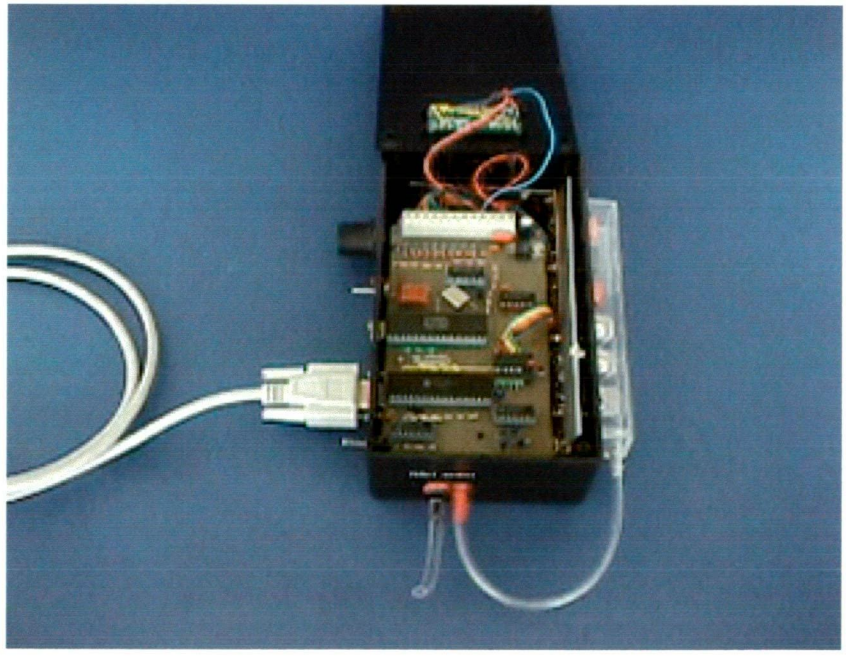

Figure 3.2. Photographs of (A) the multi-sensor array gas analyser connected to a Macintosh PowerBook computer and (B) the circuitry of the multi-sensor gas analyser.

3.2.2 Design of the Portable Gas Analyser

The portable gas analyser consists of six Taguchi type tin-oxide semiconductor sensors in a flow-through compartment, as shown in Figure 3.1. The six sensors used were the TGS880, TGS825, TGS824, TGS822, TGS813 and TGS800 types and were obtained from Figaro [25]. The TGS813 was used to replace the TGS812 as it was no longer available commercially and was reported to be similar in configuration [25]. The ethanol vapours of the standards and samples were pumped into the flow-through compartment using a diaphragm pump at a constant flow rate of 1 L / minute, using a 10 seconds sampling time. The sensors and pump were controlled by an electrical circuit operated from a battery-pack of five Ni-Cd rechargeable 1.2 V batteries. The analog voltage output was displayed on the LCD unit of the analyser, and was simultaneously converted via a 12-bit analog-to-digital converter (ADC) that transmitted through a RS232C serial output to a Macintosh PowerBook computer. Photographs of the entire portable gas analyser and the internal electronic circuitry are presented in Figure 3.2.

3.2.3 Gas Chromatography Instrumentation

A Perkin-Elmer Sigma 3 Gas Chromatograph with a Flame Ionisation Detector (FID) was used for the analysis of ethanol. A 3% Neopentyl Glycol column (6 ft in length, 1/8 in. internal diameter) was used at a temperature of 160 °C. 1.0 μL sample injection volumes were used, using a SGE 10 μL syringe. The data collected were saved as text files 'IGOR' (AD Instruments, Sydney, Australia) was used for data analysis.

3.2.4 Head-Space Analysis and Gas Chromatography Procedure

The tin-oxide semiconductor gas sensors were allowed to warm up by pumping air (carrier gas) through the analyser for 1 hour prior to measurements to ensure a stable baseline. Standard solutions as well as liquor samples were left standing at room temperature (22 ± 2 °C) for 2-3 hours and were shaken in the 100 mL volumetric flasks to produce adequate head-space vapour prior to measurement. The sample inlet tube of the gas analyser was introduced into the head-space of the flasks immediately after removing the lid, and a vapour sample was pumped

into the flow-through sensor compartment for 10 seconds at a constant temperature and relative humidity. The responses of each standard solution and beer samples for each sensor were recorded in triplicate and displayed in real-time millivolt readings on the Macintosh PowerBook computer screen using Satod ©, Version 1.46. 'IGOR' was used for data analysis and graphical representation of the data.

For the gas chromatography analysis, the same ethanol standard solutions and samples were left standing at room temperature for 2-3 hours, in order to produce adequate head-space vapour. 1.0 μL sample injection volumes were used and the data collected were stored as text files.

3.3 Results and Discussion

3.3.1 Design of the Multi-sensor Array Gas Analyser

The six Taguchi tin-oxide semiconductor gas sensors were arranged in a single flow-through compartment as shown in Figure 3.1, whereby the gas or vapour sample was pumped over the surface of the sensors. The major advantage of this arrangement is that it allows for a minimal exposure of the sensors to the gas sample and thus minimises the chance of poisoning the sensor's surface. Another advantage of this arrangement is that each sensor can be interchanged throughout the compartment.

The configuration of the Figaro gas sensors used were as follows: the TGS880 sensor has a polyamide resin base with mesh cover and is reported to be more sensitive to volatile gases for cooking processes; the TGS825 and TGS824 sensors have a heat resistant ceramic base with mesh cover and are reported to be more sensitive to sulfides and ammonia, respectively; the TGS822, TGS813 and TGS800 sensors have a polyamide resin base and housing and are reported to be more sensitive to alcohols, combustible gases and air contaminants, respectively [25]. All the gas sensors have a built-in heater in an alumina ceramic tube and the semiconductor material is mounted on the tube with two printed gold electrodes. The sensor elements were protected by a plastic housing with two flame arresters of stainless steel double-gauze on the top and bottom [25]. These low cost Taguchi sensors are compact in size (17-19.5 mm internal diameter) and easy to install [25].

The portable, multi-sensor, gas analyser is small in size (20 x 11 x 6 cm), light weight (985 g), battery-powered (6.0 V battery pack), requires low power (6.6 W), and was connected to a Macintosh PowerBook computer making it efficient for remote site monitoring. This analyser was in continuous operation for 3 hours before recharging was necessary.

3.3.2 Response to Ethanol Vapour

The response of each sensor to ethanol vapour was recorded simultaneously when the sample inlet tube was moved from ambient air into the head-space of each sample. After sampling for 10 seconds, the inlet tube was moved back into ambient air. The short sampling time resulted in a small sample zone of alcohol vapour being pumped through the sensor compartment, thereby giving a peak-shaped response. The trace on the computer screen was allowed to return to the baseline before repeat measurements were made. Triplicate peaks were obtained for ethanol at different concentrations for each sensor, as shown in Figure 3.3. All sensors exhibited a rapid response with peak widths in the range of 30-60 seconds for a 10 seconds sampling time and a constant flow rate of 1 L / minute. A peak height reproducibility of $< 3\%$ relative standard deviation (RSD) was observed for all sensors. The TGS825 sensor exhibited the highest sensitivity whereas the TGS813 sensor exhibited the least sensitive response to ethanol. However, all the six Taguchi sensors showed no loss of activity and no baseline drift during the course of the study, moreover they were resistant to poisoning and exhibited excellent durability and shock proof. These tin-oxide sensors are reported to be limited by the lack of selectivity, sensitivity and reproducibility [26]. However, these results have demonstrated that these Taguchi sensors exhibit high stability, sensitivity and reproducibility in a flow-through arrangement.

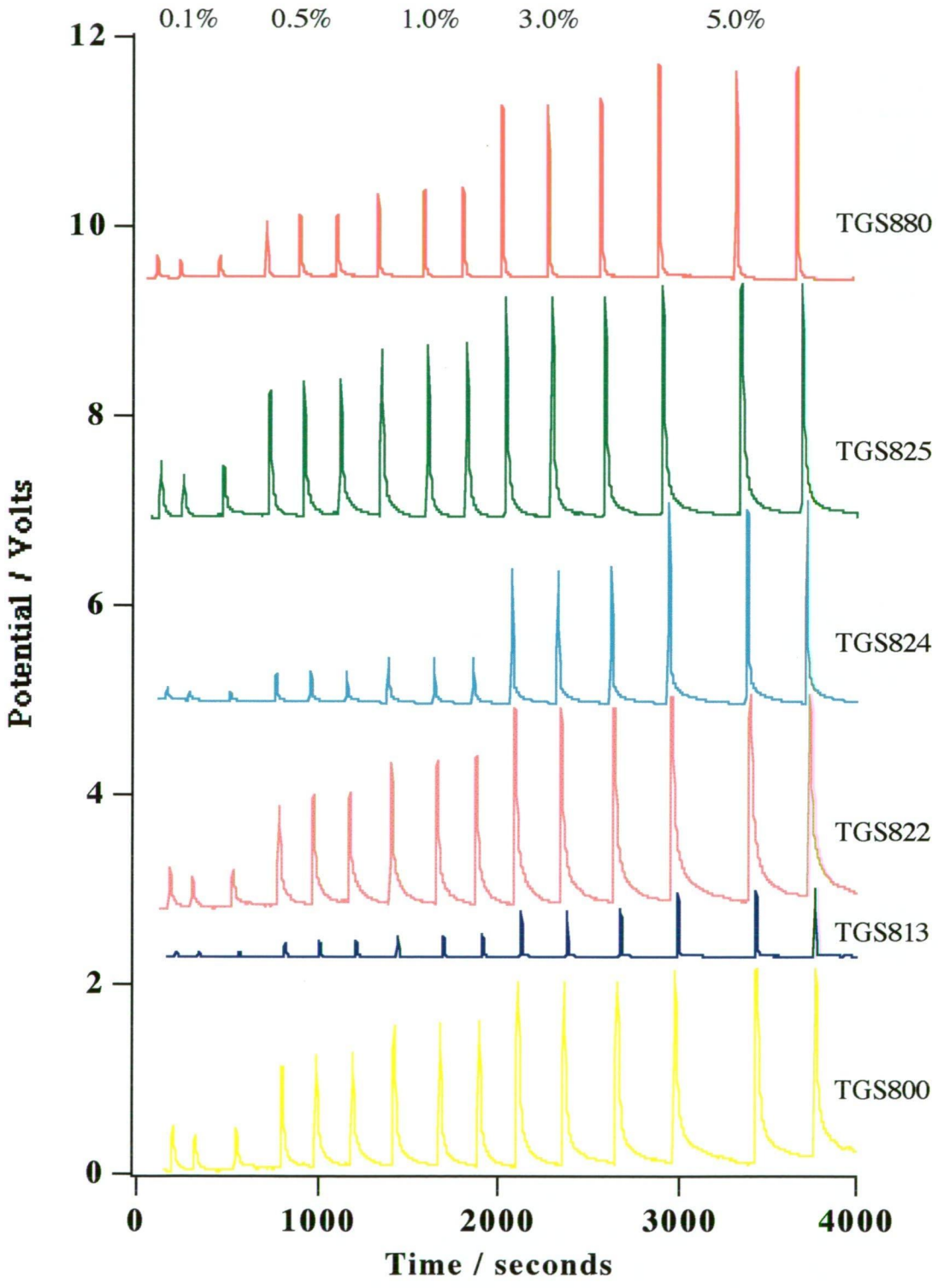

Figure 3.3. Sample peaks for increasing concentrations of ethanol for each Taguchi gas sensor.

3.3.3 Discrimination Between Varying Ethanol Concentrations

Pattern recognition techniques have been previously applied for qualitative [21,22,27] and quantitative applications [27]. In this study, the response patterns for various ethanol concentrations in the range of 0.1 to 5.0% were investigated and compared and are given in Figure 3.4. Figure 3.4, shows that the response increases as the ethanol concentration increases and that different response patterns were observed for the 3.0% and 5.0% ethanol samples compared to the ≤ 1.0% ethanol samples. In principle, this makes it possible to discriminate between high (> 3.0%) and low ethanol concentrations (<1.0%).

3.3.4 Discrimination Between Various Compounds and Functional Groups

As described earlier, the advantage of employing multi-sensor array compared to a single sensor response is that it produces a response pattern rather than a single signal, which can improve the discrimination between various compounds [1]. Figure 3.5 shows the response pattern observed for 1.0% ethanol and pure butane as examples of a polar and non-polar compounds, respectively. Clearly, a significantly different response pattern was observed for the ethanol and butane vapours, and this demonstrates the ability of the multi-sensor array employed in the portable gas analyser to selectively discriminate between two different compounds, in this case, an alkane and an alcohol. Consequently, selective response patterns can be employed for the identification of individual gas components using the multi-sensor array portable gas analyser.

Figure 3.6 presents the response patterns observed for 1.0% ethanol, propanol and butanol solutions. The response patterns observed for the ethanol, propanol and butanol were similar, since they are alcohols. However, there are observed differences between each response pattern for each alcohol, as a result of the different hydrocarbon chain, in particular the response observed for the TGS880, TGS825, TGS824 and TGS800 sensors. Consequently, selective discrimination between the different alcohol vapours was demonstrated using the portable gas analyser.

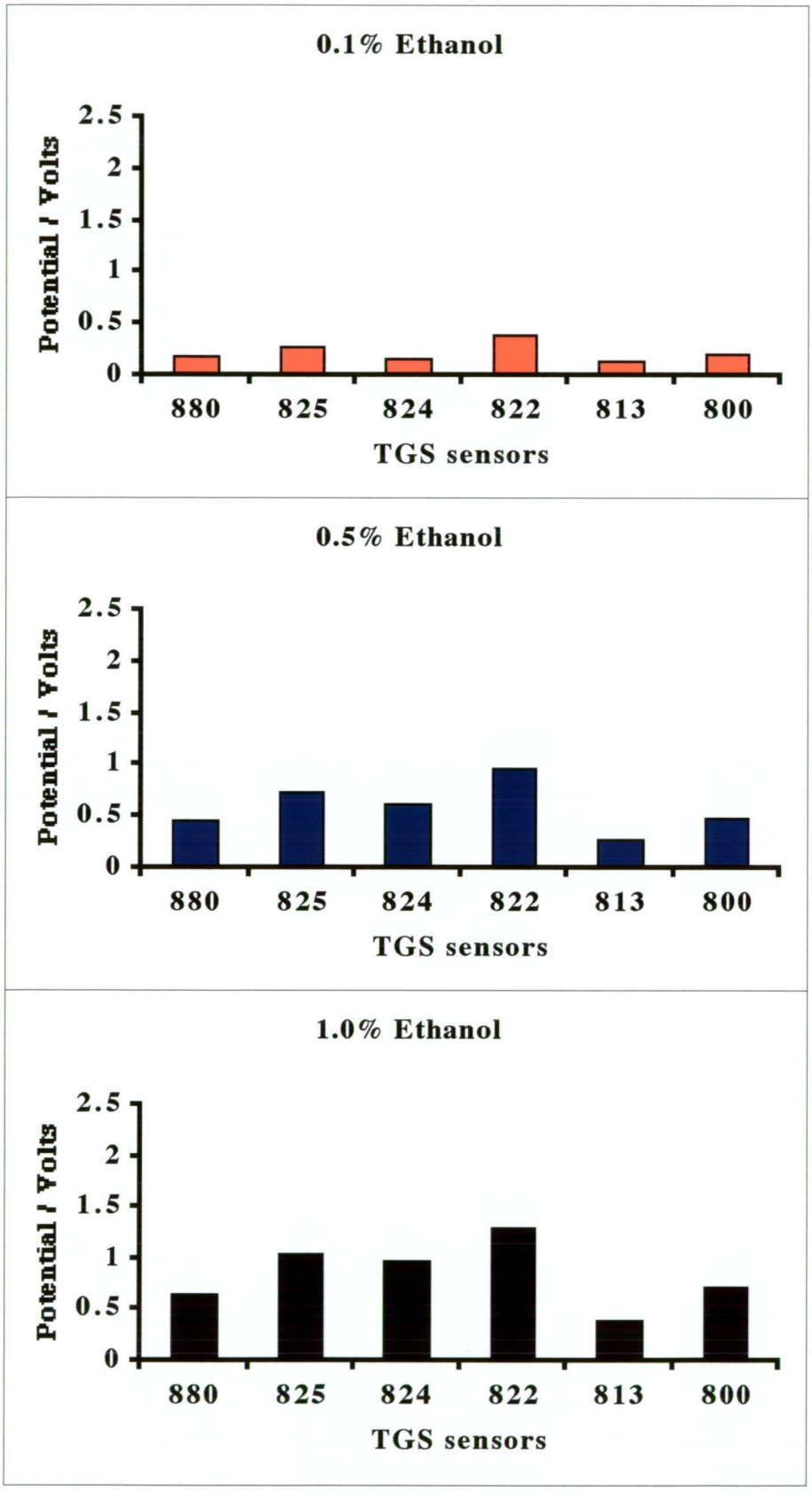

Continued on next page:

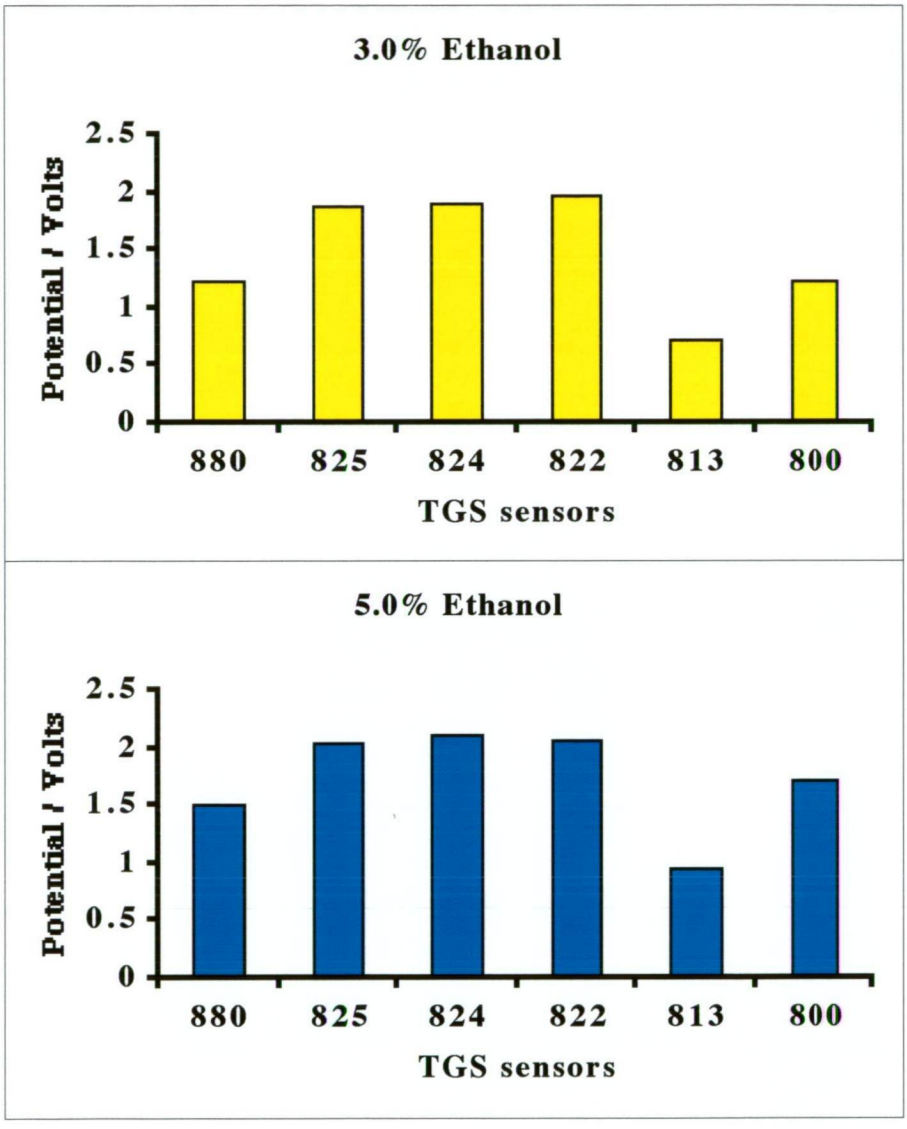

Figure 3.4. Response pattern observed for varying ethanol concentrations ranging from 0.1-5.0% (v/v) using the multi-sensor array gas analyser.

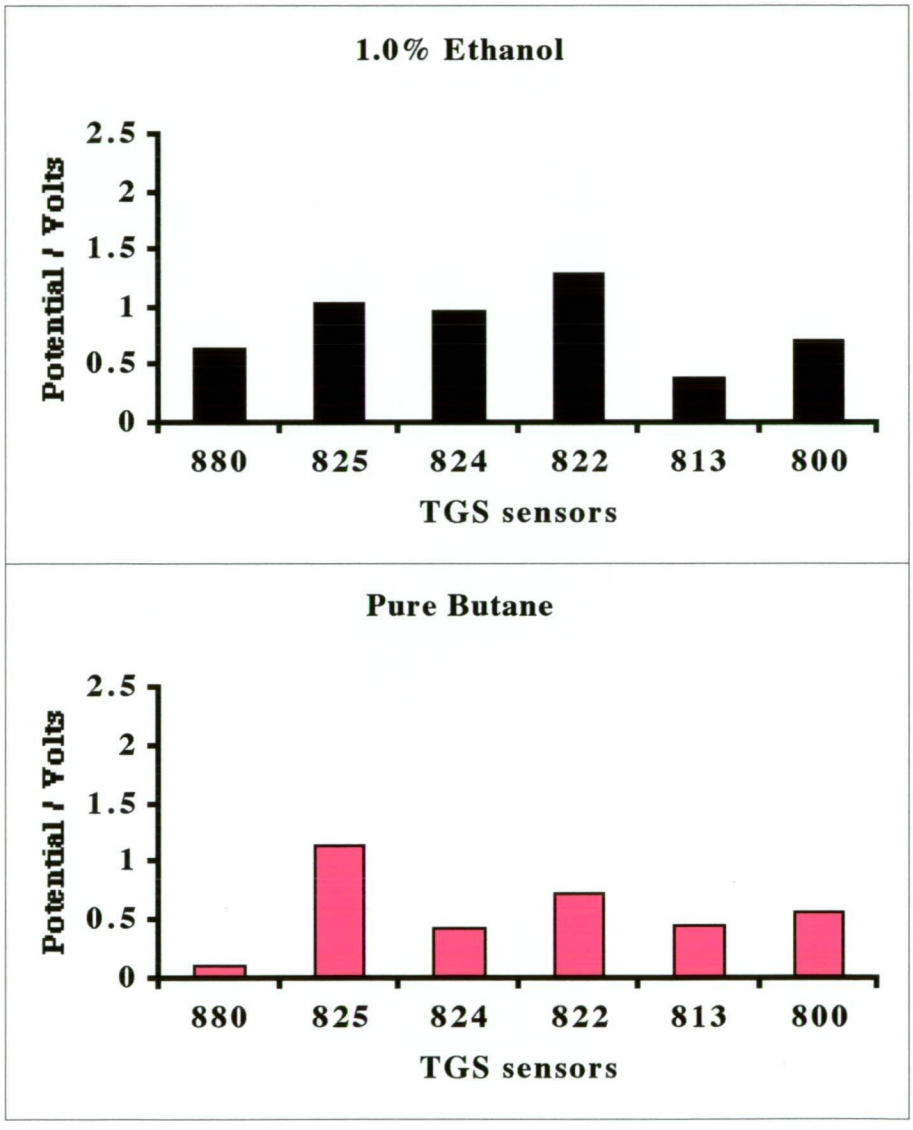

Figure 3.5. Response pattern observed for 1.0% ethanol standard solution and pure butane using the multi-sensor array gas analyser.

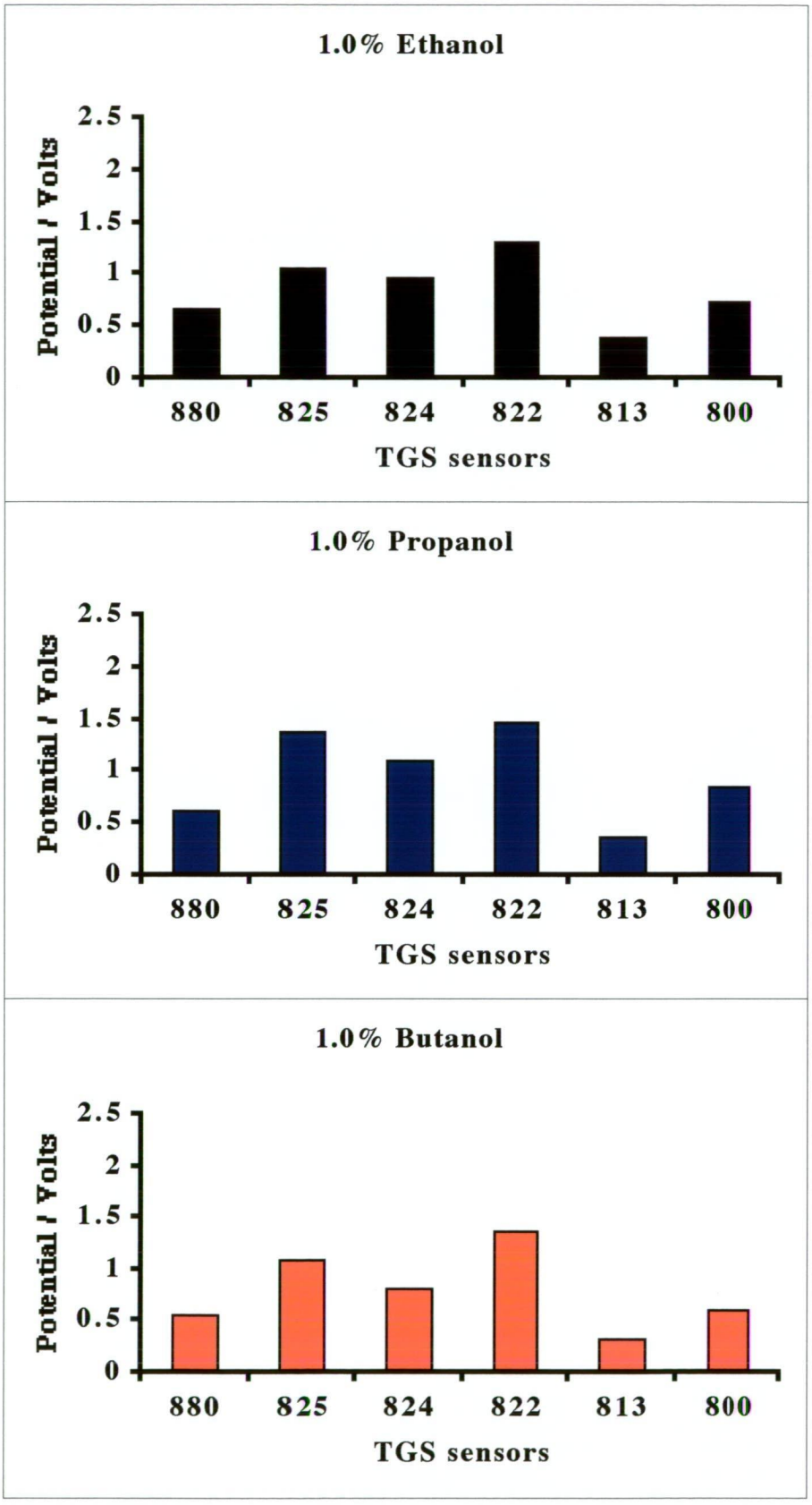

Figure 3.6. Response pattern observed for 1.0% ethanol, propanol and butanol using the multi-sensor array portable gas analyser.

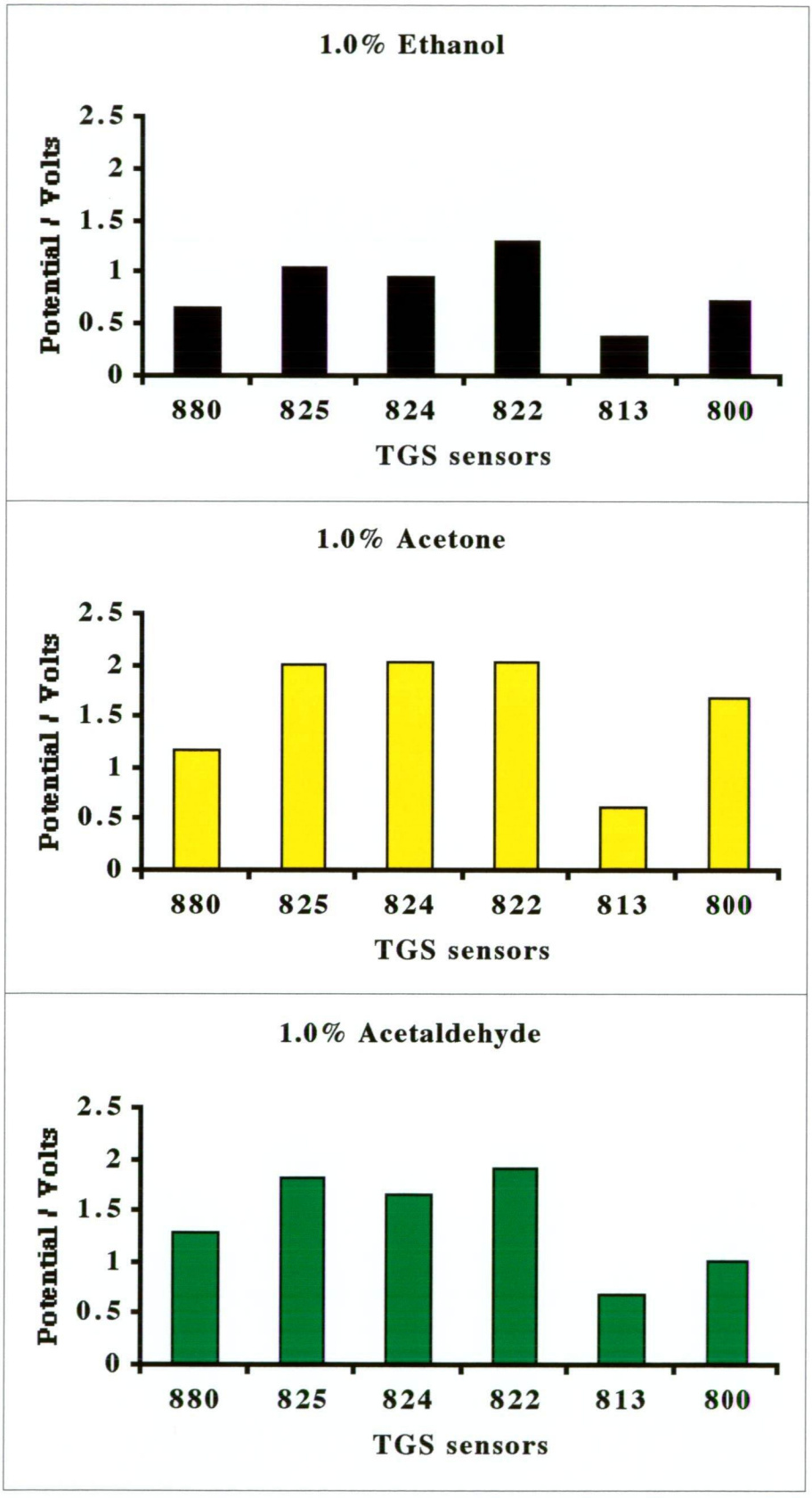

Figure 3.7. Response pattern observed for 1.0% ethanol, acetone and acetaldehyde using the multi-sensor array portable gas analyser.

Figure 3.7 presents the response pattern observed for an alcohol, a ketone and an aldehyde, namely 1.0% ethanol, acetone and acetaldehyde solutions. These three different functional groups clearly have vastly different chemical characteristics and odours between them and consequently significantly different response patterns were observed using the portable multi-sensor array gas analyser. Therefore, selective discrimination between functional groups was demonstrated with the portable gas analyser. The response pattern of the multi-sensor array is therefore useful for the identification of individual gas or vapour components due to the improved discrimination compared to a single sensor response.

3.3.5 Discrimination Between Beer Samples of Similar Ethanol Content

The response patterns of each beer sample of similar ethanol content were investigated to determine if discrimination was possible. Figure 3.8 shows response patterns of these samples compared to the 3.0% ethanol standard solution. The response of each TGS sensor for the beer samples and 3.0% ethanol solution analysed exhibited reproducibility of < 3.5% RSD. It is clear that the response pattern for the three beer samples is different from the observed response pattern of the ethanol solution. The likely reason is thought to be due to the different flavour of volatiles present in each beer sample. The flavour of beer is dependent upon many fermentation variables such as yeast strain, temperature, wort composition and aeration [28]. Therefore, it was possible to discriminate between different beer samples of similar ethanol content using the multi-sensor gas analyser.

3.3.6 Analysis of Ethanol in Beer Samples

The light beer samples were analysed for their ethanol content using the multi-sensor gas analyser. The ethanol content was determined using the Langmuir calibration plots as shown in Figure 3.9. The Langmuir isotherm is the simplest description of the adsorption mechanism and is based on the assumption that every adsorption site is equivalent and that the ability of a molecule to bind on the surface of the sensor is independent of whether or not nearby site are occupied as described in Chapter two, Section 2.4.

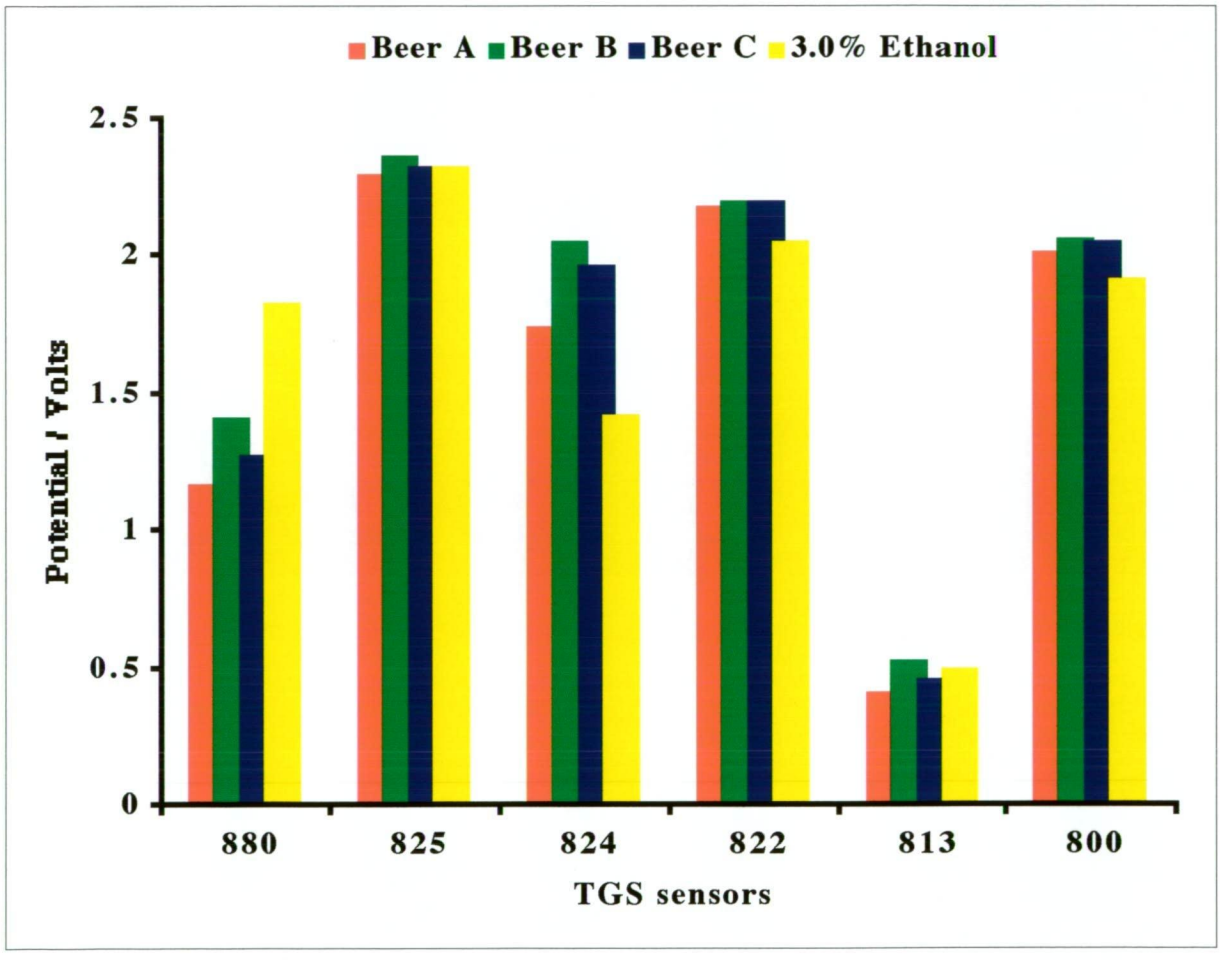

Figure 3.8. Response pattern observed for Beer A, Beer B and Beer C compared to 3.0% ethanol for the six Taguchi gas sensors.

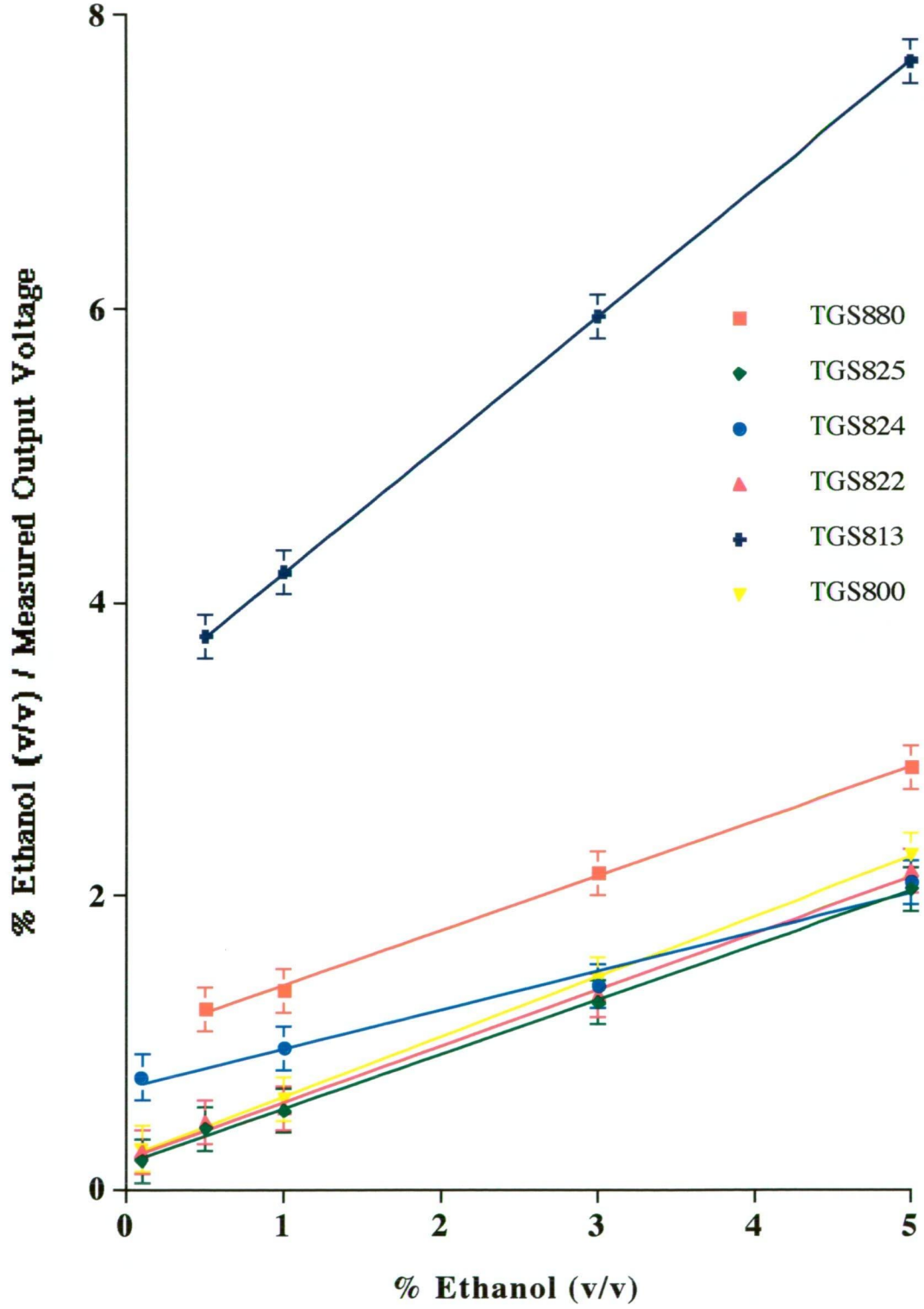

Figure 3.9. Langmuir isotherm plots for the six Taguchi gas sensors.

The results obtained for each of the six Taguchi gas sensors were compared to the gas chromatography analysis results and the labelled data and these results are presented in Table 3.1. RSD values of ≤ 2.8% were observed for all the TGS sensors for the beer samples analysed. The average ethanol content for Beer A, B and C were 2.4% 3.0% and 2.8% with corresponding RSDs of 6.5%, 4.0% and 2.9%, respectively. Therefore, analysis results for ethanol in beer samples using the multi-sensor gas analyser exhibited agreement with gas chromatography results as well as the labelled data.

Table 3.1. Ethanol content determined in light beer samples using the Langmuir isotherm plots for each of the six Taguchi gas sensors compared to gas chromatography and the labelled data.

	% Ethanol (v/v) (%RSD)								
Samples	TGS880	TGS825	TGS824	TGS822	TGS813	TGS800	Average	GC	Labelled
Beer A	2.2 (1.1)	2.5 (1.9)	2.3 (1.7)	2.6 (1.3)	2.3 (2.4)	2.5 (2.3)	2.4 (6.5)	2.5	2.7
Beer B	2.9 (1.3)	3.1 (1.4)	3.1 (0.8)	3.0 (1.8)	3.2 (2.8)	2.9 (2.1)	3.0 (4.0)	2.8	2.8
Beer C	2.9 (2.1)	2.8 (2.5)	2.9 (0.9)	2.7 (1.7)	2.9 (0.9)	2.8 (1.1)	2.8 (2.9)	2.9	2.8

3.4 Conclusions

The multi-sensor array gas analyser developed and presented in this chapter is of a simple design, portable, light weight, battery-powered, requires low power consumption and is inexpensive. The response characteristics of the gas analyser showed a stable baseline, a peak height reproducibility of < 3% RSD and a rapid response for ethanol, with peak widths in the range of 30-60 seconds for all six Taguchi type sensors. The multi-sensor gas analyser response patterns were able to selectively discriminate between samples of polar and non-polar nature such as ethanol and butane. The gas analyser was used to discriminate between functional groups such as ethanol, acetone and acetaldehyde and alcohols such as ethanol, propanol and butanol.

Due to the different flavour of volatiles commonly present in beer, the discrimination of beer samples with similar ethanol content was able to be demonstrated with this gas analyser.

Analysis results for the ethanol content in light beer samples for each of the six Taguchi gas sensors were in agreement with gas chromatography results and the labelled data. As demonstrated in this chapter, the multi-sensor gas analyser can be employed in both qualitative and quantitative applications, making this analyser a versatile portable analytical instrument.

3.5 References

1. A. D. Walmsley, S. J. Haswell and E. Metcalfe, 'Evaluation of Chemometric Techniques for the Identification and Quantification of Solvent Mixtures using a Thin-Film Metal Oxide Sensor Array', Analytica Chimica Acta, **250**, 257-264, (1991).

2. S. P. Levine and G. M. Russwurm, 'Fourier Transform Infrared Optical Remote Sensing for Monitoring Airborne Gas and Vapor Contaminants in the Field', Trends in Analytical Chemistry, **13**, 258-262, (1994).

3. P. I. Richter, 'Air Pollution Monitoring with LIDAR', Trends in Analytical Chemistry, **13**, 263-266, (1994).

4. G. Baykut and J. Franzen, 'Mobile Mass Spectrometry; A Decade of Field Applications', Trends in Analytical Chemistry, **13**, 267-275, (1994).

5. R. B. Turner and J. L. Brokenshire, 'Hand-Held Ion Mobility Spectrometers', Trends in Analytical Chemistry, **13**, 275-280, (1994).

6. S. Piorek, 'Principles and Applications of Man-Portable X-Ray Fluorescence Spectrometry', Trends in Analytical Chemistry, **13**, 281-286, (1994).

7. D. Diamond, 'Progress in Sensor Array Research', Electroanalysis, **5**, 795-802, (1993).

8. K. D. Schierbaum, U. Weimar and W. Gopel, 'Multicomponent Gas Analysis: An Analytical Chemistry Approach Applied to Modified SnO_2 Sensors', Sensors and Actuators B, **2**, 71-78, (1990).

9. H. V. Shurmer, J. W. Gardner and H. T. Chan, 'The Application of Discrimination Techniques to Alcohols and Tobaccos using Tin-Oxide Sensors', Sensors and Actuators, **18**, 361-371, (1989).

10. J. Mizsei, 'Response Pattern of SnO_2 Sensor System for Smoke of Different Origins', Sensors and Actuators B, **18-19**, 264-267, (1994).

11. C. Di Natale, F. A. M. Davide, A. D'Amico, W. Gopel and U. Weimar, 'Sensor Arrays Calibration with Enhanced Neural Networks', Sensors and Actuators B, **18-19**, 654-657, (1994).

12. J. W. Gardner, H. V. Shurmer and T. T. Tan, 'Application of an Electronic Nose to the Discrimination of Coffees', Sensors and Actuators B, **6**, 71-75, (1992).

13. H. V. Shurmer, J. W. Gardner and P. Corcoran, 'Intelligent Vapour Discrimination Using a Composite 12-Element Sensor Array', Sensors and Actuators B, **1**, 256-260, (1990).

14. J. W. Gardner, 'Detection of Vapours and Odours from a Multisensor Array using

Pattern Recognition. Part 1. Principal Component and Cluster Analysis', Sensors and Actuators B, **4**, 109-115, (1991).

15. S. J. Gentry and P. T. Walsh, 'Poison-Resistant Catalytic Flammable-Gas Sensing Elements', Sensors and Actuators, **5**, 239-251, (1984).

16. M. Nakamura, I. Sugimoto, H. Kuwano and R. Lemos, 'Chemical Sensing by Analysing Dynamics of Plasma Polymer Film-Coated Sensors', Sensors and Actuators B, **20**, 231-237, (1994).

17. W. P. Carey, K. R. Beebe, B. R. Kowalski, D. L. Illman and T. Hirschfeld, 'Selection of Adsorbates for Chemical Sensor Arrays by Pattern Recognition', Analytical Chemistry, **58**, 149-153, (1986).

18. E. T. Zellers, S. A. Batterman, M. Han and S. J. Patrash, 'Optimal Coating Selection for the Analysis of Organic Vapor Mixtures with Polymer-Coated Surface Acoustic Wave Sensor Arrays', Analytical Chemistry, **67**, 1092-1106, (1995).

19. S. L. Rose-Pehrsson, J. W. Grate, D. S. Ballantine, Jr., and P. C. Jurs, 'Detection of Hazardous Vapors Including Mixtures using Pattern Recognition Analysis of Responses from Surface Acoustic Wave Devices', Analytical Chemistry, **60**, 2801-2811, (1988).

20. J. W. Gardner, T. C. Pearce, S. Friel, P. N. Bartlett and N. Blair, 'A Multisensor System for Beer Flavour Monitoring using an Array of Conducting Polymers and Predictive Classifiers', Sensors and Actuators B, **18-19**, 240-243, (1994).

21. J. B. Tomlinson, I. H. L. Ormrod and F. R. Sharpe, 'Electronic Aroma Detection in the Brewery', Journal of American Society of Brewing Chemistry, **53**, 167-173, (1995).

22. V. P. Shiers and P. J. Farnell, 'The Electronic Nose: Aroma Profiling in the Food Industry', Food Technology International Europe, 168-171, (1995).

23. P.-M. Schweizer-Berberich, S. Vaihinger and W. Gopel, 'Characterisation of Food Freshness with Sensor Arrays', Sensors and Actuators B, **18-19**, 282-290, (1994).

24. W. R. Penrose, L. Pan, J. R. Stetter and W. M. Ollison, 'Sensitive Measurement of Ozone using Amperometric Gas Sensors', Analytica Chimica Acta, **313**, 209-219, (1995).

25. Figaro Engineering Inc., 'Figaro Gas Sensors', Product Document, Osaka, August, (1990).

26. S. R. Morrison, 'Semiconducting-Oxide Chemical Sensors', IEEE Circuits and Devices, **7**, 32-35 (1991).

27. Z. Goldring, 'A Matter of Smell', Food Manufacture, 28-68, (1997).

28. R. Kuzela, 'Control of the Levels of Flavour Active Volatile Esters and Higher Alcohols in Beers', Ferment, **10**, 35-40, (1997).

Chapter Four: The Discrimination of Beer Brands using the Portable Battery-Powered Multi-Sensor Gas Analyser and Artificial Neural Network

4.1 Introduction

In this chapter, the portable, battery-powered multi-sensor gas analyser described and evaluated in Chapter three was used with an artificial neural network to discriminate between different beer brands.

There is considerable interest in the use of multi-sensors associated with pattern recognition techniques to classify or identify various vapours and odours [1]. The pattern recognition techniques employed with solid state arrays include, principal component analysis [2-7], cluster analysis [2,3,6,7], linear discriminant analysis [7], partial least squares [2], multiple linear regression [8] and non-linear techniques [9,10] such as non-linear regression [11] and non-linear partial least squares [12].

Most solid-state sensors exhibit non-linear responses [12], and therefore cannot be adequately modelled using some of the above mentioned techniques. Artificial neural networks (ANNs) are pattern recognition techniques formed from numerous simulated neurons that are connected in much the same way as the brain's neurons and are therefore able to learn in a similar manner to people [13]. ANNs consist of parallel interconnected, and usually adaptive, processing elements used for complex, non-linear data and they are suitable for any application requiring pattern recognition [13]. ANNs learn by creating their own internal representations based on information given, have the ability to model non-linear responses and are usually able to recognise patterns even when the data are noisy, distorted or have a great amount of variation [13].

Various algorithms could be used to train a three-layer network [17]. In a three-layer network the processing are organised into three distinct layers, namely input, hidden and output layers. The back propagation [14-16] training algorithm as described in Chapter one, Section 1.4.5, was employed in this work as it was the most suitable method to identify unknown odours, after a learning process involving a set of known odours [17]. The final output from

the network for the input pattern is compared with the known correct result and a measure of the error is computed. In order to reduce this error, the weight vectors between neurons are adjusted by using the generalised delta rule and back-propagating the error from one layer to the previous layer [13]. The total error, E, is given by the difference between the correct or target output from neuron j, t_j, and the actual measured output from neuron j, O_j, [13]:

$$E = \sum_j \left(t_j - O_j\right)^2 \qquad (4.1)$$

and the critical parameter that is passed back through the layers of the network is defined as [13]:

$$\delta_j = -dE_j / dI_j \qquad (4.2)$$

where I_j is the summed input to neuron j from other neurons. For output units, the observed results can be compared directly with the target results, and

$$\delta_j = f'_j(I_j)(t_j - O_j) \qquad (4.3)$$

where f'_j is the first derivative of the sigmoid threshold function. If unit j is not an output, then,

$$\delta_j = f'_j(I_j)\sum \delta_k w_k \qquad (4.4)$$

where w_k is the weight of the connection in neurons in preceding layers. Therefore, the error is calculated first in the output layer and is then passed back through the network to preceding layers for their weight vector to be adapted in order to reduce the error.

ANNs have been used for various applications in food authentication including the assessment of the adulteration of virgin olive oils [18,19] and milk [20], the detection in the

adulteration of instant coffees [21], quantitative analysis of the adulteration of orange juice [22], the discrimination between alcoholic beverages [17] and the quality estimation of ground meat [23].

The techniques of pattern recognition described above are applied in the design and development of an 'electronic nose'. In an attempt to develop an electronic nose, researchers have attempted to mimic some of the abilities of the mammalian olfactory system by combining a multi-element array of sensors with data acquisition and processing software.

The sensation of smell arises from the stimulation of olfactory neurons, the receptor cells located high up in the nose in the olfactory epithelium. The mammalian olfactory system uses a large number of non-specific receptors that show broad patterns of response [24,25]. Typically, there are 50 million receptors in the olfactory epithelium that are exposed to the external environment [24,25]. The olfactory receptor neurons are reactive to various odourants that bind to the membrane receptors causing changes in ionic conductances; this effect produces signals that are transmitted to the olfactory bulb for processing [24,25]. Output patterns are sent to the cerebral hemispheres in the brain where they are interpreted to produce odour recognition [24]. The brain is trained to recognise which pattern corresponds to which odour description. Odourants are typically small hydrophobic organic molecules containing one or two functional groups with a mass range from 17 to 300 Da [24]. The relationship between the physiochemical properties of the odourant molecules and their odours are thought to be related to size and shape of an odourant molecule, together with the distribution of polar groups [24,25].

Beer flavour is a complex problem because there are hundreds of compounds present. Studies have shown that there are over 100 separately identifiable flavours in beer of which about 39 are present in most beers where ethanol is the main component [25]. Of these 39 key flavours in beer, 15 can be explained (eg: ethanol, estery and diacetyl), 20 partly explained (eg: hoppy, malty and worty) and 10 can not be explained at all (eg: spicy, woody and grainy) [25]. Furthermore, beer flavour is unstable and its odour will change with time as the chemical composition of beer changes [25]. Beer is prepared commercially by batch processes and it is important to ensure consistency from batch to batch and overall product quality [25]. The quality of beer is currently determined by various methods including gas chromatography or

combined gas chromatography mass spectrometry [25]. However, in the brewery, the evaluation of the olfactory aroma of a product is carried out by trained sensory experts who use a recognised vocabulary of terms to describe the character of a particular sample [24]. This organoleptic analysis is objective to a degree but is dependent on a number of factors including degree of training, personal sensitivities, diet, health and age [24]. These methods are slow and expensive and rely on large laboratory instruments or subjective sensations. Therefore, there is a need for portable battery powered instruments that can be used in the monitoring of beer flavours.

This chapter will determine whether the portable, multi-sensor gas analyser together with the back-propagation type three-layer neural network technique can be trained successfully to recognise different beer brands.

4.2 Experimental

4.2.1 Samples

The beer samples used in this study were obtained commercially from local suppliers and are listed below, with the labelled alcohol content in brackets: Beer A (2.7%), Beer B (4.9%), Beer C (4.8%), Beer D (2.8%), Beer E (4.9%) and Beer F (4.8%). Each beer sample was stored in its original bottle or aluminium can and was used for head-space analysis at room temperature, as described below.

4.2.2 Head-Space Analysis Procedure

The portable multi-sensor gas analyser described in Chapter three was employed for the work in this chapter. The head-space analysis procedure is as described in Chapter three, Section 3.2.4. The beer samples were left standing unopened at room temperature (22 ± 2 °C) for 3-4 hours to produce adequate head-space vapour prior to measurement. The sample inlet tube of the gas analyser was introduced into the head-space of the beer bottles immediately after removing the cap, and the vapour samples were pumped into the flow-through sensor compartment for 10 seconds.

The data acquired for each of the gas sensors were displayed simultaneously in real-time millivolt readings on the Macintosh PowerBook computer screen using 'Satod' and 'IGOR'

(AD Instruments, Sydney, Australia) was used for graphical representation of the data.

4.2.3 Experimental Design of Artificial Neural Networks

The application program BrainMaker Mac Release Version 1.01 (California Scientific Software, Nevada City, CA, USA) was the artificial neural network used in this study.

A three-layer network was used to model the responses of the six Taguchi gas sensors, as it can map any arbitrary continuous function given that enough neurons are present in the hidden layer [26-28].

The parameters and statistics used to train the network are presented in Figure 4.1 where the input, output and pattern windows provide a visual display of the network as it trains. The parameters window shows what BrainMaker is doing and what files are being used [13]. The 'Learning Rate' is a factor used to scale all corrections while learning which is intended to improve the speed of convergence of the network and the 'Tolerance' specifies how accurate the ANN must be to be considered correct [13]. BrainMaker has a training tolerance and a testing tolerance [13]. A different tolerance during testing is employed compared to the one used during training.

Below the parameters window is the statistics window which shows BrainMaker's progress as it trains or tests, where: 'Fact' is the sequence number of the example BrainMaker is currently evaluating, 'Total' is the cumulative number of examples that BrainMaker has evaluated, 'Bad' is the total number of examples BrainMaker got wrong so far in the run, 'Last' is the total number of examples BrainMaker got wrong in the previous run, 'Good' is the total number of examples BrainMaker got right so far in the run, 'Last' is the total number of times BrainMaker got right in the previous run and 'Run' is the total number of times BrainMaker has looked at all the examples in the training set, including the current iteration [13]. The thermometer in the input window shows the data received from a data file, the thermometer in the output window indicates BrainMaker's calculation and the thermometer in the pattern window indicates what is asserted the correct answer [13]. The thermometers in the output and pattern windows can be visually compared to determine how close BrainMaker's calculation is to the training pattern for each example BrainMaker evaluates. The 'Elapsed Time' clock starts when training begins and stops when training ends, so that training times are recorded [13].

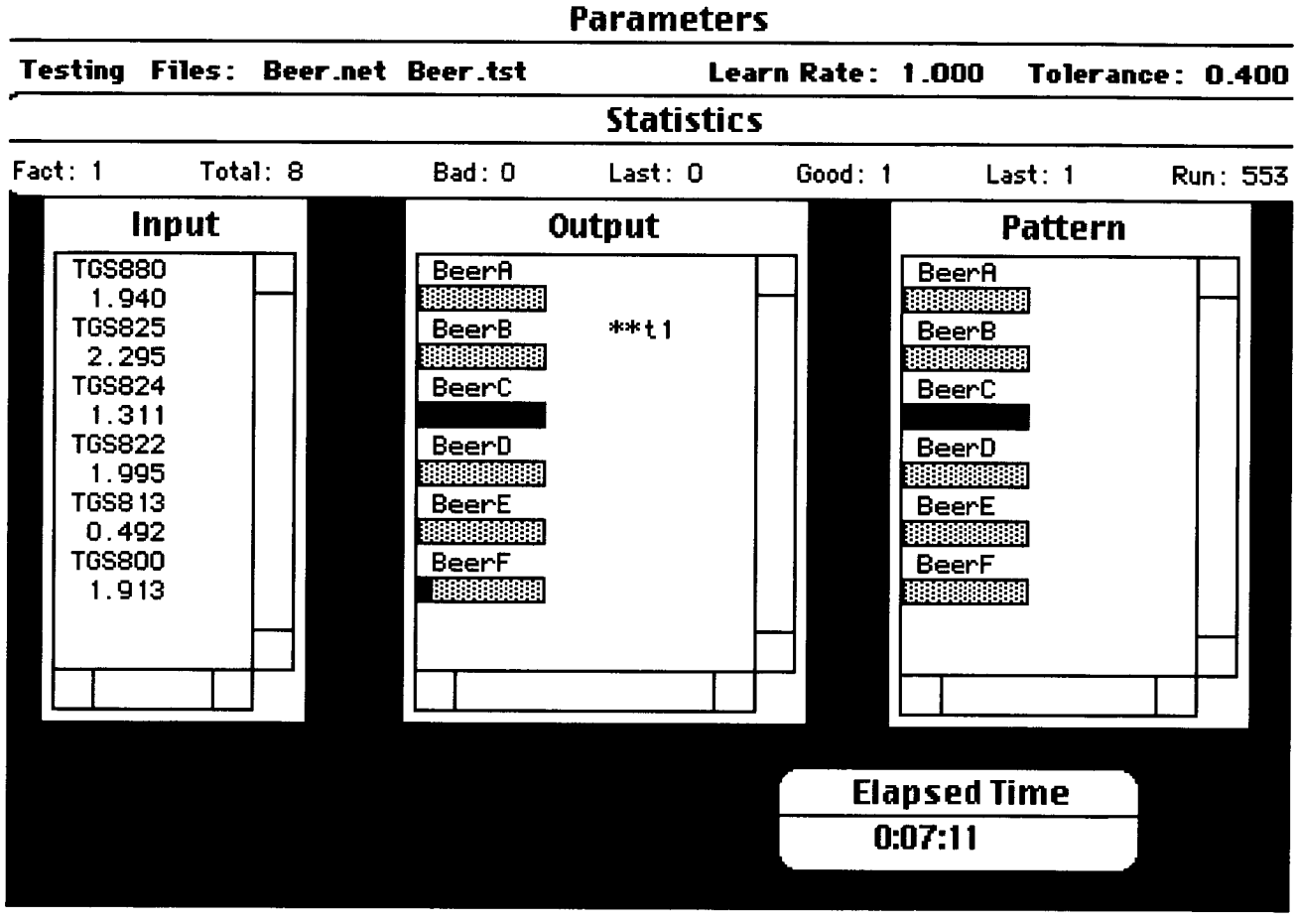

Figure 4.1. Visual display of ANN

A Macintosh PowerBook 1400cs with Power PC™ 603e at 133 MHz clock frequency and 128 kilobyte level two write-through cache memory on processor system bus was used to train the ANN.

4.3 Results and Discussion

4.3.1 Multi-sensor Response to Beer

The real-time responses of each of the six sensors to ethanol were recorded simultaneously when the sample inlet tube was moved from air into the head-space of each of the beer samples using the multi-sensor gas analyser. After sampling for 10 seconds, the inlet tube was moved back into ambient air, giving a peak-shaped response. An example of the peak response for duplicate sampling of Beer D, after the baselines were offset, is given in Figure 4.2. The TGS825 sensor was observed to be the most sensitive and the TGS813 sensor the least sensitive, with a response range between 0.0-2.0 V and 0.0-0.27 V, respectively. Response times observed for the sensors varied with peak widths over the range of 20 to 250 seconds for a 10 second sampling time and 1 L / minute flow rate. Good precision was obtained for the recorded beer samples. The relative standard deviation (RSD) of duplicate peak heights determined for each of the six different sensors were $\leq 5.0\%$.

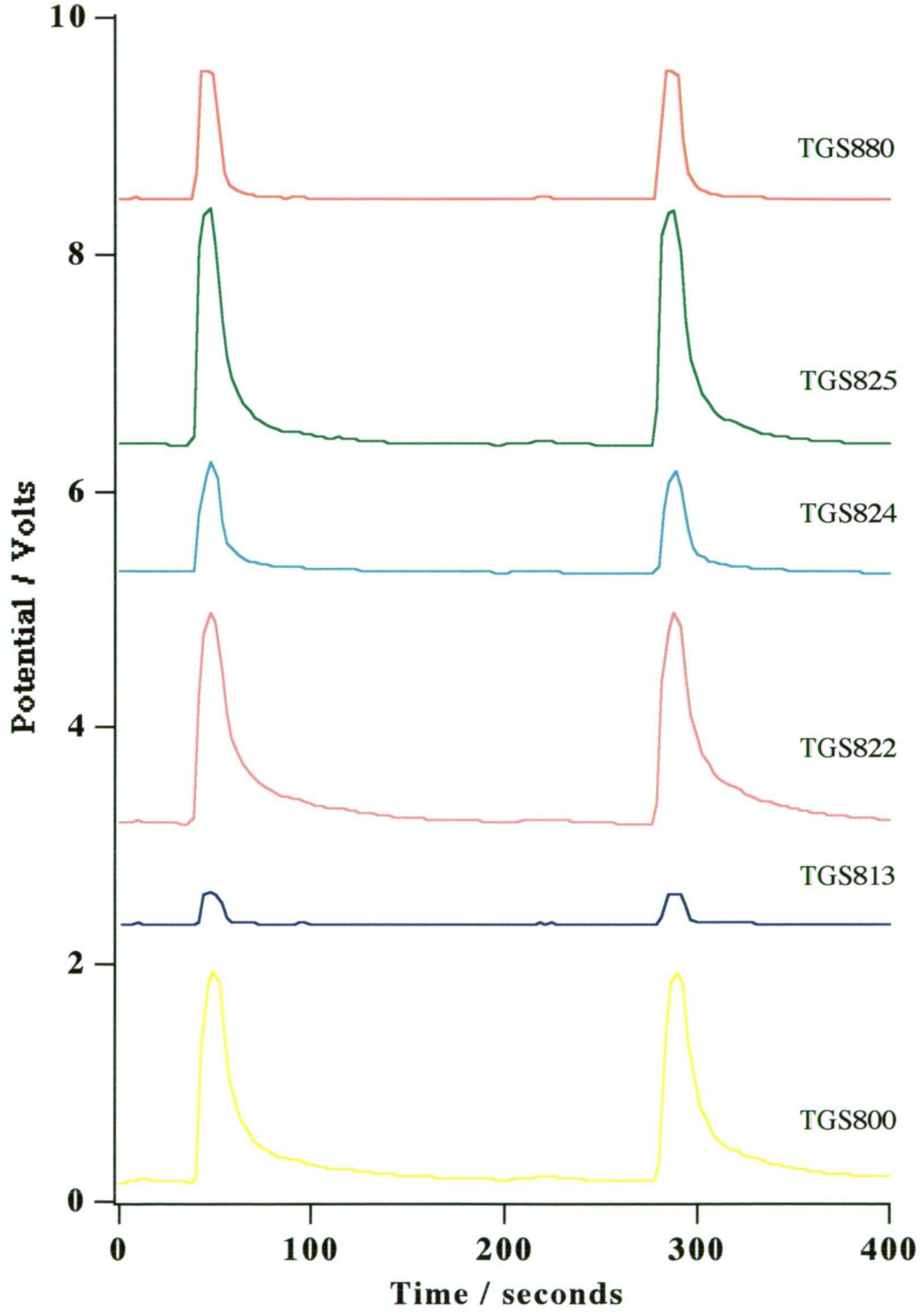

Figure 4.2. Peak response for ethanol in sample Beer D.

4.3.2 Identification of Beer Brands by Artificial Neural Network

In the three-layer artificial neural network used in this chapter there were six elements in the input layer, which received voltage data, corresponding to the peak height from each of the six gas sensors, ten elements in the hidden layer, which was calculated by BrainMaker and six elements in the output layer which provided a score for each beer indicating the certainty that the inputs were associated with the given beer brands.

In order to determine whether the back-propagation algorithm could be used to train successfully and recognise different beer samples, six beer brands were used. Two sets of beer samples were purchased, one sample set was used for training the ANN and the second set of samples were analysed as unknowns and were therefore used to evaluate the ANN.

The ideal values of the processing element in the output layer when identifying samples should be 0 unless there is correlation with the beer sample analysed, in which case it should be 1.0. In this study, an element value of 0.8 was used to indicate good identification, as has been previously reported to be acceptable [16].

A three-layer network using duplicate raw peak heights obtained for each of the six beer brands was trained in 7:11 minutes using 553 iterations at a learning rate of 1.0 and a training tolerance of 0.1. After the ANN was trained, the same raw peak heights were used to test the ANN, using a testing tolerance of 0.4. The recognition time was no more than two seconds and the results are given in Table 4.1. These results show that the outputs generated during testing were of the order of 0.900 or above compared with an ideal value of 1.0, and of the order of 0.101 or below compared with an ideal value of 0. Therefore, these results show that the ANN has trained successfully and therefore discriminates well between the beer brands.

Table 4.1. Predicted outputs for the beer brands when testing the trained ANN.

	Predicted outputs					
Brands	Beer A	Beer B	Beer C	Beer D	Beer E	Beer F
Beer A	**0.938**	0.000	0.063	0.008	0.101	0.000
Beer A	**0.954**	0.000	0.086	0.029	0.021	0.000
Beer B	0.000	**0.992**	0.023	0.000	0.014	0.076
Beer B	0.000	**0.989**	0.048	0.000	0.006	0.030
Beer C	0.001	0.047	**0.936**	0.001	0.000	0.091
Beer C	0.001	0.035	**0.950**	0.001	0.000	0.100
Beer D	0.005	0.000	0.002	**0.985**	0.033	0.003
Beer D	0.010	0.000	0.001	**0.914**	0.099	0.006
Beer E	0.042	0.000	0.001	0.012	**0.900**	0.047
Beer E	0.014	0.000	0.000	0.067	**0.900**	0.099
Beer F	0.000	0.062	0.097	0.004	0.060	**0.915**
Beer F	0.000	0.022	0.038	0.005	0.100	**0.905**

In order to validate the trained ANN, raw peak heights obtained for the unknown beer brands were used to test the trained ANN and the predicted outputs are presented in Table 4.2 and Figure 4.3.

Table 4.2. Outputs predicted from the trained ANN using unknown beer brands.

Brands	Predicted outputs					
	Beer A	Beer B	Beer C	Beer D	Beer E	Beer F
Beer F	0.000	0.128	0.164	0.002	0.042	**0.952**
Beer C	0.001	0.060	**0.924**	0.001	0.001	0.148
Beer E	0.005	0.000	0.001	0.033	**0.817**	0.084
Beer A	**0.919**	0.000	0.039	0.016	0.070	0.000
Beer D	0.018	0.000	0.002	**0.939**	0.036	0.002
Beer B	0.000	**0.990**	0.037	0.000	0.008	0.046

Sensor Response Patterns	Neural Network Prediction
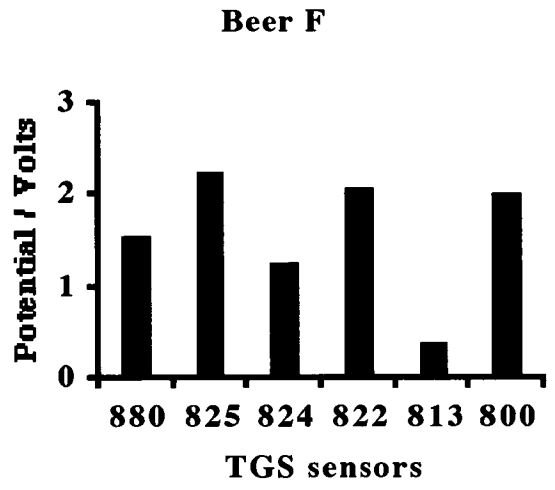	
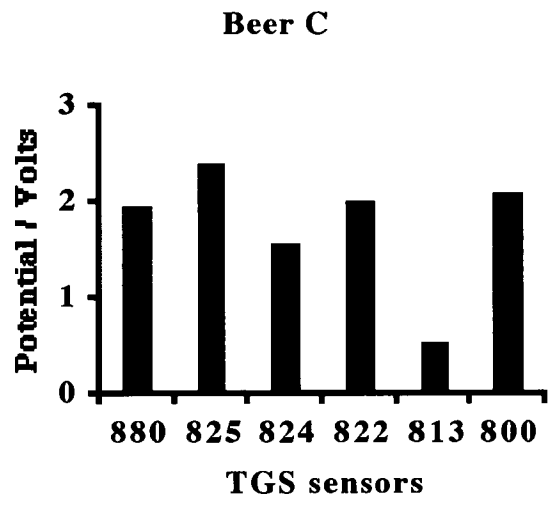	
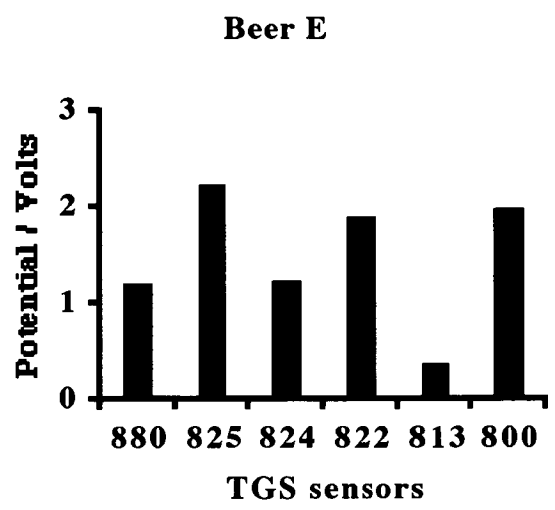	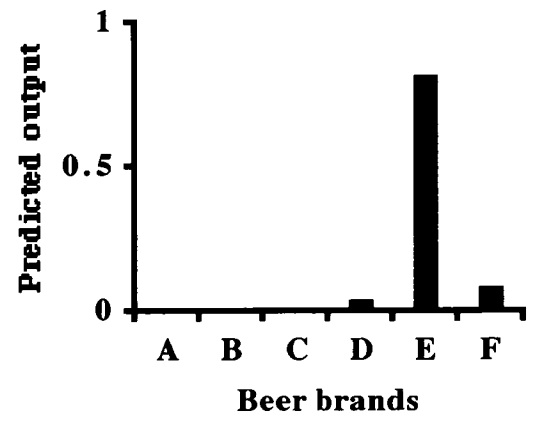

Continued on next page:

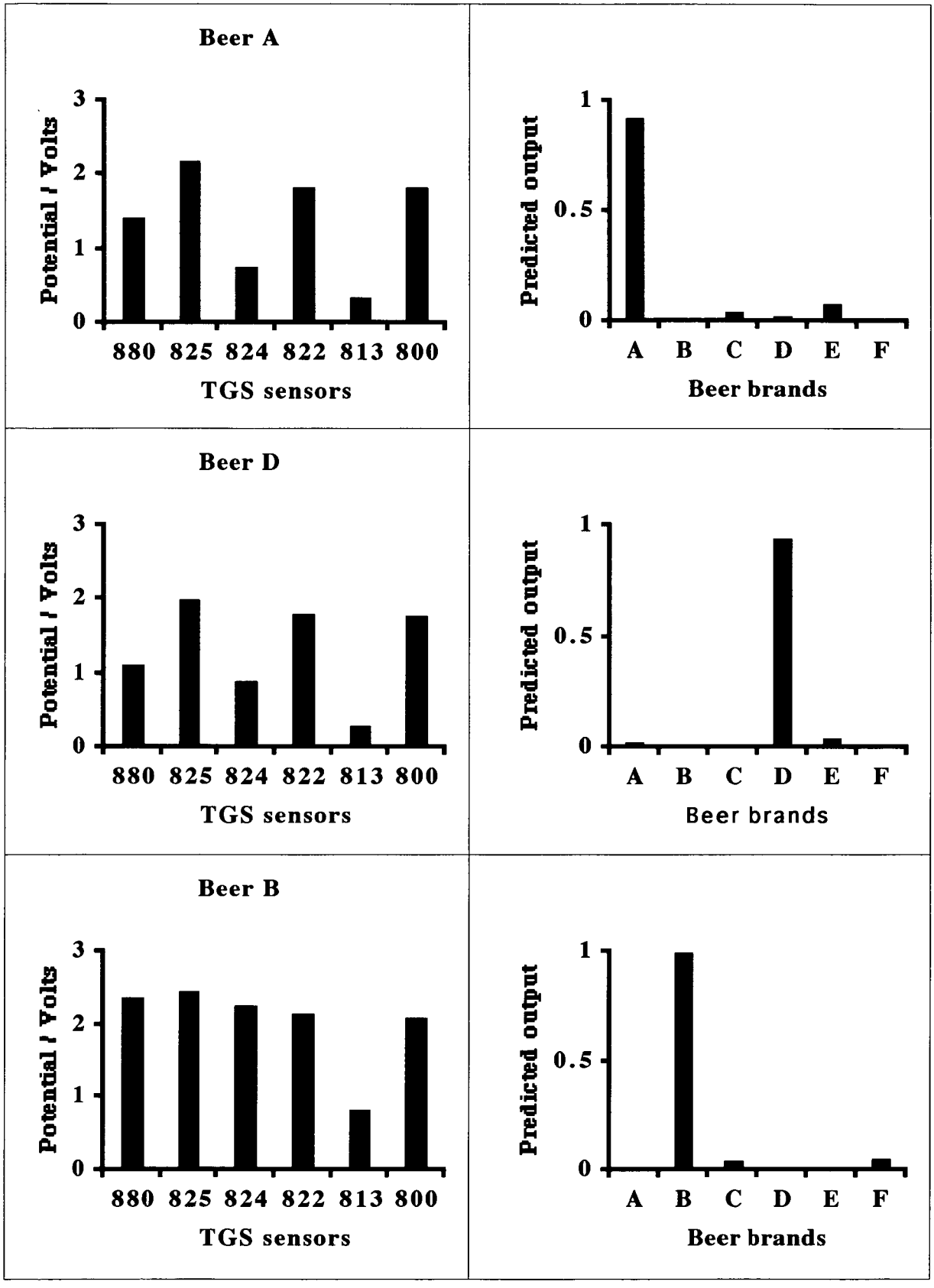

Figure 4.3. ANN predictions made from the sensor response patterns for beer brands.

These results show that in most cases the 0 output was less than 0.148, unless there was correlation with the sample analysed where an output of 0.919 or above was obtained. However, there were two exceptions to this: the lowest output value was 0.817 for an expected output of 1.0, correctly identifying Beer E, where this was significantly higher than the corresponding 0 output of 0.084 for Beer F. The largest 0 output was 0.164 which showed the characteristics of Beer C, but this was significantly smaller than the corresponding 1.0 output of 0.952, correctly predicting the identity of Beer F. Therefore, the results in this chapter show that the ANN discriminates well between the six beer brands.

4.4 Conclusions

A three-layer back propagation algorithm was used to discriminate between beer brands from the response patterns observed from the portable, multi-sensor gas analyser. The ANN used in this study was trained in 7:11 minutes using 553 iterations at a learning rate of 1.0 and a training tolerance of 0.1, which correctly identified six beer brands with an output of greater than 0.8. The work presented in this chapter shows that the portable multi-sensor gas analyser is able to discriminate among beer brands and therefore may be used to monitor beer quality in industrial processes and product quality.

4.5 References

1. C. Di Natale, F. Davide and A. D' Amico, 'Pattern Recognition in Gas Sensing: Well-Stated Techniques and Advances', Sensors and Actuators B, **23**, 111-118, (1995).

2. A. D. Walmsley, S. J. Haswell and E. Metcalfe, 'Evaluation of Chemometric Techniques for the Identification and Quantification of Solvent Mixtures using a Thin-Film Metal Oxide Sensor Array', Analytica Chimica Acta, **250**, 257-264, (1991).

3. J. W. Gardner, 'Detection of Vapours and Odours from a Multisensor Array using Pattern Recognition. Part 1. Principal Component and Cluster Analysis', Sensors and Actuators B, **4**, 109-115, (1991).

4. J. M. Slater, J. Paynter and E. J. Watt, 'Multi-layer Conducting Polymer Gas Sensor Arrays for Olfactory Sensing', Analyst, **118**, 379-384, (1993).

5. P. -M. Schweizer-Berberich, S. Vaihinger and W. Gopel, 'Characterisation of Food Freshness with Sensor Arrays', Sensors and Actuators B, **18-19**, 282-290, (1994).

6. M. Holmberg, F. Winquist, I. Lundstrom, J. W. Gardner and E. L. Hines, 'Identification of Paper Quality using a Hybrid Electronic Nose', Sensors and Actuators B, **26-27**, 246-249, (1995).

7. M. J. Martin, F. Pablos and A. G. Gonzalez, 'Application of Pattern Recognition to the Discrimination of Roasted Coffees', Analytica Chimica Acta, **320**, 191-197, (1996).

8. M. S. Nayak, R. Dwivedi and S. K. Srivastava, 'Application of Iteration Technique in Association with Multiple Regression Method for Identification of Mixtures of Gases using an Integrated Gas-sensor Array', Sensors and Actuators B, **21**, 11-16, (1994).

9. W. P. Carey, 'Multivariate Sensor Arrays as Industrial and Environmental Monitoring Systems', Trends in Analytical Chemistry, **13**, 210-218, (1994).

10. J. W. Gardner, H. V. Shurmer and T. T. Tan, 'Application of an Electronic Nose to the Discrimination of Coffees', Sensors and Actuators B, **6**, 71-75, (1992).

11. Chr. Hierold and R. Muller, 'Quantitative Analysis of Gas Mixtures with Non-Selective Gas Sensors', Sensors and Actuators, **17**, 587-592, (1989).

12. W. P. Carey and S. S. Yee, 'Calibration of Nonlinear Solid-State Sensor Arrays using Multivariate Regression Techniques', Sensors and Actuators B, **9**, 113-122, (1992).

13. J. Lawrence, 'Introduction to Neural Networks: Design, Theory, and Applications', California Scientific Software Press, Nevada City, CA, (1994).

14. D. E. Rumelhart, J. L. McClelland and the PDP Research Group, 'Parallel Distributed Processing, Explorations in the Microstructure of Cognition', Volume 1: Foundations, MIT Press, Cambridge, (1987).

15. J. L. McClelland, D. E. Rumelhart and the PDP Research Group, 'Parallel Distributed Processing, Explorations in the Microstructure of Cognition', Volume 2: Psychological and Biological Models, MIT Press, Cambridge, (1987).

16. P. J. Werbos, 'The Roots of Backpropagation: From Ordered Derivatives to Neural Networks Political Forecasting', John Wiley and Sons, New York, (1994).

17. J. W. Gardner, E. L. Hines and M. Wilkinson, 'Application of Artificial Neural Networks to an Electronic Olfactory System', Measurement Science and Technology, **1**, 446-451, (1990).

18. R. Goodacre, D. B. Kell and G. Bianchi, 'Rapid Assessment of the Adulteration of Virgin Olive Oils by Other Seed Oils using Pyrolysis Mass Spectrometry and Artificial Neural Networks', Journal of Science and Food Agriculture, **63**, 297-307, (1993).

19. R. Goodacre, D. B. Kell and G. Bianchi, 'Neural Networks and Olive Oil', Nature, **359**, 194, (1992).

20. R. Goodacre, 'Use of Pyrolysis Mass Spectrometry with Supervised Learning for the Assessment of the Adulteration of Milk of Different Species', Applied Spectroscopy, **51**, 1144-1153, (1997).

21. R. Briandet, E. K. Kemsley and R. H. Wilson, 'Approaches to Adulteration Detection in Instant Coffees using Infrared-Spectroscopy and Chemometrics', Journal of Science and Food Agriculture, **71**, 359-366, (1996).

22. R. Goodacre, D. Hammond and D. B. Kell, 'Quantitative Analysis of the Adulteration of Orange Juice with Sucrose using Pyrolysis Mass Spectrometry and Chemometrics', Journal of Analytical and Applied Pyrolysis, **40-41**, 135-158, (1997).

23. F. Winquist, E. G. Hornsten, H. Sundgren and I. Lundstrom, 'Performance of an Electronic Nose for Quality Estimation of Ground Meat', Measurement Science and Technology, **4**, 1493-1500, (1993).

24. J. B. Tomlinson, I. H. L. Ormrod and F. R. Sharpe, 'Electronic Aroma Detection in the Brewery', Journal of American Society of Brewing Chemistry, **53**, 167-173, (1995).

25. T. C. Pearce, J. W. Gardner, S. Friel, P. N. Bartlett and N. Blair, 'Electronic Nose for Monitoring the Flavour of Beers', Analyst, **118**, 371-377, (1993).

26. R. P. Lippmann, 'An Introduction to Computing with Neural Nets', IEEE ASSP Magazine, **4**, 4-22, (1987).

27. H. White, 'Connectionist Non-parametric Regression-Multilayer Feedforward Networks can Learn Arbitrary Mapping', Neural Networks, **3**, 535-549, (1990).

28. H. White, 'Artificial Neural Networks: Approximation and Learning Theory', Blackwell, Oxford, (1992).

Chapter Five: Discrimination Between Types of Olive Oils using the Portable Multi-Sensor Gas Analyser and Artificial Neural Networks

5.1 Introduction

In this chapter, the portable multi-sensor gas analyser described in Chapter three was used with an artificial neural network software described in Chapter four to discriminate between different grades of olive oils. Adulteration of olive oils has become a great temptation in today's market, because of the high price extra virgin olive oil commands due to the nutritional health benefits associated with its consumption [1].

Extra virgin olive oil is absolutely perfect in flavour and odour, and has a maximum free fatty acid content in terms of oleic acid of less than 1 gram / 100 gram [1-4]. Virgin olive oil is extracted by purely mechanical means from sound, ripe fruits of the olive tree (*Olea europaea sativa Hoffm. et Link*), whereby the oil has not undergone any treatment other than washing, decantation, centrifugation and filtration and has a free fatty oleic acid content of less than 2 gram / 100 grams [3]. Olive oil in general contains 70% monounsaturated fatty acids, 15% polyunsaturated fatty acids and 16% saturated fatty acids [4] and becomes rancid on exposure to air [5]. Olive oil is pale yellow or light greenish-yellow in colour and has a fine aroma and a pleasant taste [5], which is generally agreed to be at its best in extra virgin olive oils, and is considered to have many nutritional and health benefits [4].

There are many varied claims and suggested reasons as to the health benefits. There is very strong evidence that olive oil consumption reduces the risk of death due to circulatory system related diseases [4,6]. It is suggested that this is due at least partially to the natural antioxidants (including the bitter-tasting glycosidic compound Oleuropein) and micronutrients preventing low density lipoprotein from oxidation and so retarding the formation of atherosclerotic lesion [4]. Martin-Moreno et al. [7] have also noted that olive oils contain a

'generous amount of antioxidants' and speculate that diets high in monounsaturated fats assist in forming tissue structures that are less susceptible to antioxidative damage than would be the case in high polyunsaturated diets. They have also noted an inverse correlation between breast cancer and olive oil intake [7].

As a consequence of these health benefits, olive oil commands a much higher price compared to other edible oils. Therefore, there is a great temptation to adulterate olive oil with a cheaper oil, such as olive pomace oil, corn oil, sunflower oil or castor oil [1-4]. The necessity to detect adulterations in olive oils in general was highlighted in May 1981, when 20,000 people became ill with a severe acute respiratory illness and 350 died in Spain after consuming refined aniline denatured rape seed oil [8].

It has been reported that extra virgin oils (known as cold pressed or non-refined when referring to non-olive oils) can be distinguished by the presence of a substantial quantity of volatile components using liquid chromatography - gas chromatography - flame ionisation detection (LC-GC-FID) [9]. Therefore, it was concluded that olive oil samples which did not contain these volatile components have been treated. However, pure olive oils, being a blend of extra virgin has been difficult to distinguish since they also contain a substantial amount of these volatiles [9].

In a different study, detecting between extra virgin olive oil and adulterated olive oils with various seed oils was successful using pyrolysis mass spectrometry and artificial neural networks [2]. The same group have also used ^{13}C NMR spectra and have applied principal components analysis (PCA), principal components regression (PCR) and partial least squares (PLS) to discriminate between extra virgin olive oils from different regions of Italy [4].

The aim of this chapter is to discriminate between different grades of olive oil and estimate the age of the oil by head-space analysis using the portable multi-sensor gas analyser and artificial neural networks described in Chapters three and four, respectively.

5.2 Experimental

5.2.1 Samples

The extra virgin, pure and light grade olive oil samples used in this study were obtained commercially from local suppliers. Each olive oil sample was placed in a 100 mL glass erlenmeyer conical flask and was used for head-space analysis at room temperature using the portable multi-sensor gas analyser.

5.2.2 Head-Space Analysis and Data Analysis

The portable multi-sensor gas analyser described in Chapters three and four was used for the work presented in this chapter. The oil samples were left standing at room temperature for 1 hour and were shaken in the 100 mL erlenmeyer conical flasks to produce adequate head-space vapour prior to measurement. The sample inlet tube of the gas analyser was introduced into the head-space of the flasks immediately after removing the lid, and a vapour sample was pumped into the flow-through sensor compartment for 10 seconds at a constant temperature and relative humidity. The responses of the oil samples for each sensor were recorded in triplicate, and displayed in real-time millivolt readings on the Macintosh PowerBook computer screen using Satod ©, Version 1.46 and were saved as text files. 'IGOR' (AD Instruments, Sydney) was used for graphical representation of the data.

The ANN software package described in Chapter four (refer to Section 4.2.3) was used to discriminate between different grades of olive oils and also to determine the age of the oil samples. There were two sets of olive oil samples purchased, one sample set was used for training the ANN and the second set of samples were analysed as unknowns and used to evaluate the trained ANN.

5.3 Results and Discussion

5.3.1 Grade of Olive Oils

On the supermarket shelf, there are three main grades of olive oil available to the

consumer, extra virgin, pure and light olive oils. Extra virgin grade is the most pure and natural state of olive oil and the only process it undergoes is filtration. It has a distinctive strong fruity flavour and odour, sharply of olives, with hints of vegetables that can vary in intensity and contains a maximum of 1% free acidity as oleic acid [1-4]. Considering the significant health benefits associated with its consumption, the extra virgin grade commands a high price [1-4] and consequently, adulterating olive oils with other edible seed oils has become a great temptation in order to lower the market price.

Pure olive oil is a blend of refined olive oil and extra virgin or virgin olive oil, and has a typical composition of 75% refined and 25% extra virgin olive oils [10], but this ratio can vary between manufacturers. Pressed olive oil that does not meet the standards set by the International Olive Oil Council for virgin olive oil is refined in order to neutralise the acidity [11]. Consequently, the refined product has a bland taste and therefore must be blended with extra virgin or virgin olive oil in order to enhance the flavour, and this grade of olive oil tends to have a softer taste compared to the extra virgin grade and can also be used raw [12].

Light olive oil is similar in composition to the pure olive oil, but the proportion of extra virgin olive oil is considerably lower compared to the pure grade. Light grade olive oil has a typical composition of 90% refined and 10% extra virgin olive oils [10], but this can vary between manufacturers. This grade of olive oil has very little taste and consistency characteristics and can only be used for frying and preserving foods [10].

5.3.2 Response of Various Grades of Olive Oils

The portable battery-powered multi-sensor array gas analyser described in Chapters three and four was used for the head-space analysis of extra virgin, pure and light olive oils. The response exhibited by these different grades of olive oil samples are presented in Figure 5.1. Clearly, the extra virgin olive oil sample exhibited the largest response for all the TGS gas sensors, while the light olive oil sample exhibited the smallest. This observation correlates with the typical expectations of each grade of oil in terms of taste and odour, whereby the extra virgin

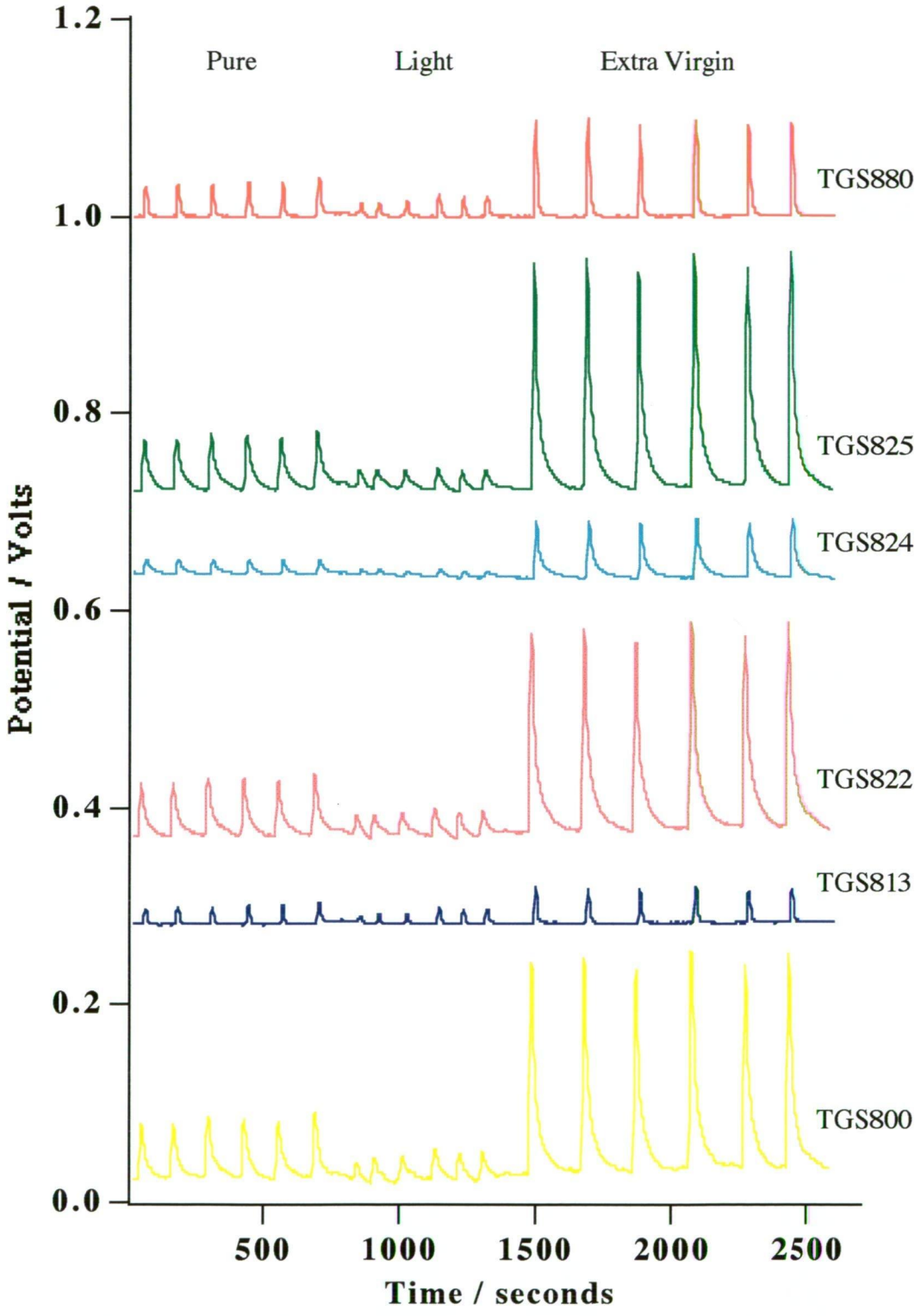

Figure 5.1. Typical response observed for the pure, light and extra virgin olive oils using the multi-sensor array portable gas analyser.

olive oil has a strong taste and odour compared to the softer taste and odour of the pure grade, while the light grade olive oil has very little taste and odour [10,12]. Therefore, it is assumed that ANN can be applied to discriminate between the grades of olive oil.

Figure 5.2, 5.3 and 5.4 shows the change of response observed for the TGS sensors over a four day period of using each grade of olive oil. As the age of each grade of olive oil increased, that is from the time they were opened and stored in the erlenmeyer conical flasks, the response exhibited by each TGS sensor in the portable gas analyser decreased significantly in intensity. However, it is important to note that the TGS sensors showed no loss of activity and no baseline drift during the course of this study. Therefore, the likely reason for the observed decrease in the gas sensor responses as the age of the oil samples increased, could be related to the increase in the oxidative rancidity process [13]. Primarily the presence of linolenic and linoleic acid in olive oil decomposes with time to form aldehydes which result in a disagreeable flavour and odour [13].

The response patterns observed for the extra virgin and the pure olive oil over a period of four days showed a decrease in the peak height by an average of 18.4%, while the peak height of the response patterns observed for the light olive oil decreased by 49.1%. As discussed in Section 5.3.1, the typical composition of the light grade olive oil is 90% refined blended in with 10% extra virgin olive oils, and this oil is reported to have very little taste and consistency characteristics [10]. Therefore, the decrease in the observed response peak height of each TGS sensor demonstrates the instability of the light grade olive oil as a result of the processes of oxidative rancidity and this is consistent with the manufacturers expectations [10].

The extra virgin grade exhibited a voltage response average decrease of 18.4% compared to 49.1% for the light grade olive oil. The likely reason for this significant difference was due to the volatile components present in the extra virgin oil [9], which give rise to the stability observed for this oil grade. The pure grade olive oil has a typical composition of 75% refined blended with 25% extra virgin and is reported to be more consistent and stable in taste compared to the light grade olive oil [10]. This was observed with the average change in voltage

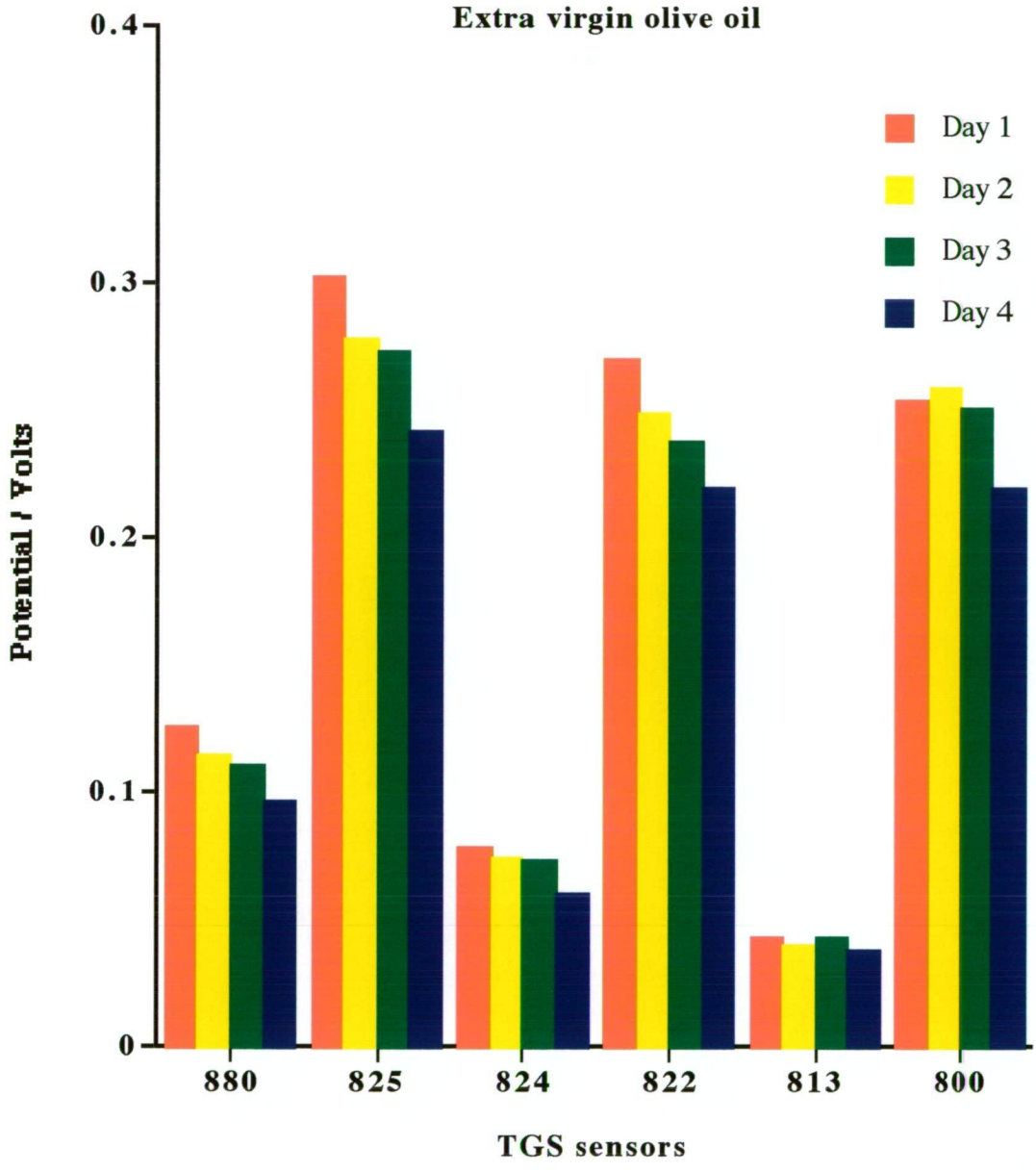

Figure 5.2. The response pattern of the extra virgin olive oil over a four day period.

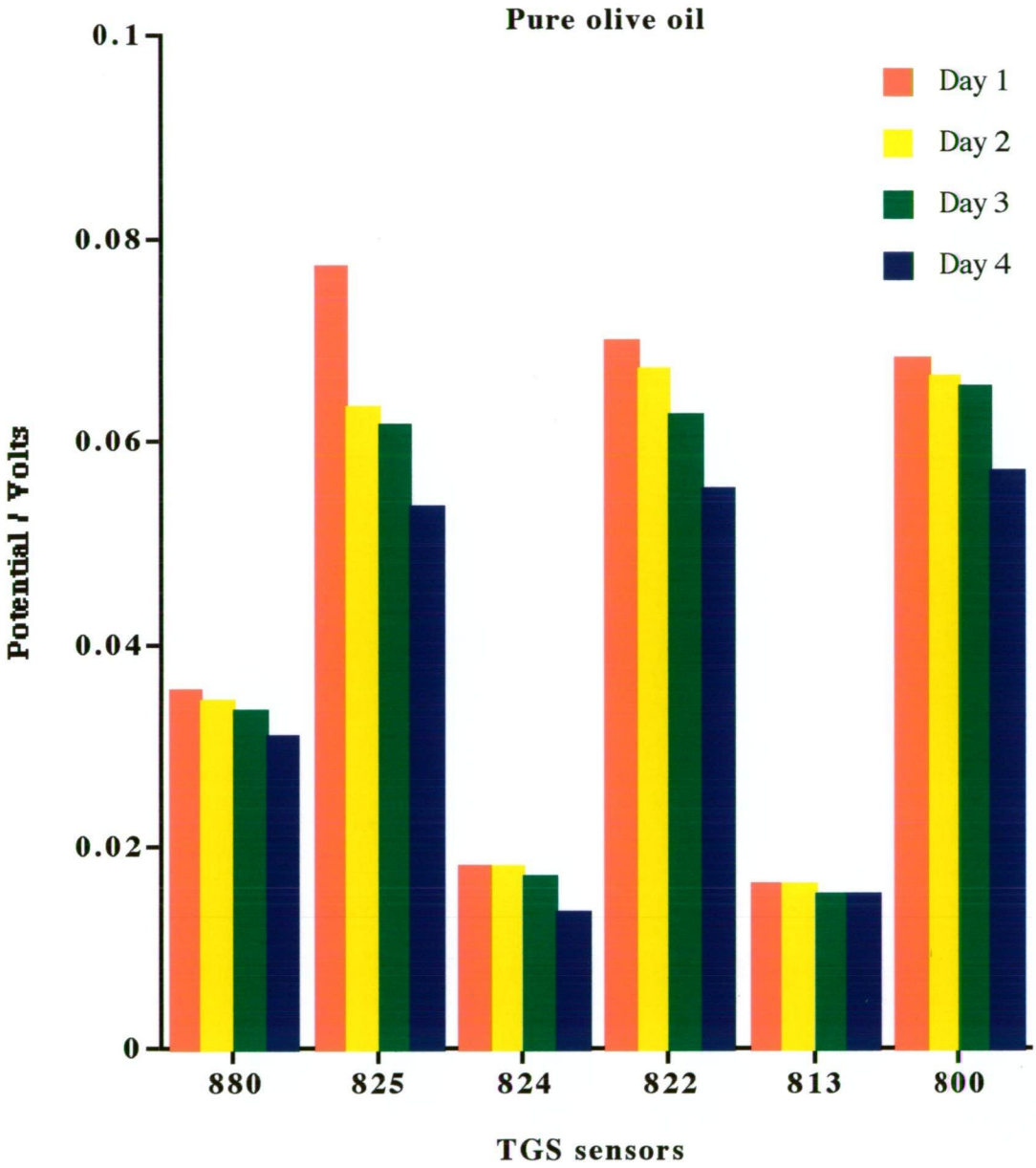

Figure 5.3. The response pattern of the pure olive oil over a four day period.

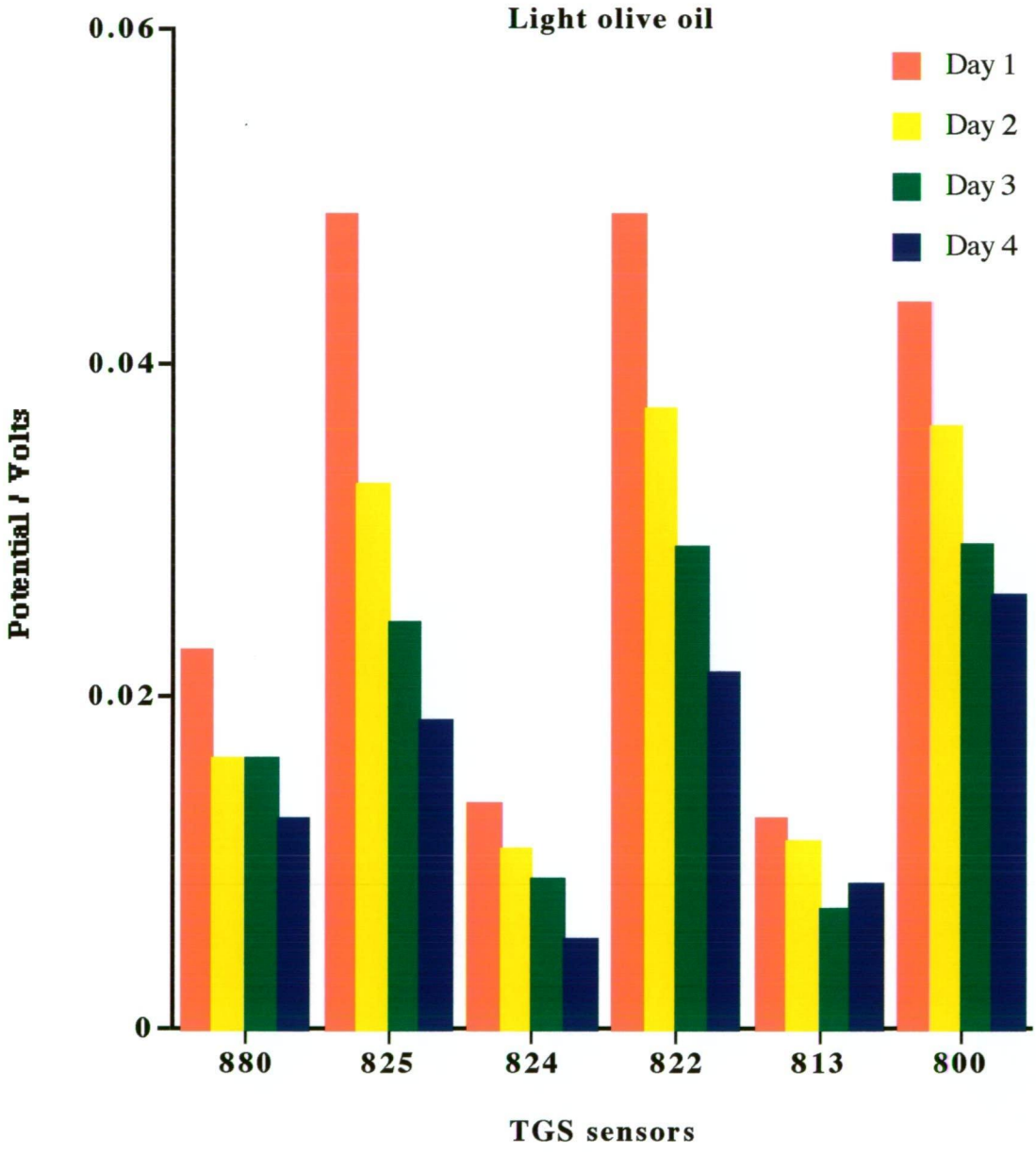

Figure 5.4. The response pattern of the light olive oil over a four day period.

of 18.4% for the TGS sensor responses compared to 49.1% for the light grade olive oil. This was surprisingly similar to that observed for the extra virgin grade, however, it has been previously reported that the pure grade of olive oil is very difficult to distinguish between the extra virgin grade, due to the presence of the volatile components present in both grades [9].

5.3.3 Discrimination Between Grades of Olive Oils using ANN

Similar to Chapter four, Section 4.3.2, the architecture of the artificial neural network used in this chapter was the three-layer network where there were six elements in the input layer, which received voltage data, corresponding to the peak height from each of the six gas sensors, ten elements in the hidden layer, which was calculated by BrainMaker and three elements in the output layer which provided a score for each olive oil indicating the certainty that the inputs were associated with the given oil grades. It is important to note that BrainMaker calculates the minimum number of neurons required in the hidden layer, and this was used throughout this work.

In order to determine whether the back-propagation algorithm could be used to train successfully and recognise different grades of olive oil, the extra virgin, pure and light grade olive oil samples were used. Two sets of olive oil samples were purchased, one sample set was used for training the ANN and the second set of samples were analysed as unknowns and were therefore used to evaluate the ANN. A decrease in the response pattern was observed with increasing age of each of the olive oil grades as discussed in Section 5.3.2. The age of the olive oil samples, that is from the time each oil sample was opened and stored in the erlenmeyer conical flasks, and were used to train and test the ANN were all 1 day old. The age of the two sets of olive oil samples had to be consistent, since the response pattern of each olive oil sample can change with time as discussed in Section 5.3.2. It was assumed that in a quality control environment, the analysis of olive oil samples would likely be performed in less than 24 hours from the time sample was opened.

Similar to Chapter four, the ideal values of the processing element in the output layer of

an ANN when identifying samples should be 0 unless there is correlation with the olive oil sample analysed, in which case it should be 1.0. In this study, an element value of 0.8 was used to indicate good identification, as it has been previously reported to be acceptable [14].

A three-layer network using duplicate raw peak heights obtained for each of the olive oil grades was trained in 2:00 minutes using 274 iterations at a learning rate of 1.0 and a training tolerance of 0.1. After the ANN was trained, the same raw peak heights were used to test the ANN, using a testing tolerance of 0.4. The recognition time was no more than two seconds and the results are given in Table 5.1. These results show that the outputs generated during testing were of the order of 0.900 or above compared with an ideal value of 1.0, and of the order of 0.110 or below compared with an ideal value of 0. Therefore, these results show that the ANN has trained successfully and therefore discriminates well between the different grades of olive oils.

Table 5.1. Predicted outputs for olive oil grades when testing the trained ANN.

	Predicted outputs		
Olive oil grades	Extra virgin	Pure	Light
Extra virgin	**0.910**	0.074	0.000
Extra virgin	**0.924**	0.098	0.000
Pure	0.094	**0.900**	0.098
Pure	0.110	**0.923**	0.058
Light	0.011	0.100	**0.960**
Light	0.011	0.090	**0.965**

In order to validate the trained ANN, raw peak heights obtained for the unknown olive oil samples (second set of samples) were used to test the trained ANN and the predicted outputs from the trained ANN are presented in Table 5.2 and Figure 5.5.

Table 5.2. Outputs predicted from the trained ANN using unknown olive oil grades.

	Predicted outputs		
Olive oil grades	Extra virgin	Pure	Light
Extra virgin	**0.920**	0.096	0.000
Pure	0.143	**0.917**	0.039
Light	0.026	0.303	**0.833**

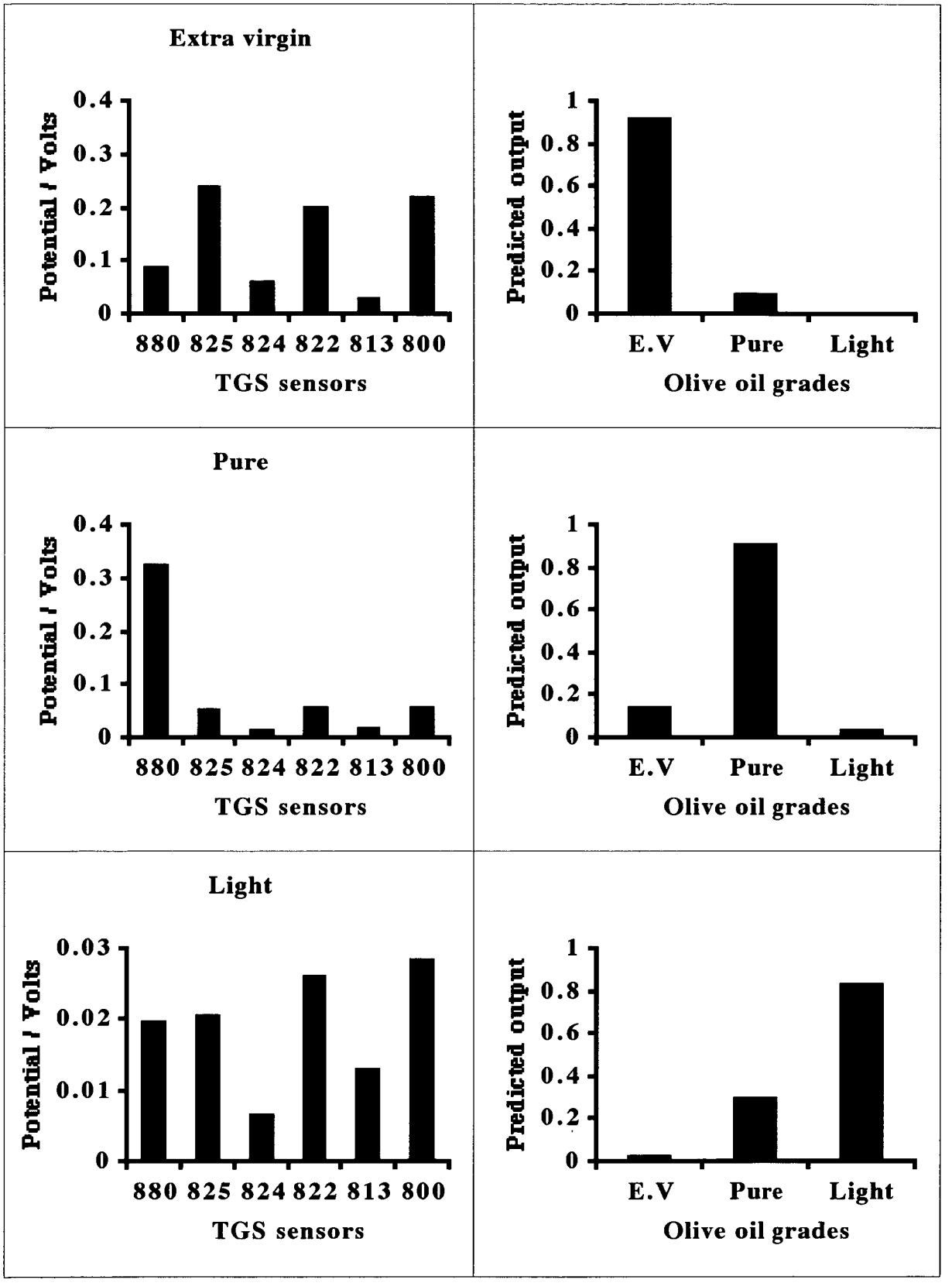

Figure 5.5. ANN predictions made from the sensor response patterns for the olive oil grades.

These results show that the 0 output was less than 0.143, unless there was correlation with the sample analysed where an output of 0.833 or above was obtained. The largest 0 output was 0.303 which showed the characteristics for pure olive oil, but this score was significantly smaller than the corresponding 1.0 output of 0.833, correctly identifying light olive oil.

5.3.4 Determination of Age of Olive Oil Samples using ANN

As discussed in Section 5.3.2, the response of the TGS sensors were observed to decrease as the age of the olive oil sample increased. Therefore, the estimation of the age of the olive oil samples was investigated using the ANN to predict the age group of a given olive oil sample. The estimation of the age groups was found to be more reliable than the specific age of the olive oil samples and was therefore used. Each olive oil sample was trained using separate ANNs. The next three sections describes the results for predicting the age group for each of the olive oil grades.

5.3.4.1 Extra Virgin Olive Oil

The architecture of the ANN employed was the three-layer network and there were six elements in the input layer, which received voltage data, corresponding to the peak height from each of the six gas sensors, ten elements in the hidden layer calculated by BrainMaker and four elements in the output layer which provided a score for each of the age groups for the extra virgin olive oil sample. Two sets of extra virgin olive oil samples were employed, one sample set was used for training the ANN and the second set of samples were analysed as unknowns and were used to evaluate the ANN.

The three-layer network using triplicate raw peak heights obtained for each age group of the extra virgin olive oil was trained in 4:59 minutes using 411 iterations at a learning rate of 1.0 and a training tolerance of 0.1. After the ANN was trained, the same raw peak heights were used to test the ANN, using a testing tolerance of 0.4. The recognition time was no more than two seconds and the results are given in Table 5.3. These results show that the outputs

generated during testing were of the order of 0.900 or above compared with an ideal value of 1.0, and of the order of 0.100 or below compared with an ideal value of 0. However, there were two exceptions to this: the lowest output value was 0.852 for an expected output of 1.0, correctly identifying day four-eight, where this was significantly higher than the corresponding 0 output of 0.308 for day thirteen-sixteen. The largest 0 output was 0.308 which showed the characteristics of day thirteen-sixteen, but this was significantly smaller than the corresponding 1.0 output of 0.852, correctly predicting the identity of day four-eight. Therefore, these results show that the ANN has trained successfully and discriminates well between the age groups for extra virgin olive oil. The estimation of the age groups instead of specific ages was found to be more reliable using the ANN and was therefore used throughout this study.

Table 5.3. Predicted outputs for the age groups of the extra virgin olive oil when testing the trained ANN.

	Predicted outputs			
Days	One-Three	Four-Eight	Nine-Twelve	Thirteen-Sixteen
	0.925	0.100	0.000	0.004
One-Three	**0.945**	0.058	0.000	0.005
	0.935	0.063	0.000	0.005
	0.045	**0.900**	0.023	0.049
Four-Eight	0.046	**0.953**	0.033	0.024
	0.012	**0.852**	0.029	0.308
	0.001	0.013	**0.953**	0.038
Nine-Twelve	0.002	0.100	**0.951**	0.009
	0.002	0.038	**0.939**	0.025
	0.045	0.007	0.000	**0.985**
Thirteen-Sixteen	0.038	0.024	0.000	**0.967**
	0.018	0.099	0.002	**0.937**

Several attempts were made to determine the specific age, in days, for the extra virgin olive oil samples. However, the ANN had difficulties in discriminating between the different ages and the reasons for these observations were not clearly understood.

In order to validate the trained ANN, raw peak heights obtained for the unknown age groups of the extra virgin olive oil sample were used and the predicted outputs from the trained ANN are presented in Table 5.4. These results show that the 0 output was less than 0.071 unless there was correlation with the sample analysed where an output of 0.938 or above was obtained.

Table 5.4. Outputs predicted from the trained ANN using unknown age groups.

	Predicted outputs			
Days	One-Three	Four-Eight	Nine-Twelve	Thirteen-Sixteen
One-Three	**0.949**	0.057	0.000	0.004
Four-Eight	0.071	**0.938**	0.022	0.017
Nine-Twelve	0.001	0.010	**0.954**	0.046
Thirteen-Sixteen	0.047	0.011	0.000	**0.976**

5.3.4.2 Pure Olive Oil

The architecture of the ANN employed was similar to that described in Section 5.3.4.1. Two sets of pure olive oil samples were employed, one sample set was used for training the ANN and the second set of pure samples were analysed as unknowns and were therefore used to evaluate the ANN.

The three-layer network using triplicate raw peak heights obtained for each age groups of the pure olive oil grade was trained in 6:05 minutes using 452 iterations at a learning rate of 1.0 and a training tolerance of 0.1. After the ANN was trained, the same raw peak heights were used to test the ANN, using a testing tolerance of 0.4 and the results are presented in Table 5.5.

These results show that the outputs generated during testing were of the order of 0.901 or above compared with an ideal value of 1.0, and of the order of 0.100 or below compared with an ideal value of 0. However, there was one exception to this: the lowest output value was 0.863 for an expected output of 1.0, correctly identifying day four-eight, where this was significantly higher than the corresponding 0 output of 0.137 for day thirteen-sixteen. Therefore, these results show that the ANN has trained successfully and discriminates well between the age groups for the pure olive oil sample.

Table 5.5. Predicted outputs for the age groups of the pure olive oil when testing the trained ANN.

	Predicted outputs			
Days	One-Three	Four-Eight	Nine-Twelve	Thirteen-Sixteen
	0.952	0.044	0.086	0.018
One-Three	**0.957**	0.028	0.047	0.030
	0.901	0.094	0.068	0.030
	0.100	**0.909**	0.093	0.040
Four-Eight	0.008	**0.902**	0.036	0.079
	0.008	**0.863**	0.028	0.137
	0.000	0.012	**0.992**	0.002
Nine-Twelve	0.000	0.027	**0.982**	0.007
	0.000	0.094	**0.963**	0.010
	0.000	0.081	0.004	**0.964**
Thirteen-Sixteen	0.009	0.077	0.000	**0.989**
	0.016	0.093	0.000	**0.985**

In order to validate the trained ANN, raw peak heights obtained for the unknown age groups of the pure olive oil sample were used and the predicted outputs from the trained ANN

are presented in Table 5.6. These results show that the 0 output was less than 0.104 unless there was correlation with the sample analysed where an output of 0.883 or above was obtained.

Table 5.6. Outputs predicted from the trained ANN using unknown age groups.

	Predicted outputs			
Days	One-Three	Four-Eight	Nine-Twelve	Thirteen-Sixteen
One-Three	**0.883**	0.096	0.058	0.032
Four-Eight	0.057	**0.960**	0.104	0.052
Nine-Twelve	0.000	0.025	**0.986**	0.005
Thirteen-Sixteen	0.000	0.001	0.008	**0.968**

5.3.4.3 Light Olive Oil

The architecture of the ANN employed was similar to that described in Sections 5.3.4.1 and 5.3.4.2. Two sets of light olive oil samples were employed, one sample set was used for training the ANN and the second set of samples were analysed as unknowns and were therefore used to evaluate the ANN.

The three-layer network using triplicate raw peak heights obtained for each age groups of the light olive oil was trained in 21:36 minutes using 1653 iterations at a learning rate of 1.0 and a training tolerance of 0.1. After the ANN was trained, the same raw peak heights were used to test the ANN, using a testing tolerance of 0.4 and the results are presented in Table 5.7. These results show that the outputs generated during testing were of the order of 0.900 or above compared with an ideal value of 1.0, and of the order of 0.102 or below compared with an ideal value of 0. However, the lowest output value was 0.811 for an expected output of 1.0, correctly identifying day four-eight, where this was significantly higher than the corresponding 0 output of 0.102 for day one-three. Therefore, these results show that the ANN has trained successfully and discriminates well between the age groups for the light olive oil samples.

Table 5.7. Predicted outputs for the age groups of light olive oil when testing the trained ANN.

Days	Predicted outputs			
	One-Three	Four-Eight	Nine-Twelve	Thirteen-Sixteen
	0.930	0.021	0.093	0.000
One-Three	**0.973**	0.007	0.094	0.000
	0.993	0.096	0.003	0.000
	0.001	**0.900**	0.098	0.000
Four-Eight	0.001	**0.901**	0.094	0.002
	0.102	**0.811**	0.031	0.000
	0.000	0.000	**0.998**	0.070
Nine-Twelve	0.005	0.099	**0.903**	0.000
	0.000	0.098	**0.980**	0.000
	0.000	0.036	0.020	**0.999**
Thirteen-Sixteen	0.000	0.022	0.033	**0.999**
	0.000	0.098	0.006	**0.999**

In order to validate the trained ANN, raw peak heights obtained for the unknown age groups of the light olive oil sample were used and the predicted outputs from the trained ANN are presented in Table 5.8. These results show that the 0 output was less than 0.093 unless there was correlation with the sample analysed where an output of 0.930 or above was obtained.

Table 5.8. Outputs predicted from the trained ANN using unknown age groups.

Days	Predicted outputs			
	One-Three	Four-Eight	Nine-Twelve	Thirteen-Sixteen
One-Three	**0.930**	0.021	0.093	0.000
Four-Eight	0.020	**0.987**	0.022	0.000
Nine-Twelve	0.000	0.000	**0.999**	0.000
Thirteen-Sixteen	0.000	0.042	0.012	**0.999**

Therefore, the results in this chapter show that the ANN discriminates well between the grades of olive oil and the age groups of each grade of oil sample.

5.4 Conclusions

The portable multi-sensor gas analyser with the three-layer ANN was used to successfully discriminate between different olive oil grades and the age groups of each oil. The extra virgin olive oil was observed to give a significantly higher response pattern compared to the pure and the light olive oil, most likely due to its distinctive taste, odour and strong fruity flavour. The observed response pattern for the pure olive oil was less in magnitude compared to the extra virgin, but higher than the light olive oil. This was most likely due to pure olive oil which typically contains a blend of 25% extra virgin and 75% refined olive oil, while light olive oil contains a blend of 10% extra virgin and 90% refined olive oil. Therefore, the ANN was able to discriminate between the three olive oil grades with an output of greater than 0.833.

The multi-sensor gas analyser with the three-layer ANN was also employed to determine the age group of a given olive oil grade with an output of greater than 0.883. The estimation of the age groups was found to be more reliable than the specific age of the olive oil samples.

5.5 References

1. R. Goodacre, D. B. Kell and G. Bianchi, 'Neural Networks and Olive Oil', Nature, **359**, 594 , (1992).

2. R. Goodacre, D. B. Kell and G. Bianchi, 'Rapid Assessment of the Adulteration of Virgin Olive Oils by other Seed Oils using Pyrolysis Mass Spectrometry and Artificial Neural Networks', Journal of Science Food and Agriculture, **63**, 297-307, (1993).

3. E. Li-Chan, 'Developments in the Detection of Adulteration of Olive Oil', Trends in Food Science and Technology, **5**, 3-11, (1994).

4. A. D. Shaw, A. di Camillo, G. Vlahov, A. Jones, G. Bianchi, J. Rowland and D. B. Kell, 'Discrimination of the Variety and Region of Origin of Extra Virgin Oils using ^{13}C NMR and Multivariate Calibration with Variable Reduction', Analytica Chimica Acta, **348**, 357-374, (1997).

5. The Merck Index, An Encyclopedia of Chemicals, Drugs and Biologicals, 12th Edition, Merck Research Laboratories, New Jersey, (1996).

6. G. E. Fraser, 'Diet and Coronary Heart Disease: Beyond Dietary Fats and Low-Density-Lipoprotein Cholesterol', American Journal of Clinical Nutrition, **59**, 1117S-1123S, (1994).

7. J. M. Martin-Moreno, W. C. Willett, L. Gorgojo, J. R. Banegas, F. Rodriguez-Artalejo, J. C. Fernandez-Rodriguez, P. Maisonneuve and P. Boyle, 'Dietary Fat, Olive Oil Intake and Breast Cancer Risk', International Journal of Cancer, **58**, 774-780, (1994).

8. W. N. Aldridge, 'The Toxic Oil Syndrome (TOS, 1981): from the Disease towards a Toxicological understanding of its Chemical Aetiology and Mechanism', Toxicology Letters, **64-65**, 59-70, (1992).

9. K. Grob, M. Biedermann, M. Bronz and J. P. Schmid, 'Recognition of Mild Deodorization of Edible Oils by Loss of Volatile Components', Zeitschrift fur Lebensmittel-Untersuchung und -Forschung, **199**, 191-194, (1994).

10. F. di Monteriggioni, Private Communication, Olio Di Oliva Maroni s.n.c., Siena, Italy, (1998).

11. International Olive Oil Council, International Trade Standard Applying to Olive Oils and Olive Promace Oil, Sousse, Tunisia, (1996).

12. P. Hymel, Private Communication, Chaparral WesternFoods, L. L. P., Houston, TX, USA, (1998).

13. McGraw-Hill Encyclopedia of Science and Technology, Volume 7, 8th Edition, McGraw-Hill, New York, (1997).

14. P. J. Werbos, 'The Roots of Backpropagation: From Ordered Derivatives to Neural Networks Political Forecasting', John Wiley and Sons, New York, (1994).

Chapter Six: Conclusions

The results presented in this thesis demonstrate the novelty of the portable multi-sensor gas analysers described. The analysers can be operated in a totally portable manner with low power consumption, using a six 1.2 V Ni-Cd rechargeable battery-pack to run the analog-to-digital converter and the gas sensors. The analysers described in this study weighed no more than 1.1 kg. The use of a PowerBook computer allows for real time plotting of data at remote locations away from conventional laboratories.

Initially, the performance of the twin gas sensor based portable flow-through analyser was developed and evaluated in this study. The twin gas analyser was of a simple design, light weight, battery-powered and required low power consumption. The gas analyser was used continuously for up to 4 hours, before recharging was necessary. The use of gas sensors in flow-through analysis allows the operator to conduct rapid measurements without interference from other volatile organics in the liquor samples analysed.

The TGS812 and TGS824 gas sensors exhibited excellent peak height reproducibility (up to 3% RSD), good baseline stability and sensitivity and a rapid response with peak widths of 30 seconds for ethanol in the range between 0.1 to 20% (v/v). A calibration plot of $1 / V_S$ versus $1 / C_S$ exhibited a linear plot for the TGS812 and TGS824 sensor response to ethanol and this plot was employed to determined the ethanol content in beer and wine samples, and the results were in good agreement compared to gas chromatography analysis.

The ethanol response exhibited by the TGS812 and TGS824 gas sensors were fitted to the Langmuir isotherm model and a linear calibration plot was achieved. The Langmuir isotherm model plots were validated by determining the ethanol content in various beer and wine samples and these results were in good agreement compared to gas chromatography analysis.

Extending the number of Taguchi gas sensors from two to six in order to improve the discrimination characteristics of the portable gas analyser was also investigated and evaluated in this work. The six-sensor array gas analyser developed was of a simple design, portable, light

weight, battery-powered, requires low power consumption and was inexpensive. The response characteristics of the gas analyser showed a stable baseline, a peak height reproducibility of < 3% RSD and a rapid response for ethanol, with peak widths in the range of 30-60 seconds for all six Taguchi type sensors. The multi-sensor gas analyser response patterns were able to discriminate between samples of polar and non-polar nature such as ethanol and butane, between different functional groups such as ethanol, acetone and acetaldehyde, alcohols such as ethanol, propanol and butanol and also between beer samples with similar ethanol content. Analysis results for the ethanol content in light beer samples for each of the six Taguchi gas sensors were in good agreement with gas chromatography results and the labelled data.

A three-layer back propagation algorithm was used to discriminate between different beer brands from the response patterns of the portable six-sensor gas analyser. The ANN employed in this study was trained in 7:11 minutes using 553 iterations at a learning rate of 1.0 and a training tolerance of 0.1, which correctly identified six beer brands with an output of greater than 0.8. The work presented in Chapter four shows that the portable multi-sensor gas analyser was able to discriminate among beer brands and therefore may be used to monitor beer quality in industrial processes and product quality.

The portable multi-sensor gas analyser with the three-layer ANN was used to successfully discriminate between different olive oil grades and the age groups of each oil. The extra virgin olive oil was observed to give a significantly higher response pattern compared to the pure and the light olive oil, most likely due to the distinctive taste, odour and strong fruity flavour of the extra virgin olive oil. The observed response pattern for the pure olive oil was less in magnitude compared to the extra virgin, but higher than the light olive oil. This was most likely due to pure olive oil typically containing a blend of 25% extra virgin and 75% refined olive oil, while light olive oil contains a blend of 10% extra virgin and 90% refined olive oil. Therefore, the ANN was able to discriminate between the three olive oil grades with an output of greater than 0.833.

The multi-sensor gas analyser with the three-layer ANN was also employed to determine the age group of a given olive oil grade with an output of greater than 0.883. The estimation of the age groups was found to be more reliable than the specific age of the olive oil

samples.

Therefore, the portable multi-sensor gas analyser described in this work can be applied to field measurements at remote site locations. An operator would need to calibrate the portable multi-sensor gas analyser and then take measurements on site and store the acquired data on the PowerBook computer, and then move onto the next site and repeat the procedure. The advantage of the data acquisition program used in this study was that it can display each sensor response simultaneously on the PowerBook computer screen and therefore an operator can monitor the performance of each Taguchi gas sensor employed in the field and use it as a diagnostic tool.

Appendix 1

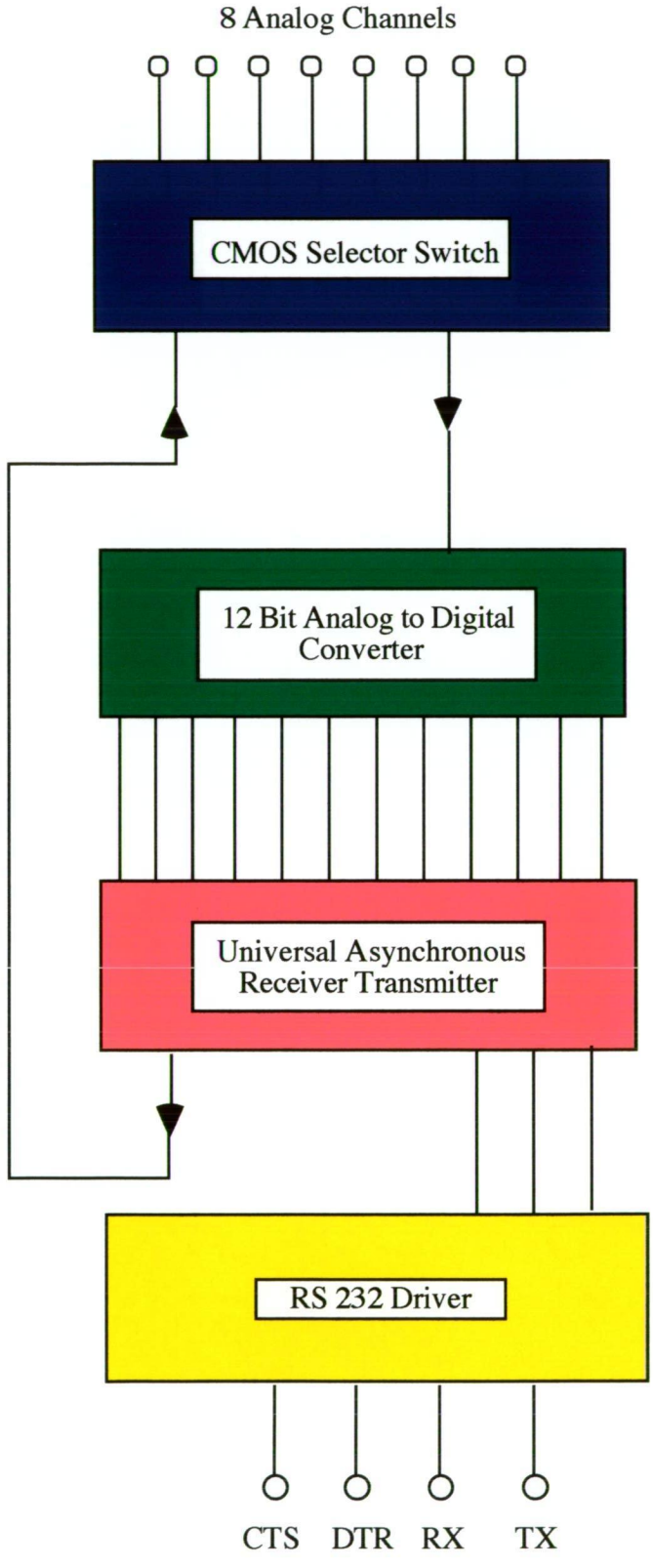
8 Analog Channels
CMOS Selector Switch
12 Bit Analog to Digital Converter
Universal Asynchronous Receiver Transmitter
RS 232 Driver
CTS
DTR
RX
TX

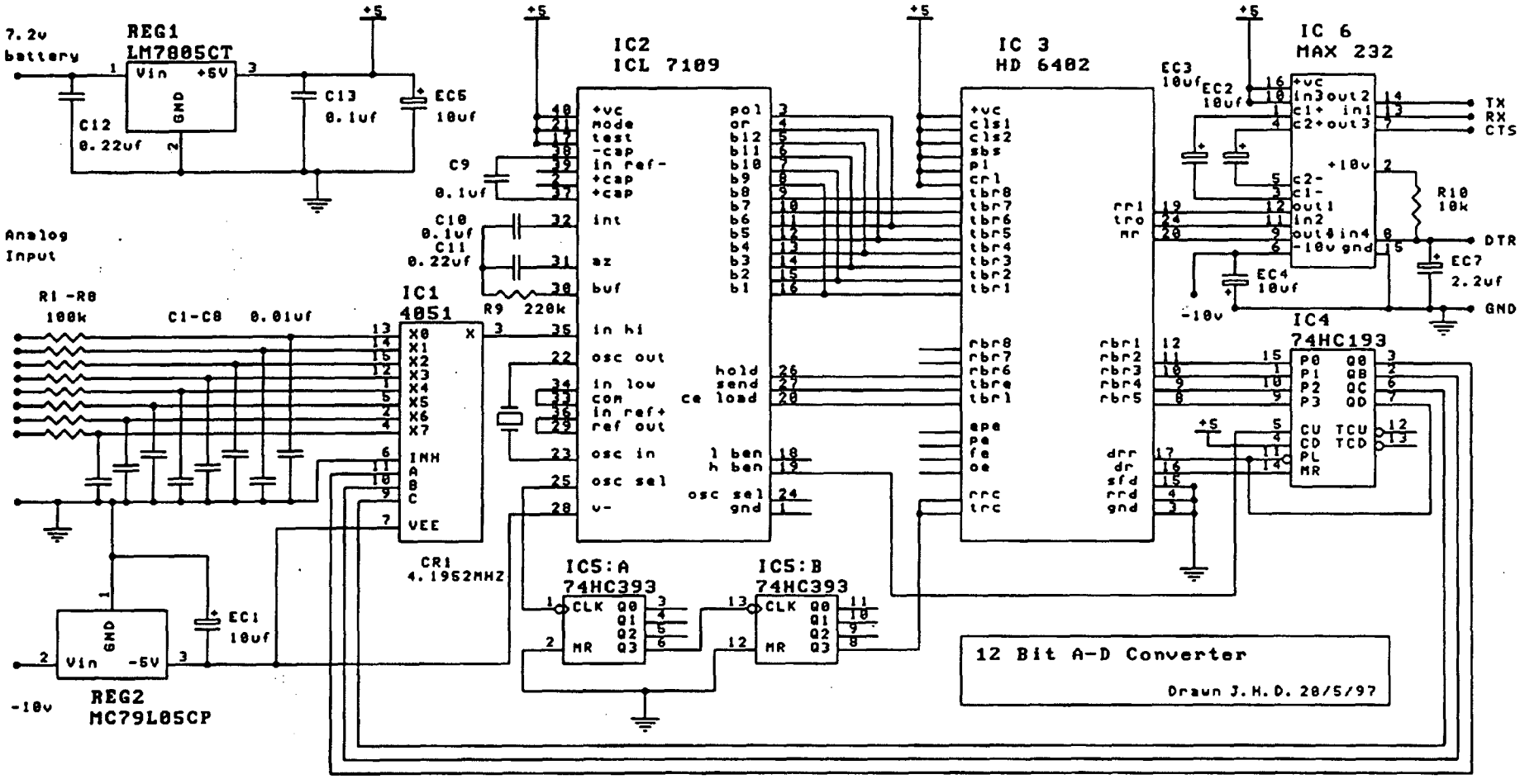
7.2v battery
REG1 LM7805CT
Vin +5V GND
C12 0.22uf
C13 0.1uf
EC5 10uf
+5
IC2 ICL 7109
+vc mode test -cap in ref- +cap +cap int az buf in hi osc out in low com in ref+ ref out osc in osc sel v-
pol or b12 b11 b10 b9 b8 b7 b6 b5 b4 b3 b2 b1 hold send ce load l ben h ben osc sel gnd
C9 0.1uf
C10 0.1uf
C11 0.22uf
R9 220k
Analog Input
R1 -R8 100k
C1-C8 0.01uf
IC1 4051
X0 X1 X2 X3 X4 X5 X6 X7 X INH A B C VEE
CR1 4.1952MHZ
IC 3 HD 6402
+vc clsl cls2 sbs pl crl tbr8 tbr7 tbr6 tbr5 tbr4 tbr3 tbr2 tbr1 rbr8 rbr7 rbr6 tbre rbr4 epe pe fe oe rrc trc
rri tro mr rbr1 rbr2 rbr3 rbr4 rbr5 drr dr sfd rrd gnd
IC 6 MAX 232
+vc in3out2 c1+ in1 c2+out3 c2- c1- out1 in2 out4 in4 -10v gnd
EC3 10uf
EC2 10uf
+10v
R10 10k
TX
RX
CTS
DTR
GND
EC7 2.2uf
EC4 10uf
-10v
IC4 74HC193
P0 P1 P2 P3 CU CD PL MR Q0 Q1 Q2 Q3 TCU TCD
IC5:A 74HC393
IC5:B 74HC393
CLK MR Q0 Q1 Q2 Q3
EC1 10uf
REG2 MC79L05CP
Vin -5V GND
-10v
12 Bit A-D Converter
Drawn J.H.D. 28/5/97